# Analysis of Reliability of Fueling Machine Head Encoders

by

Nigel Fluegel

A thesis
presented to the University of Waterloo
in fulfillment of the
thesis requirement for the degree of
Master of Applied Science
in
Civil Engineering

Waterloo, Ontario, Canada, 2021

## Author's Declaration

I hereby declare that I am the sole author of this thesis. This is a true copy of the thesis, including any required final revisions, as accepted by my examiners.

I understand that my thesis may be made electronically available to the public.

## Abstract

The objective of this thesis is to investigate in-service performance and reliability of four principal encoders used to guide the motion of the fueling machine (FM), which is used to support the fueling operation in a CANDU nuclear power reactor.

A primary function of an encoder is to track the precise position of a fueling component, such as the charge tube and ram. However, the tracking of position is occasionally prone to error due to faults in the encoder operation. The sequence jump is such a fault in which the encoder output about the position of a component suddenly increases by a large magnitude in a spurious manner. The sequence jump error is normally a result of unavoidable noise and disturbances in electric circuits and buses connecting the encoder with the fuel handling computers. In such case, the encoder functionality is restored by simple fault recovery process. However, the sequence jump error is also triggered by mechanical faults, such as worn tracking gears or faulty bit readings. In such cases, the sequence jump error continues to occur so frequently that fueling operation is significantly interrupted. This prompts the replacement of the encoder via a maintenance outage, which also costs resources and lost power generation.

At present, there is no capability to predict the reliability and lifetime of encoders as well as no health monitoring strategy. This study aims to tackle these challenges by investigating the three particular aspects of encoder performance: (1) estimation of the lifetime distributions, (2) stochastic modelling of the occurrences of encoder errors, and (3) analyzing the bit patterns of encoder sequence jump errors for health monitoring purposes.This study is based on about 20 years of historical operating data related to these encoders from a nuclear station in Canada.

The encoder lifetime distributions are estimated using the lifetime histories collected from the plant maintenance database. These distributions are used to estimate the Mean Time To Failure (MTTF) and mission reliability over an operating interval. The stochastic process modelling and probabilistic bit pattern assessment during a sequence jump error helps to formulate a health monitoring strategy for encoders.

The models developed in this research will help to improve reliability of fueling operation, and reduce the unavailability and generation losses caused by abrupt encoder failures.

**Acknowledgements**

I would like to praise God for giving me the strength to accomplish this achievement. I would also like to thank my supervisor, Professor Mahesh Pandey, for the opportunity and for his patience, knowledge, and guidance throughout my time as a Graduate student at the University of Waterloo. Finally, I would like to acknowledge my wife for her love and support that allowed me to persevere through the ups and downs of my graduate education.

## Dedication

To God, my wife, and our family.

# Table of Contents

# List of Figures

# List of Tables

# List of Abbreviations

**BM** Bit Mismatch 77–81, 87, 89–91, 93, 94

**CDF** Cumulative Distribution Function 23

**CHF** Cumulative Hazard Function xiv, 26–28, 32, 36

**COV** Coefficient of Variation 23, 26, 27, 35

**FM** fueling machine iii, 1

**FM** fuel machine xiv, 1–3, 9–12, 18, 21, 37, 45, 75, 94

**FMH** fueling machine head 1, 18, 77

**GEH-C** General Electrical-Hitachi Nuclear Energy Canada Inc. 16

**HPP** Homogeneous Poisson Process 41, 42

**IST** in-service testing 89

**MLE** Maximum Likelihood Estimation xiv, 21, 26, 28, 32, 34–36, 39, 40, 96

**MTTF** Mean Time To Failure iii, 23, 26, 27, 35, 36, 96, 97

**NHPP** Non-Homogeneous Poisson Process 3, 17, 37, 39, 41–45, 53, 75, 80–82, 87–91, 93–97

**PDF** Probability Density Function 21, 22, 24, 28

**ROCOF** rate of occurrence of failure 41

**SECHK** Shaft Encoder Check 13

**TTF** Time-to-Failure 26, 27

**WO** Work order x, xiv, 11–21, 38, 43, 75, 77, 81, 90, 96

# Chapter 1

# Introduction

## 1.1 Motivation

The fueling machine (FM) Head is used for refuelling and defueling of the fuel channels in a CANDU reactor. Each reactor consists of 480 fuel channels that need frequent additions of new fuel to maintain reactivity. Two FM heads work on opposite sides of a fuel channel, with the help of the carriage assembly, to complete the fueling process (see Figure 1.1). One of the FM heads inserts new natural uranium fuel bundles, pushing the irradiated fuel bundles out the other side where the other FM head accepts them. The fueling process is carried out when the reactor is operating at full power. This is accomplished with the help of numerous sensors and instrumentation. This thesis specifically focuses on the shaft encoder that serve as the main sensors to allow the fueling to be done remotely.

The fueling machine head (FMH) is equipped with 4 primary encoders that guide the motion of the head during the opening/closing of the shield plug and channel plug and pushing a fuel bundle into a channel at a precise location. In essence, these encoders act as the eyes of the FM head. The success of the FM head operation depends on an accurate and reliable performance of all the encoders. A malfunction in an encoder could disrupt the operation, ranging from a short stoppage in the fueling to long unavailability for a maintenance outage while performing complex recovery operations. A critical situation can arise when a fueling machine containing an irradiated bundle cannot be removed from the channel due to an encoder failure. The encoder sensor is critical to the fuelling process being achieved safely, while maintaining maximum power output.

At present, there is no systematic approach available for monitoring the health and tracking the reliability of encoders in the fuel handling system. The encoders are subjected to a time-based maintenance policy and are typically replaced during the overhaul of the entire fueling machine. Because of this, fuel handling operators occasionally experience encoder errors and they deal with them based on their experience.

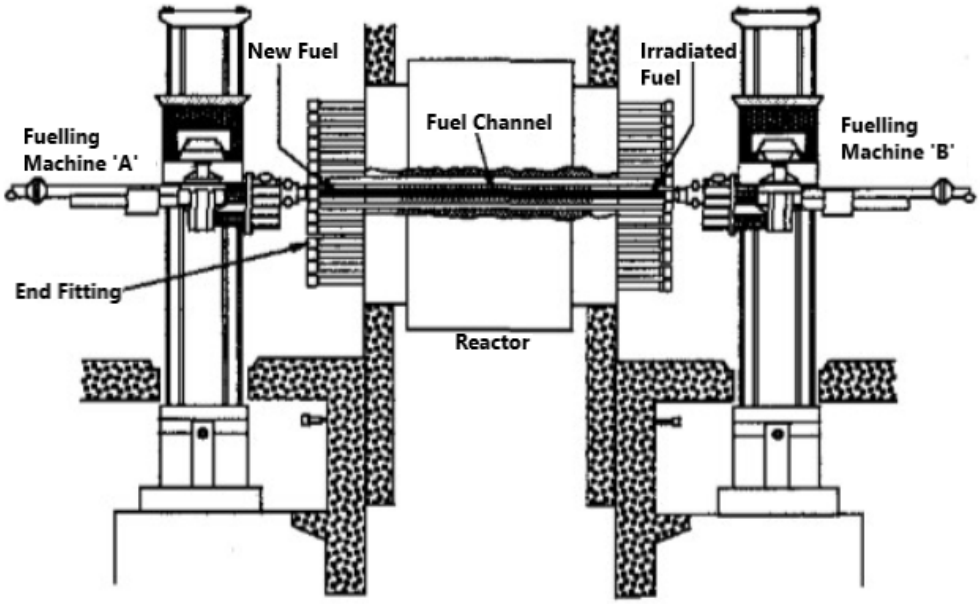


Figure 1.1: Arrangement Of Fuelling Machines During Fuelling Operations [1]

## 1.2 Research Objectives

Therefore, the primary goal of this thesis is to develop a probabilistic model of reliability of FM encoders using the operating data from a fuel handling system at a nuclear station. The specific objectives of the thesis are as follows:

1. Estimate the lifetime distribution of FM encoders,
2. Investigate the stochastic sequence of patterns of encoder errors for health monitoring purposes,
3. Investigate the probabilistic pattern of a specific "sequence jump" error in encoders, and
4. Determine a reliability centered maintenance strategy for FM encoders.

## 1.3 Approach

This thesis analyzes the performance of four main encoders used in the FM head, which are namely: (1) Charge Tube Axial, (2) Charge Tube Rotary, (3) Ram Axial, and (4) Magazine Rotary. The analysis is based on historical operating data of encoders in 8 fueling machines over about 15 years. The work-order data for encoder repair and replacement is used to estimate the lifetime distributions.

Occurrences of various types of encoder errors are continuously logged in computer-generated log files of the fuel handling system. Using these data sets, error occurrences are modelled as the Non-Homogeneous Poisson Process (NHPP) and their probabilistic characteristics are investigated. The sequence jump error, a serious type of encoder error, is further analyzed using the log file data. Here, bit mismatch patterns causing the sequence jump are investigated.

## 1.4 Organisation of Thesis

Chapter 1 introduces the problem to the reader, discusses the studies preceding approach, and gives all the information necessary on the encoder. Chapter 2 provides basic information about the encoder and its operation. The analyses will utilize the historical data available on the component with the complete breakdown of the data and use within the rest of the study found in Chapter 3. Chapter 4 defines the method for retrieving the specified distribution, presents the analysis results, and finishes with a summary breakdown. Chapter 5 presents all relevant stochastic models of the lifetimes after defining the process of creation. It also finishes with a summary analysis of the resulting models. Chapter 6 presents a methodology for accurate and effective bit mismatch pattern retrieval and then concludes with a case study with examples of the two types of lifetimes. Chapter 7 recommends ways for applying the outputs of the analyses into the maintenance protocols and workforce. It also presents a health monitoring tool by combining two of the analyses. The document then ends with a conclusion of its entire contents.

# Chapter 2

# FM Encoders

## 2.1 Fueling Machine Head Encoders

In the FM Head component there are four main drive systems that enable the refuel/defuel process; charge tube axial, charge tube rotation, ram axial, and magazine rotation (a detailed view of each of these drive systems can be found in Appendix A). Encoders are installed in the drive systems for the charge tube axial and rotary motion, the ram axial and the magazine. The magazine encoder is installed adjacent to the magazine hydraulic motor on the left hand gearbox assembly, the other three encoders being mounted on the input drives. The encoders provide digital information of the position of the various systems to the computer. This information is used to provide the control console readout, the printout information and control program permissives [2].

### 2.1.1 The Refuel/Defuel Process

Each trolley carries two FM Heads on either side of itself at one time. One FM Head carries new fuel bundles to push into the fuel channels and the other accepts irradiated fuel bundles for proper disposal. The two Fueling Machine Rooms contain the New Fuel ports, Spent Fuel ports, and each room has its respective control system. With the Fueling Machine Rooms Shielding Gates closed, it allows for maintenance on the FM heads and for them to be removed and replaced with overhauled FM heads. Given the three trolleys only allow for six FM heads in operation at one time, that leaves two FM heads to be overhauled and prepped as spare parts.

On the initiation of the "Move Fuel" sequence at the control panel of each FM head, the FM head carrying the new fuel automatically starts an "Eject Fuel" sequence while the other FM head starts its "Accept Fuel" sequence [2].

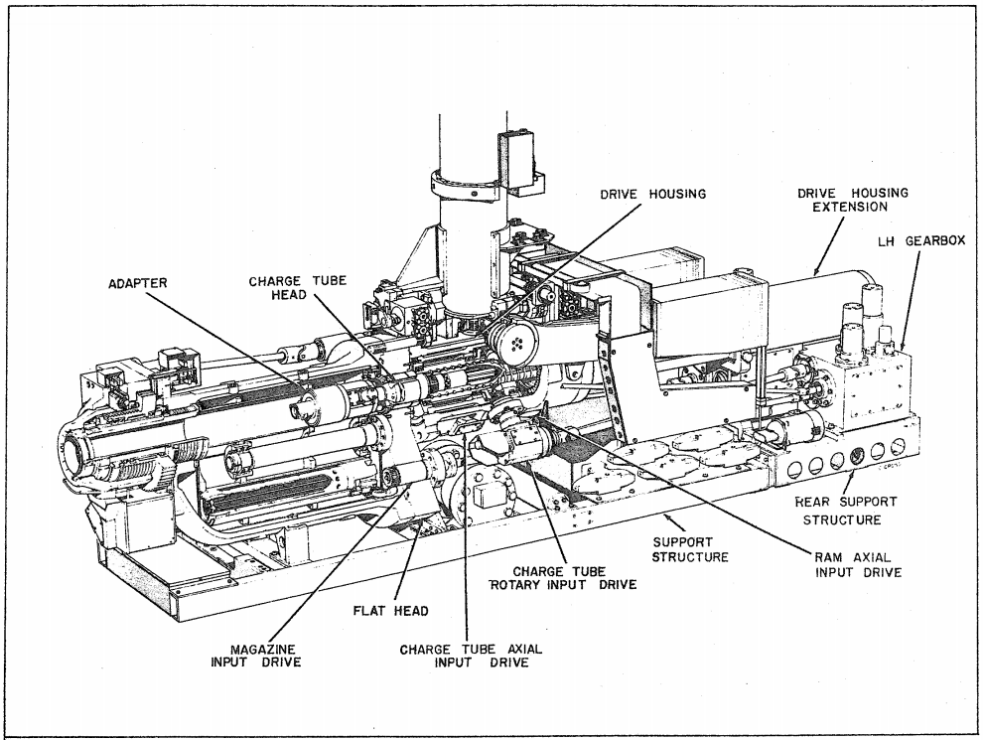


Figure 2.1: Fuel Machine Head Diagram [2]

The accepting FM head rotates its magazine to align an empty fuel carrier with the charging tube and ram. The charging tube and ram of the accepting FM head then lock on to the fuel carrier, unlocking it from the magazine and moving it forward readying it to accept the irradiated fuel bundle(s). The magazine of the ejecting FM head rotates to align a new fuel bundle carrier with the charging tube and ram. The charging tube of the ejecting FM head then locks on to the fuel carrier, unlocking it from the magazine and moving it forward into the fuel channel. The ram movement then pushes the fuel bundle from the carrier causing the entire column of fuel bundles to move one bundle length along the fuel channel. This ejects the irradiated fuel bundle into the carrier of the accepting FM head. Both charging tubes then retract to withdraw the fuel carriers into the magazine. The charging tubes lock the fuel carriers into the magazines and are in turn unlocked from the fuel carriers. If this is the end of the fuelling operation, the magazines are then rotated to align the plugs and adapters with the charging tubes and the plugs are both replaced [2].

### 2.1.2 Charge Tube Axial Encoder

The axial position of the charge tube is continuously monitored by a shaft encoder and is mounted on the input drive and driven from the input drive shaft. This is used in conjunction with four pressure switches CFHP and CFLP (charge forward high and low pressure) and CRHP and CRLP (charge retract low and high pressure) for control logic [2].

### 2.1.3 Charge Tube Rotary Encoder

The charge tube rotary position is monitored by an encoder and is installed on the input drive to provide the necessary signals for the control system. This is used in conjunction with three pressure switches ACCLP (A-motion, counter-clockwise, low pressure), ACWLP, and ACWHP (A-motion counter-clockwise, low and high pressure). The control logic is done in a similar manner to the charge tube axial encoder and switches [2].

### 2.1.4 Ram Axial Encoder

Four pressure switches are used in conjunction with an encoder to detect ram force and position RFLP and RFHP (ram forward low and high pressure) and RRLP and RRHP (ram retract low and high pressure). The pressure switches and encoder work in conjunction to detect force and position in a similar manner to those in the charge tube axial system [2].

### 2.1.5 Magazine Rotation Encoder

The magazine position is controlled entirely by the encoder. The magazine drive provides indexing to any of the six magazine channels, locking and aligning each magazine channel with the snout centerline and charge tube, with sufficient accuracy to permit reliable fuelling operations. The cam of the indexing drive makes 6 revolutions to rotate the magazine 60 degrees from one channel to an adjacent position. The magazine encoder positions are set at the middle of a cam dwell, thus effectively locking the magazine in each position. The magazine makes two revolutions to cover the total encoder bits of 4096 and, due to this, there are two unique encoder readings for each magazine channel [2].

### 2.1.6 Operation

The input signals from each of these four motions (charge tube rotary and axial, ram axial, and magazine rotation) are provided by shaft encoders. Shaft encoders are devices which produce a unique code for a given shaft position. A typical encoder is a brush type $2^{12}$ (12-bit) Gray code encoder producing 4096 discrete positions and require 16 turns to produce the complete 4096 discrete positions.

The code is produced by brushes sliding over discs with concentric tracks coded with conducting and non-conducting segments. The conducting segments producing a digital value of 1 and the non-conducting segments producing a digital value of 0. Each line on the track, therefore, produces a binary code that is transmitted to the computer interface to identify its position. However, the tracks use a canonical binary single-distance code commonly referred to as Gray code. Gray code is, therefore, a numbering system made up of ones and zeroes (binary) that has only a single-digit changing between each position. The reason for using the Gray code is to prevent ambiguity of the read out, it does this by limiting the bit changes to one always, whereas, with a typical binary code bit changes can be up to 5 or 6 for one positional change. With manufacturing tolerances in the brushes and disc contacts, it is impossible for all the brushes to change from one digit to the next in the same instant. Meaning lots of different binary code combinations can be made when switching from one position to another. For example, the Figure 2.2 shows a transition from position 3 to 4 in the binary coded $2^3$ (3-bit) encoder disc, however the position output could be 3 or 4 or 5 or 6. When compared to the Gray coded encoder disc in the same Figure, the position can only be 2 or 6 based on track 4 being the only track to change. In the Figure the dots • represent the brush contacts sliding over the coded discs and the discs are shown expanded linearly rather than on a circular representation (as seen in Figure 2.3). The x-axis is a binary to decimal conversion and the y-axis is the track numbers for a $2^3$ (3-bit) encoder disc ($2^0$ (1), $2^1$ (2), $2^2$ (4), and $2^3$ (8)) [2].

The $2^{12}$ encoders use two discs geared together with a gear ratio of some power of two between them. This is because it is practical to put only a limited number of tracks on a single disc because of the tolerance buildup and brush size. To ensure that the backlash in the gears and any misalignment between the brushes for one disc and the other is kept to a minimum, the low speed disc has two identical disc patterns, lead and lag. At all times, either the lead or the lag pattern is energized by a switching track on the high speed disc.

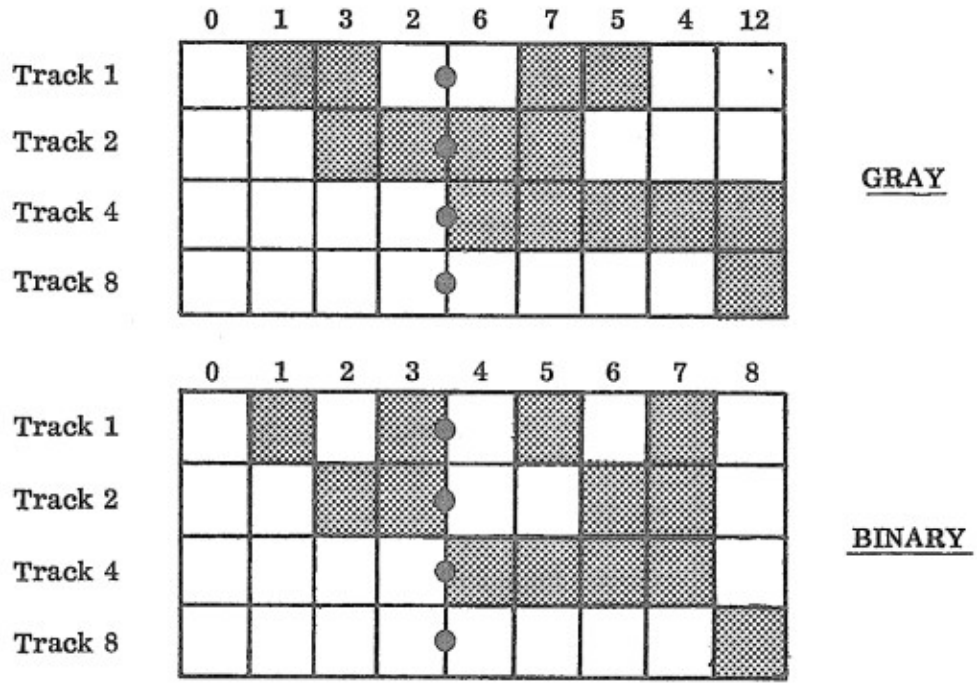


Figure 2.2: Encoder Operation Gray Versus Binary Diagram [2]

The 12-bit encoders have lead and lag outputs for the computer word bits 0 to 4 inclusive and single outputs for the remaining bits. A switching track output is provided and inputs for the lead and lag buses are required [2].

The $2^{12}$ (12-bit) encoders on the drive systems, allow for the refuel/defuel process to be done safely, remotely, and efficiently.

### 2.1.7 Notation

The four encoders is identifiable in four different ways, as shown in Table 2.1.

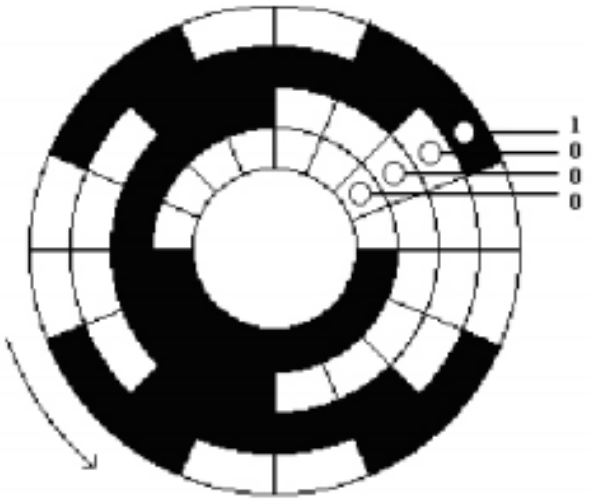


Figure 2.3: $2^3$ (3-bit) Gray Code Shaft Encoder Disc [3]

Table 2.1: Names of FM encoder

| **Encoder Number** | **Full Name** | **Short Form** |
|---|---|---|
| 1 | Charge Tube Axial Encoder | CA or CTA |
| 2 | Charge Tube Rotary Encoder | CR or CTR |
| 3 | RAM Axial Encoder | RA |
| 4 | Magazine Rotary Encoder | MR |

The component identification and short form terms were used to identify the encoders throughout the historical data to properly analyze them. Any of these notation styles can be used to identify specific encoders within this case study. There are eight fuel machine heads throughout the plant, therefore using one of these terms identifies eight potential encoders. Pairing these terms with a head number (1 to 8) identifies one singular encoder.

## 2.2 Summary

In this chapter, the FM Head, refuel/defuel process, and the four main encoders are described. Two FM Heads simultaneously push and receive fuel bundles from a single fuel channel to complete the refuel/defuel process. Furthermore, this chapter goes in-depth on the exact operation and design of the brush type shaft encoders utilized within each FM Head that enable this process. Each encoder is a 12-bit encoder using gray code to identify the positions and allow for this process to be done safely and remotely. Finally, the notation utilized to describe each respective encoder throughout the thesis is stated here as well.

# Chapter 3

# FM Head Encoder Performance Data

## 3.1 Introduction

This chapter presents an overview of operating history and performance of four FM Head encoders that are used in this study as a basis for reliability analysis and stochastic modeling of encoder errors. The overview includes types of data sets available and assumptions made in the interpretation of data in the statistical analysis. Furthermore, it will define the concept of clamp ups as the metric for this study.

## 3.2 Work Order

WOs are submitted by maintenance personnel to initiate and track the maintenance of a component in the plant. They usually provide a short reasoning for the work and a description of the work done, start and end dates, associated costs and hours, the type, and identifying values. This information is compiled by hand and placed into a maintenance database by one or more maintenance personnel. Each WO has a reference number and can have one or more tasks associated with it. The data has two types of tables, a summary table with only the distinct WOs and a task level table with all tasks shown for each respective WO number. This study uses 372 WOs related to FM encoders over a period from 1998-2019 and their respective breakdown is shown in Figure 3.1.

The WO database provides all the maintenance information performed on the components of interest. The maintenance information is the source for determining the lifetimes of encoders. The idea is to follow each new encoder until replacement or overhaul and collect these lifetimes for further analysis. An overhaul is the complete rejuvenation of the component or system, either by replacement or significant repair. The encoders are all a part of the FM head system and they all are replaced at the time of an overhaul of the

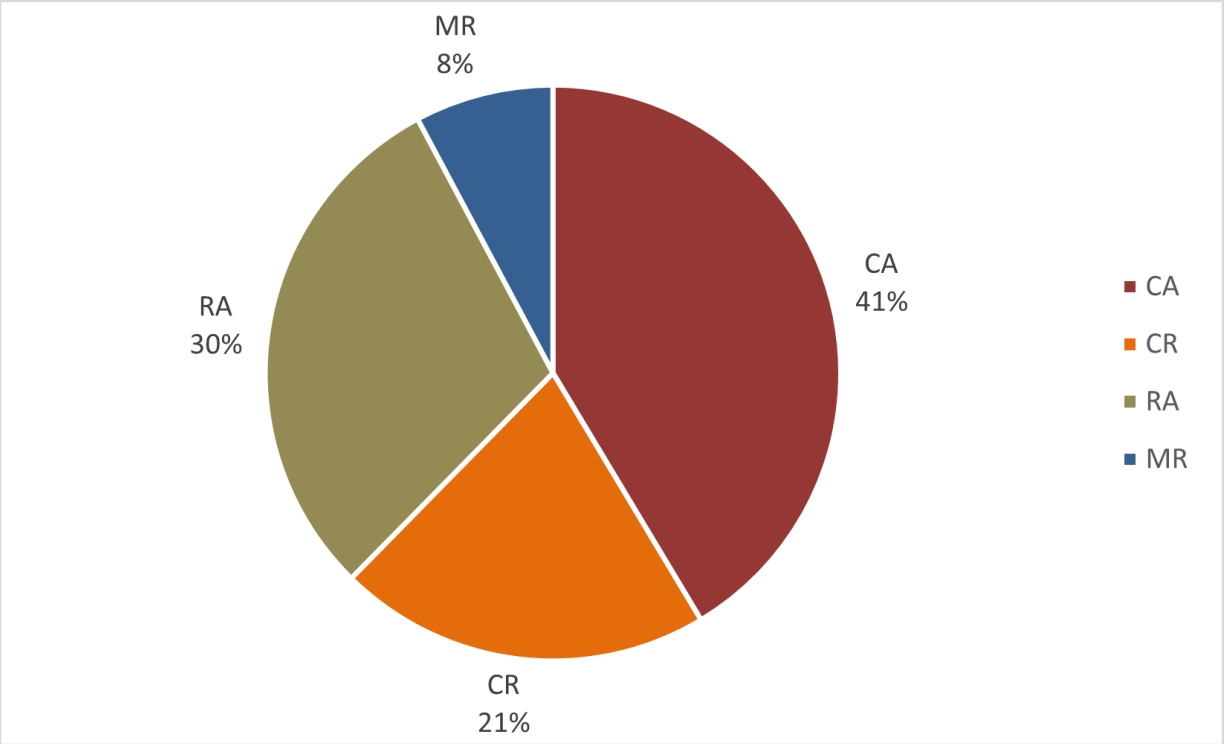


Figure 3.1: Distribution of the number of WOs among 4 encoders

FM head. In case of a malfunction, encoders are also replaced before the overhaul of the FM head.

The reason for the replacement of an encoder is carefully analyzed, since this information is necessary for the lifetime distribution analysis presented in Section 4. The reason identifies the type of lifetime and a proper determination is imperative for an accurate lifetime distribution. In this case, there are two possible reasons; replacement due to failure and a contingency replacement. The lifetimes further provide the necessary date intervals for the stochastic process models in Section 5 and the probabilistic assessment of the bit mismatch patterns in Section 6.

Table 3.1: Example of Work Order Task Level Entry with 1 Task in WO

| Title | SCI | Component | Work Order Number | WO Description | Work Order Task | Task Description | Work Order Type | Start Date Start Date Start Date | Completion Date | Parts Cost | Parts Hours | Labor Cost | Labor Hours | Miscellaneous Cost | Miscellaneous Hours | Estimated Hours | Failure Mode |
|---|---|---|---|---|---|---|---|---|---|---|---|---|---|---|---|---|---|
| FM HEAD | 63521 | ZE1-CA(H2 | 01306152 | F/H 0-63521-ZE1-CA(H2 MANY SEQUENCE JUMPS AND FWD BITS | 01 | (*) FHMC REPLACE ZE1-CA(H2 | OM | 11/29/2005 | 11/29/2005 | | | 1314.24 | 24 | | | 8 | T |

### 3.2.1 Assumptions

The maintenance staff file the WO entries in the database. Each maintenance personnel has a style for filling a WO and this makes it complicated to categorize them. The WOs go through a cleaning process of identifying them as a replace/repair, no failure, minor issue, no issue, ignored, misplaced, or test. The explanation of all the categories is in Table 3.2. After the cleaning process, only two types matter for the lifetime calculation; replace/repair and no failure. The starts of the lifetimes are the completion dates of the replace/repair or no failure type of WO. The ends of the lifetimes are start dates of the replace/repair or no failure type of WO. Ending a lifetime with a replace/repair type WO identifies a complete lifetime, and ending with a no failure type identifies a right-censored lifetime (please see Section 4 for more information regarding complete and right-censored lifetimes). Overhauls WOs are in most cases a no failure type. However, in some cases, a failure occurs, and the plant chooses to replace the failed encoder in an overhaul instead, making it a replace/repair type. A python code was written to extract information from the WOs and then calculates the lifetimes.

## 3.3 Types of Encoder Errors

The main reason for the encoder error data is to determine an exact time of failure for a respective component. This information is significant for complete lifetime retrievals and component distributions. This section describes encoder errors, their usefulness to the study, and how it pertains to the components of interest.

All shaft encoder data is read and evaluated by the Shaft Encoder Check (SECHK) task via the multiplexer. The purpose of this task is to error check the shaft encoders and their

Table 3.2: Filtering Logic For Classifying WO

| **WO Type** | **Description** |
|---|---|
| Replace/Repair | Part is replaced or repaired to good as new due to failure. |
| No Failure (Replace) | No failure has occurred, however the part is replaced or repaired to good as new. |
| Minor Issue | Minor issue was found with the component, simple repair was performed and will be considered a non-failure. |
| No Issue | No issue was found with the component per WO description and/or notes (no failure). |
| Ignored | WO is deemed not important for an identified reason, this reason is documented within the comment section of the WO. |
| Misplaced | The WO is categorized within a different component number then identified within the WO description and notes (no failure). |
| Test | WO describes tests performed on specified components (no failure). |

respective buses. The errors from the encoder component divide into two major types, single card/encoder errors and bus errors. Examining a single encoder's data and data from many encoders from a particular bus determines single card errors and bus errors, respectively [4]. The point of interest for this study is in the first type of errors (single card/encoder errors). There are four possible single card errors;

1. redundant error,
2. encoder removed error,
3. bus mismatch error, and
4. sequence jump error.

### 3.3.1 Redundant Error

A redundant error is only valid with paired encoders that are generally in use with the bridge and carriage encoders. The components in this study do not have paired encoders. This error, therefore, did not log and gave no information to the analysis.

### 3.3.2 Encoder Removed Error

The encoder removed error logs when an encoder reading returns zero, which is generally unusual. For the magazine encoder, a zero reading is possible and the test is modified so that an error logs with a zero reading and a considerable sequence jump or logged sequence jump error. An analysis of the error data identifies that it logs primarily during the maintenance staff's removal or reinstatement of encoders. This error logging otherwise indicates some form of electrical short during operation via wire failure or ingress of water, for example. Given the point for using encoder error data, both of these reasons for this specific error do not help determine an exact failure date, and the remainder of this study does not consider it. However, this error could help confirm removal and installments of encoders given the WO start and end dates. Although prevalent during the removal and install of encoders, it is not reliable. This data is mainly disregarded, given its unreliability and the reliability of clamp-up data.

### 3.3.3 Bus Mismatch Error

The bus mismatch error and the sequence jump error are the two most common errors when looking at the four encoders of interest. Bus mismatch error is logged on an encoder when the data between bus 1 and 2 do not match and surpass a preset limit. Both buss are read virtually simultaneously and should be close to identical at all times. This error is not sufficient in determining which bus contains valid data. In most cases, this error will occur first, and other related errors will come after. The correlated errors, to the initial bus mismatch error, determine which bus, if any, contain any valid data [4]. This error is more likely to indicate electrical failure or environmental factors (dust, water, etc.) on either bus. If the encoder fails and a bit(s) produces false readings, this error would not trip given both buss would still read the same. For this error to indicate a failed encoder one of

the buses would need to breakdown simultaneously with the false reading. Trend plotting the bus mismatch error with WO data further confirms its lack of consistent usefulness in determining encoder failures. Comparing the two most common error reliability trend plots with correlating WO data further confirms this diagnosis. The bus mismatch error data is, therefore, disregarded.

### 3.3.4 Sequence Jump Error

The sequence jump error is when the current reading from the encoder to the succeeding reading change beyond expectation. This error can log for either bus 1 or 2. The two main causes for this error are the encoder moving faster than expected or a bad data bit as identified by a tech document provided by General Electrical-Hitachi Nuclear Energy Canada Inc. (GEH-C) [4]. When an encoder fails, the selected output value freezes at the last valid data for the encoder. It will remain frozen until the encoder returns to normal operation or the operator disables error logging for the encoder [4]. The error can log and return to normal operation hundreds of times in a couple of hours. The operators can mitigate the nuisance of repetitive error logging by disabling error logging. Encoder errors can also log due to associating components failing or minor issues described in the section above. Plotting errors with correlating WOs provide the necessary insight to confirm error trends, given the other possibilities. The disabling of error logging also means there might not always be a definitive trend to follow before the WO. The possibility of an associating component or a minor issue being the cause of the error means a definitive failing trend does not always indicate a failed encoder and can not be assumed. The WO is therefore imperative to confirm any trend discovered. The sequence jump error logs independently on either bus 1 or 2. Therefore, a sequence jump error logging on one bus can occur without logging on the other. One bus logging a sequence jump error can aid bus mismatch error determination of which bus holds valid data; whichever bus logged is the bus with invalid data. However, if both buses log a sequence jump error, the correct bus would not be possible to determine. Both buses logging a sequence jump error is the most indicative of a bad bit(s) or failed encoder and is the most common within the data. The bus mismatch error and the sequence jump error can occur together in a failing encoder. With a failed bit, the Grey code of the encoder and the ambiguity of the encoder's readout are affected and allows for the buses to potentially read differently (see Section 2.1.6). The bus

mismatch error shows its inconsistency by comparing error trends with the sequence jump error leading to work order numbers. The sequence jump error shows a definitive failing trend accompanied by a failed encoder replacement order. Plotting the bus mismatch error shows inconclusive results of a failed encoder and for an exact failure date.

The sequence jump error documentation identifies it as the error for identifying a failed bit(s). An error trend plot of the sequence jump error correlated with the respective WO dates; confirms its ability to identify a failed encoder. The WO data identifies failed encoders, and the sequence jump error data identifies the exact dates of failure. For each complete lifetime, the specific date of failure or change point is vital to obtain for accurate lifetimes and component lifetime distributions (further discussed in Section 3.4 and Chapter 4). The NHPP models and the bit mismatch patterns also use sequence jump error for accurate tracking of the encoder reliability in Chapter 5 and Chapter 6 respectively.

### Data Processing Procedure

The encoder outputs a 12-bit length Grey string (13 digits in total), and the computer converts this value to an octal number for the encoder error logging. The current and previous bus values for both bus 1 and 2 need conversion to the original Grey values for assessment of the bit mismatch patterns in Chapter 6. However, the usual octal to Grey conversion will not work on this data. Although the encoder is outputting a 12-bit grey code value to the computer, computers do not understand Grey, and it perceives it as a binary number. Therefore, the conversion needs to be octal to binary to regain the original values outputted from the encoder, and this allows for a proper analysis of the bit mismatching. Table 3.3 shows an example of the conversion on each respective value. A Python code was written to process the encoder error data for this study.

Table 3.3: Octal to Grey (Binary) Conversion Example from Encoder 1 Head 1 Previous Bus 1

| **Logged Octal Value** | **Original Encoder Grey Value** |
|---|---|
| 012100 | 1010001000000 |

## 3.4 Clamp-Ups

In reliability modeling, a measure of equipment usage is needed to define its lifetime. For continuously operating machines lifetime is quantified in terms of hours, days, months, years, etc. However, FM encoders are used only when a fueling machine is either pushing a new fuel bundle in a channel or receiving an irradiated buncle. Such discrete operations of FMH are referred to as "clamp-ups", which are recorded in log files of the fuel handling system. Therefore, an encoder's lifetime is defined in terms of the cumulative number of clamp-ups from the time of installation to the time of replacement.

The clamp-ups further aids the encoder error data and extraction of exact failure dates for complete lifetimes. The error data has a CSF flag value for each error logging. The CSF flag value is the clamp-up count when the error logs. After an overhaul of the encoder components, the maintenance staff reset the CSF flag value to zero and can aid in further confirming the occurrence of an overhaul. The CSF flag value also allows for proper grouping of encoder errors for further analysis. Grouping errors by the metric day posed a problem when the same error would occur over several days, or several different errors would log in one day. Grouping the errors by CSF flag value resolves the issue because the value freezes on the failures and is not constrained to the day. A change in the CSF flag value indicates the encoder operated without error for the difference. The error trends are now more apparent and accurate. Extracting the exact failure date of an encoder is very important for the lifetime retrieval of a complete lifetime. Finding the starting point or change point of the failing trend can become complex when looking at the data based on days. On the other hand, the clamp-up data is certain when identifying errors that have occurred closer together, allowing the retrieval of the change point to become a trustworthy process.

Furthermore, the clamp-up data is an essential tool for checking assumptions on WO data and overhaul dates. The clamp-up data is very reliable information, unlike the WO data which has human error involved and the encoder error data, which carries a lot of assumptions on the meaning of the errors. The clamp-up data can reliably identify when an encoder is working or not. Making it easy to confirm overhaul dates in correlation with CSF flag resets or other WO maintenance.

## 3.5 Applications of Data

Table 3.4 shows the utilization of the historical data. Solving for the lifetime distributions produces lifetimes of each respective encoder over each respective head. The lifetimes identify intervals in the encoder error data and aid the stochastic process modelling in Chapter 5 and the probabilistic assessment of the bit mismatch patterns in Chapter 6.

Table 3.4: The use of the Historical Data throughout this Study

| | **Historical Data Type** | | |
|---|---|---|---|
| **Analysis** | **Work Order** | **Encoder Error** | **Clamp-Ups** |
| **Lifetime Distribution** | ✓ | ✓ | ✓ |
| **Stochastic Process Model** | | ✓ | ✓ |
| **Bit Mismatch Patterns** | | ✓ | |

### Lifetime Distribution

The lifetime distributions use the WO data to uncover the replacement dates and the lifetimes. In the case of complete lifetimes, the encoder error data identifies the exact failure date by following the error trend before a failed encoder. Finally, the lifetimes provide the dates to calculate the total clamp-ups over each lifetime, respectively.

### Stochastic Process Model

The stochastic process models use the encoder error data and separate it based on the intervals found in the lifetime retrieval process. The errors in each respective interval receive a clamp-up value based on the clamp-ups that occurred from their interval start. This value is from the clamp-up data.

#### Probabilistic Assessment of Bit Mismatch Patterns

The bit mismatch assessment also separates the encoder error data based on the intervals from the lifetime retrieval process. Then the bit mismatching analysis occurs based on the encoder error data seen in each respective interval.

## 3.6 Summary

In this chapter, different types of historical encoder operating data from the encoder are described.

The WO data involves the maintenance information on each respective encoder from the 32 within the study. Each WO receives a type, as shown in the filtering logic Table 3.2, and these types aid in the lifetime retrieval process in the next chapter. These types also aid in further analyzing the encoder errors and clamp-ups.

There are four types of encoder errors logged for each encoder. A discussion on their respective relevancy in the study occurred, and it found the sequence jump error to be the only encoder error of intrinsic value to the study. For this reason, it is the only encoder error utilized throughout the rest of the analyses. Also, the processing procedure of this data type for Chapter 6 is determined.

The chapter then describes clamp-ups and their importance in calculating the reliability of the encoder and in being able to discuss and make assumptions on the results from the analyses. The clamp-up data also aids in determining overhaul intervals of the components.

Finally, the chapter discusses the aforementioned historical data types utilization on the chapters within the study. A summary of this utility found in Table 3.4.

# Chapter 4

# Lifetime Distribution

## 4.1 Introduction

This section presents the statistical analysis of historical WO data for the estimation of lifetime distribution of FM encoders. The MLE method is applied to estimate parameters of the candidate probability distributions, e.g., the Weibull and lognormal distributions. From WO data, complete and censored lifetime histories were extracted. Figure 4.1 illustrates the types of lifetime data, namely, complete, right-censored, and interval-censored, with the red dot in the figures indicating a failed encoder. The WO data identifies two types of replacements of the encoders; corrective replacement and preventive replacement at the time of head maintenance. The encoder errors allow for the faulty WOs to become complete lifetimes and increase the accuracy of the model (see Section 3.3). The right-censored data occurs on the replacement of an encoder before its failure. The MLE is used due to its versatility in dealing with censored data in the parameter estimations.

## 4.2 Probability Distribution Models

The Weibull distribution is a preferred model for the component lifetime distribution, since the Weibull distribution is well-known in the lifetime analysis of engineering components when describing ageing and provides diverse shapes for product life modelling. The Weibull distribution Probability Density Function (PDF) is as follows:

$$f(x) = \frac{\alpha}{\beta}\left(\frac{x}{\beta}\right)^{\alpha-1} \mathrm{e}^{-\left(\frac{x}{\beta}\right)^{\alpha}}, x, \alpha, \beta > 0. \tag{4.1}$$

$\alpha$ is the shape parameter and reflects the ageing and $\beta$ is the scale parameter. $\beta$ is called the "characteristic life," which corresponds to the time at which 63.2 % of the components

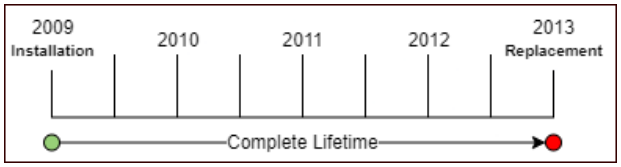


(a) Complete Lifetime

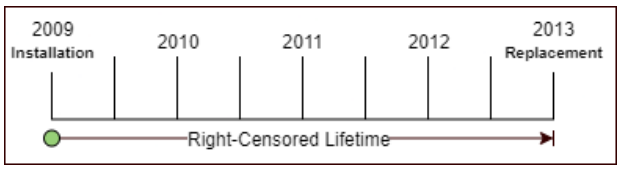


(b) Right-Censored Lifetime

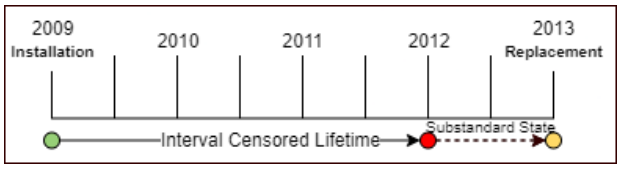


(c) Interval Censored Lifetime

Figure 4.1: Lifetime Datatypes

will fail [5] ($\alpha$ and $\beta$ are only positive values and make it suitable for a life [6]). Two special cases exist within the Weibull distribution when $\alpha = 1$ or $\alpha = 2$; becoming the exponential distribution or the Rayleigh distribution, respectively [6]. In lifetime modelling, the continuous random variable is the lifetimes of the components, and the PDF curve represents the probability content of the lifetimes. The area under the PDF, given a range of the lifetime, denotes the probability of this being the life of the component, with the total area under the PDF equalling 1.

The Lognormal distribution is used for comparison, and the PDF is as follows:

$$f(x) = \frac{1}{\sqrt{2\pi}\zeta x} \mathrm{e}^{-\frac{(\ln(x)-\lambda)^2}{2\zeta^2}} \tag{4.2}$$

where $\zeta$ and $\lambda$ are the shape and scale parameters, respectively.

### Reliability Analysis Equations

The Cumulative Distribution Function (CDF) of the Weibull distribution is shown in Equation 4.3. The CDF is the probability of the component failing before a specific clamp-up count.

$$F(x) = 1 - \mathrm{e}^{-\left(\frac{x}{\beta}\right)^{\alpha}}, x \geq 0 \tag{4.3}$$

Inverting the CDF gets the percentile equation, where $x_p$ is the $p^{th}$ percentile value. Equation 4.4, therefore, returns the quantile value and is useful for determining the median.

$$x_p = \beta[-\ln(1-p)]^{\frac{1}{\alpha}} \tag{4.4}$$

The mean time to failure (MTTF) is another measure of reliability. The mean of the Weibull distribution is as follows:

$$\mu = \beta\Gamma\left(1 + \frac{1}{\alpha}\right) \tag{4.5}$$

Calculating the Coefficient of Variation (COV) of the lifetime distribution involves dividing the standard deviation by the mean. The COV is the measure of randomness in the data and is a dimensionless quantity valuable when comparing different datasets contingent to the central location and dispersion [5]. Equation 4.6 identifies the variance for the Weibull distribution.

$$s^2 = \beta^2\left[\Gamma\left(1 + \frac{2}{\alpha}\right) - \Gamma\left(1 + \frac{1}{\alpha}\right)^2\right] \tag{4.6}$$

Therefore, the reliability curve for a Weibull distribution is as follows:

$$R(x) = 1 - F(x) = \mathrm{e}^{-\left(\frac{x}{\beta}\right)^{\alpha}} \tag{4.7}$$

The reliability represents the probability of no failure up to the given clamp-up count, $x$. The hazard rate is the instantaneous probability of failure of the component at age $x$.

The derivation is from taking the PDF over the reliability function, Equation 4.8 is the calculation output.

$$h(x) = \frac{\alpha}{\beta}\left(\frac{x}{\beta}\right)^{\alpha-1} \tag{4.8}$$

$h(x)$ increases with clamp-ups for an $\alpha > 1.0$ and decreases with time when $\alpha < 1.0$ and for a $\alpha = 1.0$ (the exponential distribution), the failure rate is constant [6]. The Weibull hazard rate can also depict three types of component ageing given the estimated $\alpha$ parameter is greater than one [5].

- $1.0 < \alpha < 2.0$ the hazard rate is increasing at a decreasing rate.
- $\alpha = 2.0$ the hazard rate is increasing at a constant rate
- $\alpha > 2.0$ the hazard rate is increasing at an increasing rate

These abilities of the Weibull distribution made it well-liked for life data analysis.

## 4.3 Maximum Likelihood Method

The Maximum Likelihood Method is an approach that uses a function maximization algorithm to find the distribution parameter(s) that maximize the likelihood of obtaining the data set. The maximization of the log-likelihood function is done instead for convenience, given the likelihood function's multiplication. For a probability density function with two or more parameters, the likelihood function becomes given a Weibull distribution and where $k$ is total number of complete lifetimes, $f(t)$ is the two-parameter PDF, and $t_i$ is the $i^{th}$ complete lifetime:

$$L\left(t_1, ..., t_k; \alpha, \beta\right) = \prod_{i=1}^{k} f\left(t_i; \alpha, \beta\right) \tag{4.9}$$

However, the datasets contain right-censored data, and the likelihood function needs to be changed accordingly. Including the right-censored data, the equation becomes:

$$L\left(t_1, ..., t_k, t_{k+1}, ..., t_N; \alpha, \beta\right) = \prod_{i=1}^{k} f\left(t_i; \alpha, \beta\right) \prod_{j=k+1}^{N} R\left(t_j; \alpha, \beta\right) \tag{4.10}$$

Where $N$ is the total number of right-censored lifetimes, $R(t_j)$ is the reliability function, and $t_j$ is the $j^{th}$ right-censored lifetime. Taking the logarithm of the likelihood function, it becomes:

$$\ln L\left(t_1, ..., t_k, t_{k+1}, ..., t_N; \alpha, \beta\right) = \sum_{i=1}^{k} \ln f\left(t_i; \alpha, \beta\right) \sum_{j=k+1}^{N} \ln R\left(t_j; \alpha, \beta\right) \tag{4.11}$$

Maximizing simultaneous equations, shown in Equation 4.12, allow for the retrieval of the Weibull parameters of each data set.

$$\frac{\partial \ln L\left(t_1, ..., t_k, t_{k+1}, ..., t_N; \alpha, \beta\right)}{\partial \alpha} = 0, \frac{\partial \ln L\left(t_1, ..., t_k, t_{k+1}, ..., t_N; \alpha, \beta\right)}{\partial \beta} = 0 \tag{4.12}$$

## 4.4 Results

After the lifetimes retrieval, a python code outputs the lifetime model, failure rate curve, reliability curve, and associating statistics.

### 4.4.1 Distribution Parameters

Table 4.1 is a summary of the datasets for all four components within this study. As shown below, the encoder MR's data is almost all right-censored.

Table 4.1: Summary of Time-To-Failure Data

| Encoder | Lifetime Data Type | No. of Data Points | Sum of Lifetimes (Clamp-Ups) | Average (Clamp-Ups) |
|---|---|---|---|---|
| CA | Complete Lifetime | 35 | 45854 | **1310.11** |
| | Right-Cens. Lifetime | 32 | 57859 | **1808.09** |
| | Total Lifetime | 67 | 103713 | **1547.96** |
| CR | Complete Lifetime | 7 | 12814 | **1830.57** |
| | Right-Cens. Lifetime | 35 | 96349 | **2752.83** |
| | Total Lifetime | 42 | 109163 | **2599.12** |
| RA | Complete Lifetime | 28 | 53411 | **1907.54** |
| | Right-Cens. Lifetime | 34 | 59129 | **1739.09** |
| | Total Lifetime | 62 | 112540 | **1815.16** |
| MR | Complete Lifetime | 3 | 1355 | **451.67** |
| | Right-Cens. Lifetime | 32 | 105251 | **3289.09** |
| | Total Lifetime | 35 | 106606 | **3045.88** |

MLE results are given in Table 4.2 and shows the calculation of the respective MTTF and the calculation of the COV and median on the datasets or Time-to-Failure (TTF) data. A lognormal distribution has also been fitted to the respective datasets using the MLE method and is for comparison with the Weibull distribution. The lognormal parameters and metrics are also shown in the same table below.

### 4.4.2 Goodness of Fit with Cumulative Hazard Plots

Wayne Nelson in [7] provides a method for plotting the sample CHF to approximate the true function called hazard plotting. Hazard plotting was developed for analysis on multiply censored data and can better appropriate the goodness of fit of the models than probability paper plotting, given this data present. First, the hazard function can be found by Equation (4.13) and then the corresponding CHF can be found by equation (4.14) shown below.

$$h(x) = f(x)/(1 - F(x)) \tag{4.13}$$

Table 4.2: MLE Parameter Results & Distribution Metrics

| Encoder | Distribution Type | Shape Parameter | Scale Parameter | MTTF (Clamp-ups) | COV TTF | Median TTF |
|---|---|---|---|---|---|---|
| CA | Weibull | 0.95 | 3011.31 | 3,083.32 | 1.0542 | 2,046.59 |
| | Lognormal | 1.46 | 7.55 | 5,544.03 | 2.7478 | 1,895.96 |
| CR | Weibull | 1.18 | 12446.79 | 11,772.61 | 0.8536 | 9,112.60 |
| | Lognormal | 1.45 | 9.31 | 31,571.73 | 2.6667 | 11,085.41 |
| RA | Weibull | 1.11 | 3843.92 | 3,698.08 | 0.9022 | 2,763 |
| | Lognormal | 1.72 | 8.04 | 13,579 | 4.2389 | 3,117.84 |
| MR | Weibull | 0.52 | 275184.82 | 509,670.39 | 2.1063 | 136,387.68 |
| | Lognormal | 3.30 | 12.20 | 45,577,240.60 | 229.18 | 198866.619 |

$$H(x) = \int_{-\infty}^{x} h(x)\,dx = -ln(1 - F(x)) \tag{4.14}$$

For the Weibull distribution case, the cumulative distribution equation is shown by (4.3) and with it the corresponding Weibull hazard function equation becomes;

$$h(x) = \frac{\alpha}{\beta^{\alpha}} x^{\alpha-1}, x > 0 \tag{4.15}$$

The Weibull distribution is an exponential distribution and has a constant failure rate and, therefore, its CHF equation becomes;

$$H(x) = (\frac{x}{\beta})^{\alpha}, x > 0 \tag{4.16}$$

Wayne Nelson continues to present within [7] a basic method for hazard plotting multiply censored data. It begins by taking the reverse rank of the failure times and taking the hazard and cumulative hazard values for complete lifetimes. The hazard value is taken as the inverse of the reverse rank and the cumulative hazard value is the sum of the hazards values up to the respective failure time entry. For the Weibull hazard plot, the ln is taken for the failure time and cumulative hazard value and plotted with the ln of the cumulative hazard value on the x-axis and the ln of the failure time on the y-axis. For the Lognormal

hazard plot, the percentile value of $1 - e^{cumulativehazardvalue}$ is found using the Normal distribution percentile function ($x^p$) and is on the x-axis and the ln of the failure times is on the y-axis. For the Normal hazard plot, the percentile value of $1 - e^{cumulativehazardvalue}$ is again on the x-axis and the failure times are on the y-axis. The hazard plots are shown by Figures 4.2, 4.3, and 4.4 for encoder CA, CR, and RA, respectively.

From the hazard plots, estimates for the shape and scale parameter can be found with the line of best fits. With the line of best fit on the Weibull plots, estimates of the Weibull distribution shape and scale parameters are made by dividing one by the slope and taking the exponential of the y-intercept, respectively. The shape and scale parameters estimates are found by the slope and y-intercept, respectively, with the Lognormal distribution cumulative hazard plot. Table 4.3 identifies the line of best-fit estimates for the shape and scale parameters for the Weibull and Lognormal distributions from the CHF method. The table also contains the MLE method estimates for comparison. Per the line of best-fit estimates, encoder CA and RA are very close to being reduced to an exponential distribution, given their Weibull shape parameters close approximation with 1. Encoder CA and RA also associate well with the Weibull distribution; however, encoder CA seems to also associate well with a lognormal distribution, while encoder RA does not. Encoder CR also associates reasonably with a Weibull distribution but slightly better with a lognormal distribution. For these reasons the Weibull distribution is chosen as a good fit of the data and was taken as the distribution of choice for the encoders. Between the methods for estimation, the MLE parameters were chosen for plotting in the following sections and for the applications chapter.

### 4.4.3 Lifetime Models

Inputting the Weibull parameters from Table 4.2 to the Weibull PDF from Equation 4.1 outputs the Weibull lifetime distribution models for each component. Inputting the Lognormal parameters from Table 4.2 to the Lognormal PDF from Equation 4.2 outputs the Lognormal lifetime distribution models for each component. The red curve on each figure is the estimation of the respective Weibull model and the green curve is the estimation of the respective Lognormal model. Figure 4.5, 4.6, and 4.7 is the models of encoder CA, CR, and RA, respectively. Encoder MR plots have been removed due to insufficient data.

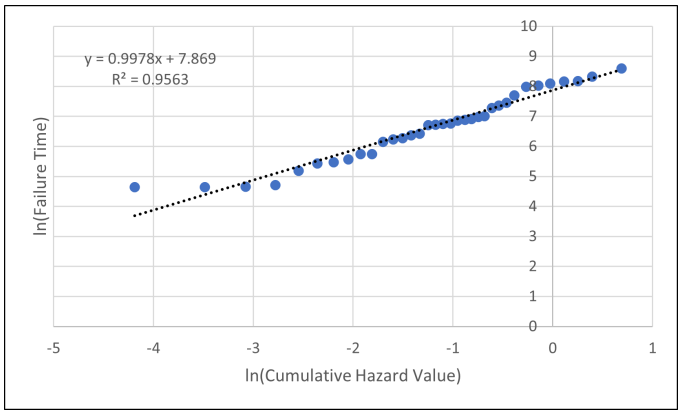


(a) Weibull

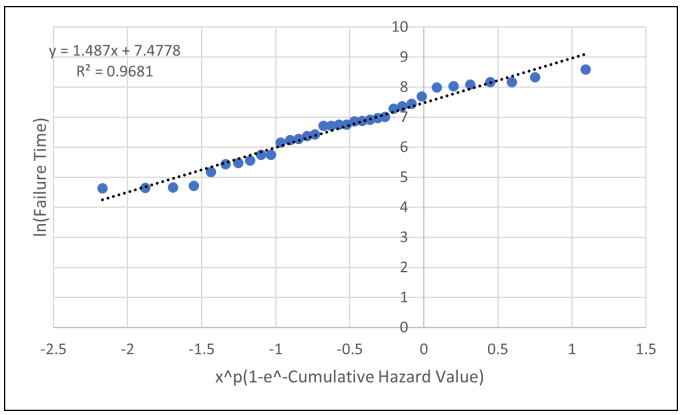


(b) Lognormal

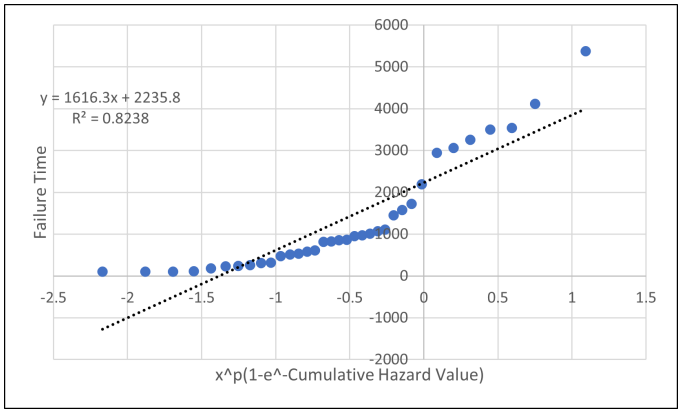


(c) Normal

Figure 4.2: Encoder CA Cumulative Hazard Plots

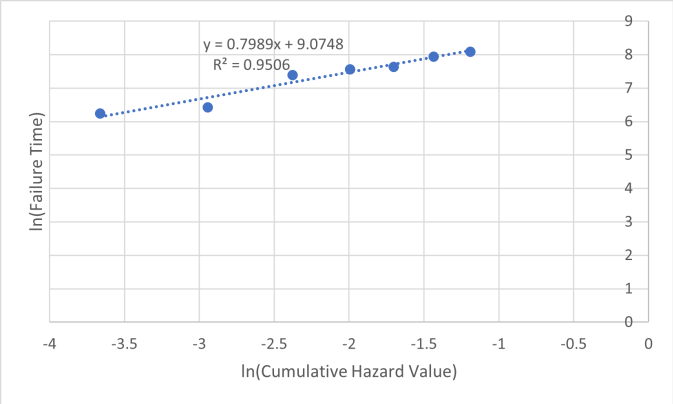


(a) Weibull

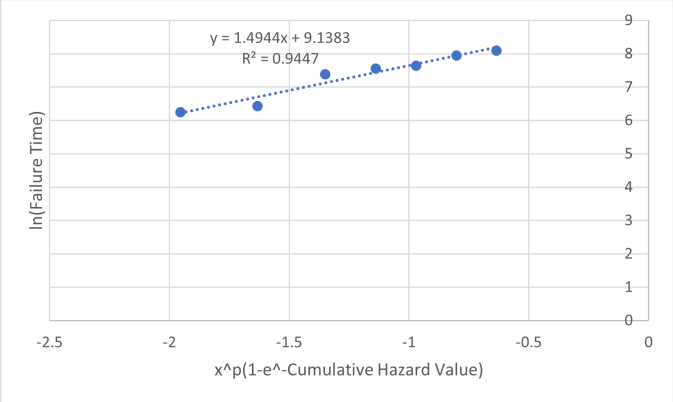


(b) Lognormal

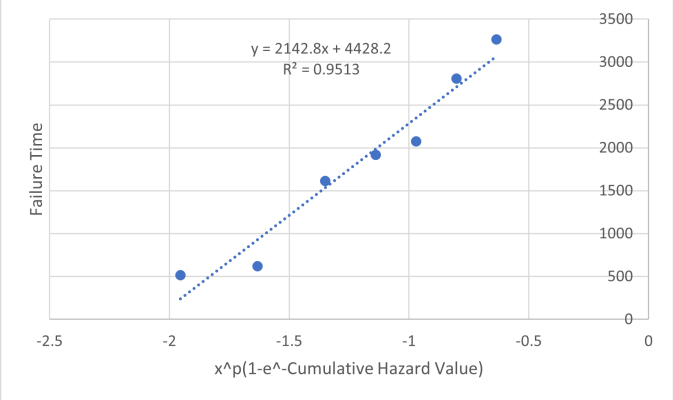


(c) Normal

Figure 4.3: Encoder CR Cumulative Hazard Plots

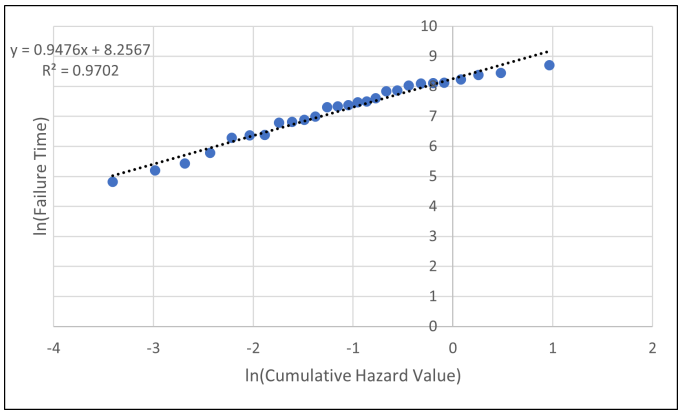


(a) Weibull

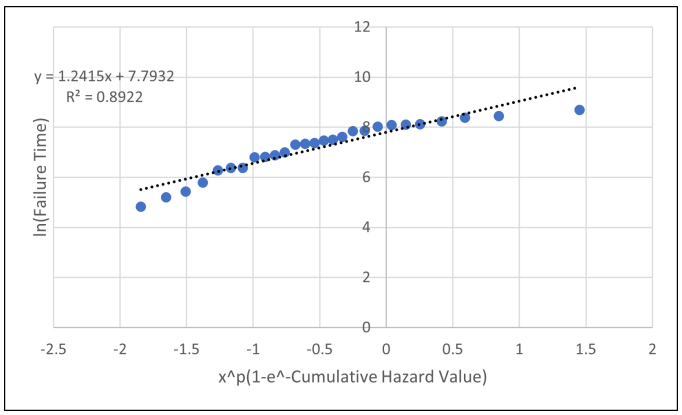


(b) Lognormal

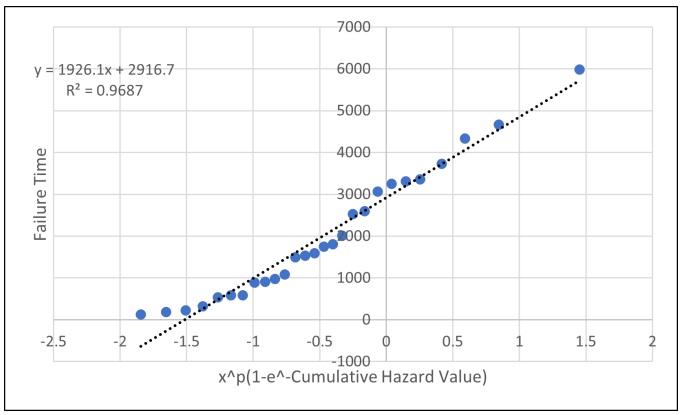


(c) Normal

Figure 4.4: Encoder CA Cumulative Hazard Plots

Table 4.3: Estimates of the CHF and MLE methods for Weibull and Lognormal Distributions

| Encoder | Method | Distribution | Shape | Scale |
|---|---|---|---|---|
| CA | CHF | Weibull | 1.002 | 2614.949 |
| | | Lognormal | 1.487 | 7.478 |
| | MLE | Weibull | 0.95 | 3011.31 |
| | | Lognormal | 1.46 | 7.55 |
| CR | CHF | Weibull | 1.252 | 8732.439 |
| | | Lognormal | 1.494 | 9.138 |
| | MLE | Weibull | 1.18 | 12446.79 |
| | | Lognormal | 1.45 | 9.31 |
| RA | CHF | Weibull | 1.055 | 3853.357 |
| | | Lognormal | 1.242 | 7.793 |
| | MLE | Weibull | 1.11 | 3843.92 |
| | | Lognormal | 1.72 | 8.04 |

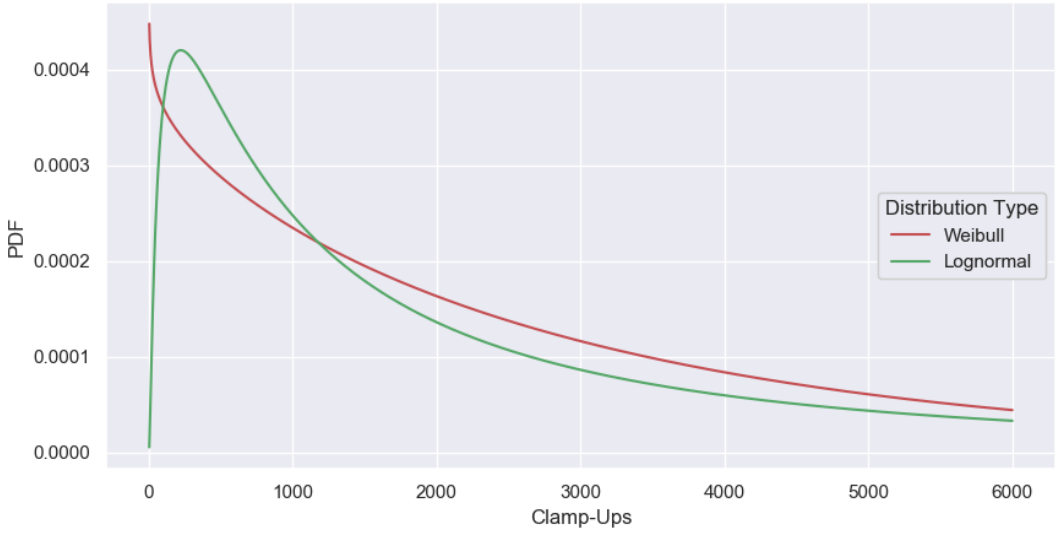


Figure 4.5: Lifetime Models for Encoder CA

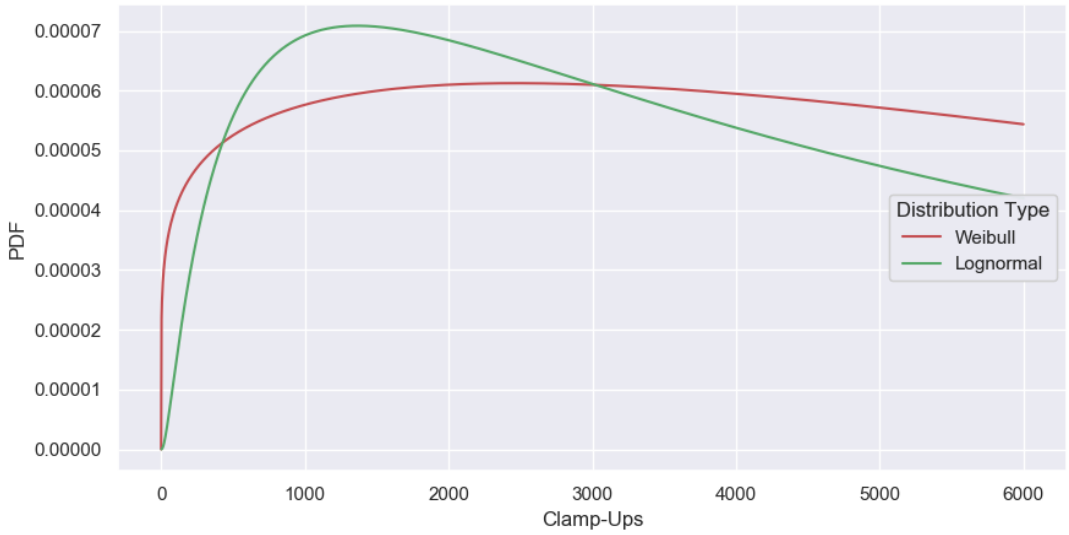


Figure 4.6: Lifetime Models for Encoder CR

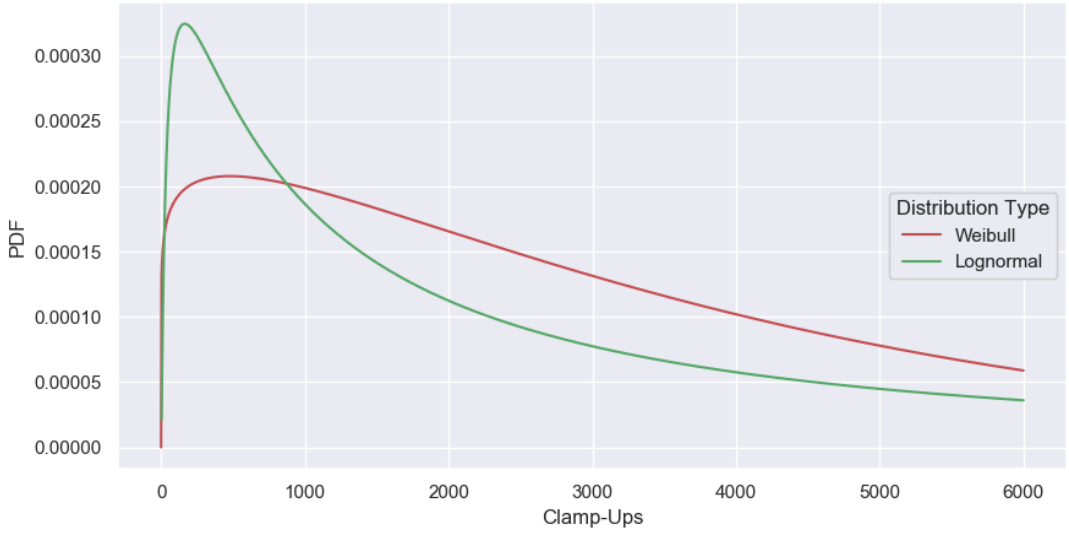


Figure 4.7: Lifetime Models for Encoder RA

### 4.4.4 Reliability Curve

The reliability curve identifies the probability of no failure in an interval $(0, t)$, where $t$ is the maximum clamp-ups for the interval and Equation 4.7 defines the reliability for the Weibull distribution. Figure 4.8 depicts the reliability of each encoder with an interval of $(0, 10,000)$ clamp-ups using the Weibull distribution and the MLE parameters. With the desired overhaul interval of $5,000$ clamp-ups for the FM head system, the reliability that the encoders survive is approximately 19.83%, 71.01%, and 26.21 % for encoder CA, CR, and RA, respectively.

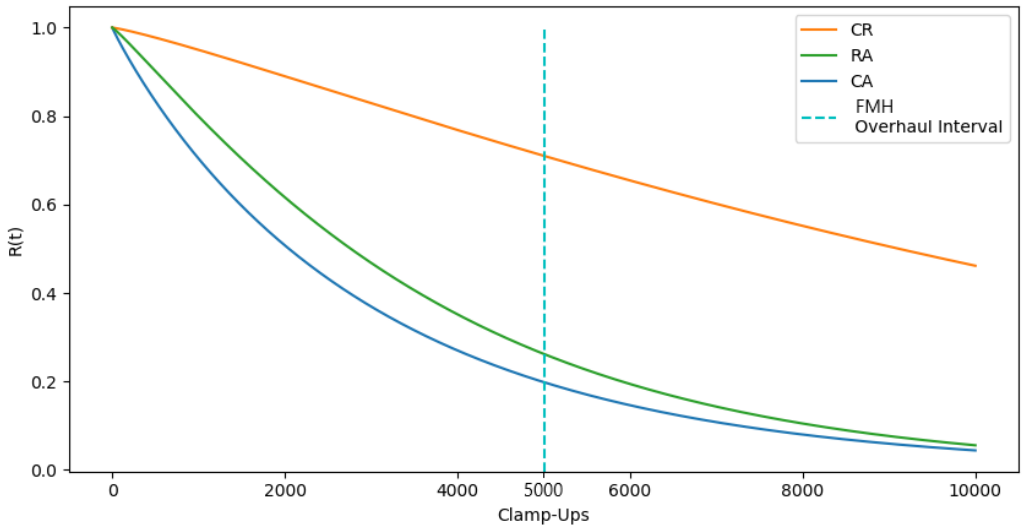


Figure 4.8: Reliability Curves for the three encoders

### 4.4.5 Hazard Rate Plot

Figure 4.9 shows the hazard rate curve of each encoder, with a clamp-up range of $(0, 10,000)$. The hazard curves are calculated using the MLE paramters for the Weibull Distribution. With the $\alpha < 1.0$ encoder CA is prone to early failures, and with an $\alpha > 1.0$ encoder CR and RA are prone to failure with age. Meaning, with encoder CA, the focus should be towards their early life, and with encoder CR and RA, the focus should be on the wear-out

phase in terms of failure. However, encoder CA, CR, and RA are close to having a constant failure rate with $\alpha \approx 1.0$, meaning their models are close to an exponential distribution.

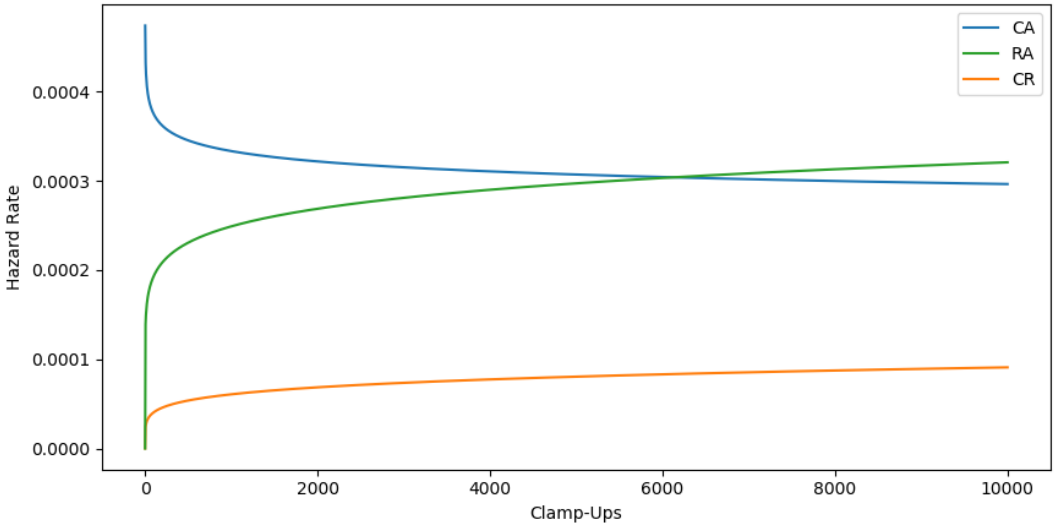


Figure 4.9: Hazard Rate Plots for the three encoders

### 4.4.6 Discussion

This chapter describes the creation of lifetime distributions, failure rate plots, and reliability curves for each encoder. Furthermore, the MLE algorithm estimated the Weibull and lognormal distribution parameters, which allow for the calculation of the MTTF, COV, and median of each respective model. Goodness of fit models are also produced using the cumulative hazard function (CHF) plotting technique for censored data, where the Weibull distribution is confirmed viable.

With encoder CR the MTTF and median values are large given the large $\beta$ parameter estimation by the MLE method. The Encoder CR dataset has low percentage of complete lifetimes, which has drastically affected the results and is concerning when trying to make reliability assumptions for these encoders. Potentially a similar accelerated degradation test might be needed to be implemented as described in [8] to confirm these results or to provide the data necessary to complete a lifetime analysis on encoder MR.

On the other hand, encoder CA and RA datasets seem to provide an accurate model with an approximately even distribution of type of lifetimes. The lifetime distribution models and the metrics make sense. Encoder CA and RA models identify MTTFs of approximately 3,083 and 3,698 clamp-ups, respectively. Given the low reliability for encoder CA and RA (19.83% and 26.21%) to survive without failure to $5,000$ clamp-ups, the encoders should have an overhaul before the FM head overhaul interval.

## 4.5 Summary

In summary, lifetime distributions for encoder CA, CR, and RA were found and fitted to their respective datasets using the MLE and CHF methods. The CHF method was used to show goodness of fit of the Weibull distribution when compared to the Lognormal and Normal distribution instead of probability paper plot given the censored data, while the MLE parameters were used for the final plotting of the lifetime distributions. The primary distribution is the Weibull distribution, and the lognormal distribution is fitted and shown for comparison. The Weibull distribution MLE parameters are then used to create reliability curves and hazard rate plots. The reliability curve shows that encoder CA and RA have a 19.83% and a 26.21% reliability to make it to the system desired overhaul interval of 5,000 clamp-ups, while encoder CR shows a 71.01%. The lifetime distributions and this section's applications are further discussed in Chapter 7.

# Chapter 5

# Stochastic Model of Encoder Errors

## 5.1 Introduction

During the fueling operation, encoders can experience four types of errors, as discussed in Section 3.3 of the thesis. The fuel handling control computers log each occurrence of any one of these errors. With the use of this data, sequences of occurrences of encoder errors can be constructed. This chapter aims to evaluate the application of stochastic process models to determine a failed or non-failed encoder during its life. These insights, gained from probabilistic characteristics of the stochastic model, are expected to help develop health monitoring strategies for FM encoders. Such work has not been undertaken in the nuclear system's reliability literature.

Only the "sequence jump" error is analyzed in this chapter, as it is a more critical error that impairs the encoder function. Error occurrences are modelled as a Non-Homogeneous Poisson Process (NHPP), due to its "minimal repair" property. After the occurrence of a sequence jump error, the control computer resets the encoder to mitigate this error. This resetting of the encoder can be treated as a "minimal repair" action, as it does not fully renew the encoder, i.e., it does not reset the age to zero. Thus, NHPP model implies that an encoder in-service continues to age irrespective of resetting of the encoder, such that the propensity to the occurrence of errors with age does not change.

## 5.2 Processing of Error Occurrence Data

Figure 5.1 shows a graphical representation of the processing procedure put in place for this chapter. The plot shows a typical example of errors over an encoder's entire lifetime. The lifetime is indicated by the dates encapsulated by the purple vertical band and the red vertical line. The purple vertical band indicates an overhaul of a FM head system,

including the installation of a new encoder. The red vertical line signifies the date of a failed encoder and the end of its lifetime. A lifetime could also be between two overhauls or two failures or the vice-versa of the current example. A right-censored lifetime is when the life of the encoder ends with an overhaul or a contingency WO and a complete lifetime is when the life of the encoder ends with a failure WO.

The raw encoder error data is indicated on the plot as blue x's. Often the raw data can mislead in identifying failed encoders when trying to model the encoder errors. Hundreds of errors can populate for numerous reasons in the middle of an encoder's lifetime that could be regarded as a failed encoder. However, when referencing the WO data, it is clear it was not a failed encoder that caused the errors, or it was a minor issue. Furthermore, upon looking at the clamp-up number, the error occurrence can identify if the system moved ahead and continued to fail or it continued to fail in the same position. For noise reduction in the error data, the errors are grouped based on their clamp-up number within the respective lifetime; this is shown in the plot as the orange x's. Clamp-up number grouping is done instead of date grouping due to its overall relevancy to this study and that errors with the same clamp-up number can span multiple days. This process of grouping errors by clamp-up number can be hereafter be described as unique faults. Taking the unique faults of the encoder error data allows for independent events for modelling and will increase its overall accuracy and usefulness in determining and analyzing failed encoders. The plot also identifies the point of failure for a more accurate calculation of a complete lifetime via the green x's, which was used in Chapter 4. The value of this processing is further discussed and analyzed below.

With the processing techniques described above, the historical example shown in Figure 5.1 has been processed. For stochastic modelling, clamp-up number grouped data is taken (the orange x's) for each historical lifetime within the indicated time range with 15 or more errors for encoder CA, CR, and RA. Encoder MR is removed from this chapter of the study due to lack of data, for this encoder.

## 5.3 Parameter Estimation

Definition 33 from [9] states that *"if the testing of the repairable system stops after a predetermined number of failures say "n" then the data are said to be failure truncated.*

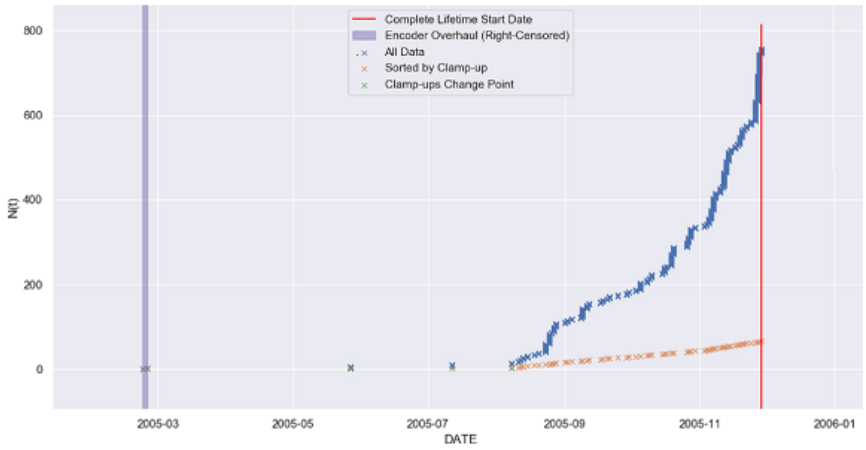


Figure 5.1: Encoder Error Sequence Jump Plot With Processing Over a Historical Lifetime

*If testing stops at a predetermined time "t" then the data are said to be time truncated."* The termination of the data collection in this study falls under the time truncated case, and this information is valuable for the statistical inference procedure for determining the parameters of $\beta$ and $\theta$ in the NHPP model. The $\beta$ parameter affects how the system deteriorates or improves over time, and $\theta$ is the scale parameter. In this case, the number of failures, $N$, is random, and clamp-ups, where the data retrieval stops, are fixed, $T_{max}$.

### 5.3.1 Point Process Estimation

Let the denotation of the observations of failures before $T_{max}$ be $T_1 < T_2 < \cdots < T_N < T_{max}$. Given the number of failures, $N$, are random, the time truncation case produces a random number of random variables at random times. Therefore, the likelihood takes into account the randomness of $N$ and the randomness of the failure times $t_1 < t_2 < \cdots < t_N$. If the observation of failures is zero before $T_{max}$, $N = 0$, the MLE for the parameters do not exist. The derivation for $\beta$ and $\theta$ is found in [9] and is as follows. The joint density of $(N, T_1, \cdots, T_N)$ is given by Equation (5.1).

$$f(n, t_1, ..., t_n) = \begin{cases} f_N(n) f(t_1, ..., t_n | n), & n \geq 0 \\ f_N(0), & n = 0. \end{cases} \tag{5.1}$$

The random variable $N$ has a Poisson distribution with mean $\left(\frac{t}{\theta}\right)^{\beta}$, so the distribution is;

$$f_N(n) = \frac{\left[\left(\frac{t}{\theta}\right)^{\beta}\right]^n \mathrm{e}^{\left[-\left(\frac{t}{\theta}\right)^{\beta}\right]}}{n!}, \qquad n = 0, 1, \cdots . \tag{5.2}$$

Given $N = n$ and the power law process, the distribution of $T_1 < T_2 < \cdots < T_n$ is therefore;

$$f(t_1, t_2, \cdots, t_n|n) = n! \prod_{i=1}^{n} \frac{\beta}{T_max} \left(\frac{t_i}{T_max}\right)^{\beta-1}, \qquad 0 < t_1 < t_2 < \cdots < t_n < t. \tag{5.3}$$

The joint density of $N$ and $T_1 < T_2 < \cdots < T_N$ is thus;

$$f(n, t_1, t_2, \cdots, t_n) = \frac{\beta^n}{\theta^{n\beta}} \left(\prod_{i=1}^{n} t_i\right)^{\beta-1} \mathrm{e}^{-\left(\frac{t}{\theta}\right)^{\beta}}, \qquad n \geq 1, 0 < t_1 < t_2 < \cdots < t_n < t \tag{5.4}$$

and

$$f(0) = \mathrm{e}^{-\left(\frac{t}{\theta}\right)^{\beta}}, \qquad n = 0. \tag{5.5}$$

The MLEs retrieval is done on the logarithm of the joint density, shown by Equation (5.6).

$$L(\theta, \beta|n, t) = n \log \beta - n \log \theta + (\beta - 1) \sum_{i=1}^{n} \log t_i - n(\beta - 1) \log \theta - \left(\frac{t}{\theta}\right)^{\beta}. \tag{5.6}$$

When at least one failure occurs before $T_{max}$ then MLEs for the parameters exist. Differentiating the log-likelihood with respect to $\beta$ and $\theta$, setting the results equal to zero, and then solving for the parameters yields the MLE equations, with $\theta$ being in terms of $\beta$ (Equation (5.7) and Equation (5.8) respectively, where $\hat{\beta}$ and $\hat{\theta}$ are the maximum likelihood estimates).

$$\hat{\beta} = \frac{N}{\left[N \ln T_{max} - \sum_{i=1}^{N} \ln T_i\right]} \tag{5.7}$$

$$\theta = \frac{T_{max}}{N^{\frac{1}{\hat{\beta}}}} \tag{5.8}$$

If $n \geq 1$ then;

$$E\left(\frac{N-1}{N}\hat{\beta}\middle|N = n\right) = \beta. \tag{5.9}$$

Thus the conditionally unbiased estimator for $\beta$ becomes;

$$\bar{\beta} = \left(\frac{N-1}{N}\right)\hat{\beta} \tag{5.10}$$

The NHPP models have an intensity function with the form;

$$\lambda(t) = \frac{\beta}{\theta}\left(\frac{t}{\theta}\right)^{\beta-1} \tag{5.11}$$

Equation (5.11) is also referred to the failure rate or rate of occurrence of failure (ROCOF) and defines the average number of failures per unit time. If $\beta > 1$, then the $\lambda(t)$ is increasing, and the failures tend to occur more frequently. If $\beta < 1$, then $\lambda(t)$ is decreasing, and the system is improving. If $\beta = 1$, then NHPP reduces to Homogeneous Poisson Process (HPP) with intensity $1/\theta$ [9].

### 5.3.2 Tests of Hypotheses

The basis of the confidence intervals and tests of hypotheses for $\beta$ is the Theorem 32 from [9]. The chi-square distribution is customary for hypothesis testing and confidence interval construction for the variance. $1-\alpha$ is the probability that the confidence interval includes the true value of $\beta$ when the data is collected and calculated in a defined way. The confidence is in the method that produces the interval rather than in the interval itself.

A wide confidence interval identifies that the information for defining the parameters is little. For this chapter the $\alpha = 0.05$, giving a probability of 95% for the confidence interval calculations in Section 5.3.3. Thus a $100(1-\alpha)\%$ confidence interval for $\hat{\beta}$ is given by Equation (5.12), shown below.

$$\frac{F^{-1}_{\chi^2}(\alpha/2; 2n)\hat{\beta}}{2n} < \beta < \frac{F^{-1}_{\chi^2}(1-\alpha/2; 2n)\hat{\beta}}{2n}. \tag{5.12}$$

Where $F^{-1}_{\chi^2}(p; 2n)$ is the inverse of the chi-square distribution with $2n$ degrees of freedom, and $p$ is the desired probability level. It is also of interest to identify if the confidence interval for $\beta$ includes or excludes the value of $\beta = 1$ (HPP). Using Theorem 32 from above again allows the construction of size $\alpha$ test of;

$$H_0 : \beta = \beta_0 \quad \text{versus} \quad H_1 : \beta \neq \beta_0. \tag{5.13}$$

Where $\beta_0 = 1$. The rule is to reject $H_0$ if;

$$\hat{\beta} < \frac{2n\beta_0}{F^{-1}_{\chi^2}(1-\alpha/2)} \quad \text{or} \quad \hat{\beta} > \frac{2n\beta_0}{F^{-1}_{\chi^2}(\alpha/2)} \tag{5.14}$$

For the time truncation case, there is no current method for obtaining exact confidence intervals for $\theta$, given the parameter has no simple interpretation.

### 5.3.3 Statistical Analysis: Example

Given the historical data available described in Section 3.2, 39 sample paths over the three encoders (CA, CR, and RA) have been chosen to be useful for modelling due to them consisting of 15 or more unique faults. The breakdown is as follows; 6, 11, and 22 sample paths for encoder CA, CR, and RA, respectively. This section will consist of a complete analysis of encoder CR's sample-path 7, which is a right-censored lifetime. The analysis will look at the raw data and the processed data for comparison. For each data set, a NHPP model will be fitted to it, which outputs a $\beta$ and $\theta$ value to be inputted into the Weibull pdf formula, shown by Equation (4.1). The NHPP model can define three types of fault trends within the data given the parameter $\beta$. With $\beta < 1$, the faults are becoming

less frequent. With $\beta \approx 1$, the faults are constant. With $\beta > 1$, the faults are becoming more frequent. A model will be described as having stationary behaviour when the $\beta$ value, based on the hypothesis test described above, can be approximated by 1. It will also be described as stationary when the null hypothesis is disregarded, and the $\beta$ value can be described as less than one. A model will be described as having non-stationary behaviour when the null hypothesis of the $\beta$ value is disregarded and can be assumed as greater than 1. The encoder error trend plots will be the cumulative number of errors, $N_f$, versus the occurrence in the encoders operating life. A dashed vertical line will also show the encoder replacement clamp-up number for the respective plot. The following example shows where the processing procedure of the encoder errors correctly indicated a non-failed encoder and will demonstrate the methods utilized on the remaining sample paths.

Table 5.1: Encoder CR sample path 7 information table for raw and unique encoder error data

| **Data Type** | **Encoder Name** | **Type of Lifetime** | **Lifetime (Clamp-ups)** | **No. of Data Points** | **beta** | **theta** | **beta >** | **beta <** |
|---|---|---|---|---|---|---|---|---|
| Raw | CR | right-cens. | 5429 | 994 | 2.9382 | 513.1967 | 0.9406 | 1.0652 |
| Unique | CR | right-cens. | 5429 | 24 | 0.716 | 67.2311 | 0.6905 | 1.5775 |

Table 5.1 shows the model calculation results for the encoder CR sample-path 7, and Figure 5.2 and 5.3 visualize them with the raw and unique data, respectively. Remember that the complete lifetime types in the summary tables show the clamp-ups until the change point and not until replacement in the lifetime (Clamp-Ups) column. The raw encoder error data for sample-path 7 has 994 data entries but only occurs at 24 clamp-up numbers, with the most errors occurring at approximately the 4300 clamp-up number. Including all the error logs when calculating the model creates a model that indicates the faults are becoming more frequent with the operation and, therefore, a failing encoder. However, as indicated in Table 5.1, the encoder did not fail and was replaced before failure creating a right-censored lifetime. Processing the errors as described above produces the unique data plot in Figure 5.3. The corresponding $\beta$ value from the unique faults model indicates the faults are constant and the encoder has not failed, which implicates with the WO and the right-censored lifetime identification from Chapter 4. Here the raw data NHPP model imply a failed encoder while the sample path was indicated as a right-censored lifetime

type. Upon processing the raw data to include only the unique faults the NHPP model indicates a more well behaved encoder that is in line with the sample paths' right-censored lifetime type. The raw data model can be defined as non-stationary, and the unique data can be defined as stationary, which matches a right-censored lifetime type.

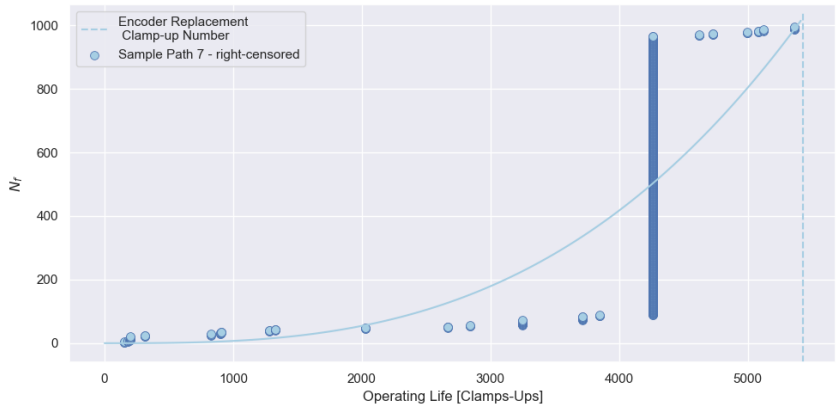


Figure 5.2: Encoder error trend using raw error data (encoder CR sample path 7)

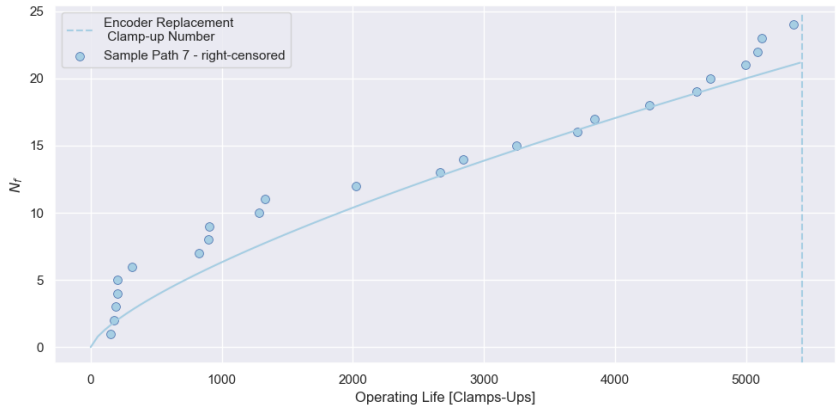


Figure 5.3: Encoder error trend using unique error data (encoder CR sample path 7)

## 5.4 Numerical Results

For each sample-path, NHPP models are fitted to both the raw and processed data. These models are split into stationary and non-stationary type, described in the above example, and separated by encoder position within the FM head. Within their encoder names, the stationary and non-stationary models are compared.

The analysis of the processing procedure involves looking at the change from the raw data model to the processed data model. In the above example in Section 5.3.3, the processed model effectively indicated a non-failed encoder. When comparing the change from raw data to processed data, two things can occur; either there is a change in interpretation between them (failed to non-failed or vice-versa), or there is no change. Furthermore, given a change in interpretation from raw to processed, it can either better implicate to the indicated sample paths' lifetime type, make the implication worse, or not change it at all. Therefore, there are four types of occurrences when comparing the raw and processed data; positive implication with no change in interpretation, positive implication with a change in interpretation, negative implication with no change in interpretation, and negative implication with a change in interpretation. A positive implication is when the lifetime type is visible in the encoder error model of the lifetime; with a constant failure rate model positively implicating to a right-censored lifetime type and an increasing failure rate positively implicating to a complete lifetime type. A negative implication occurs when the opposite occurs, with a right-censored lifetime type being modelled with an increasing failure rate and a complete lifetime type modelled with a constant failure rate. A positive implication with a change of interpretation indicates where the processing is actively effective, and a negative implication with a change in interpretation indicates an adverse change has occurred. When there is no change in interpretation, and a positive implication remains, the processing procedure was passively effective. If a negative implication remains, the processing procedure made no difference in determining a failure or non-failure. Visual examples of these four different occurrences are as follows:

#### Positive Implication With No Change In Interpretation

The positive implication involves a constant failure rate linked to a right-censored lifetime and an increasing failure rate linked with a complete lifetime. The unchanging interpreta-

tion means that the raw model indicates the same failure rate as the processed data model. Two examples are given for a right-censored and complete lifetime with sample path 14 from encoder RA in Figure 5.4 and sample-path 2 from encoder CA in Figure 5.5.

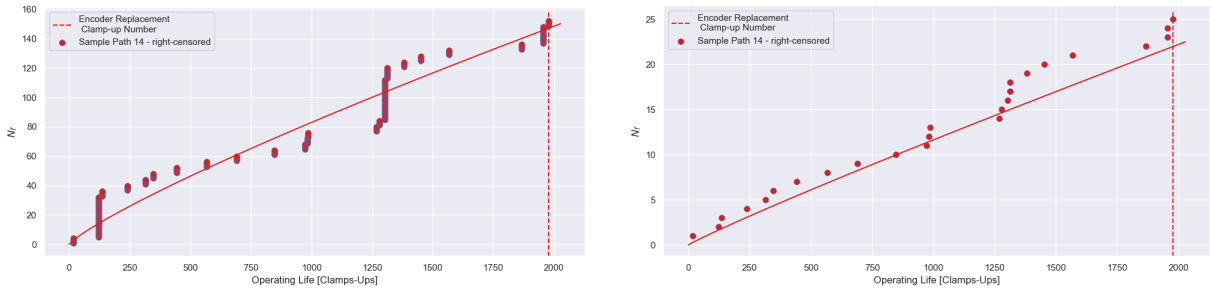


(a) Raw encoder error data (b) Processed encoder error data (unique faults)

Figure 5.4: Encoder error trend plots: encoder RA sample path 14 - right-censored lifetime

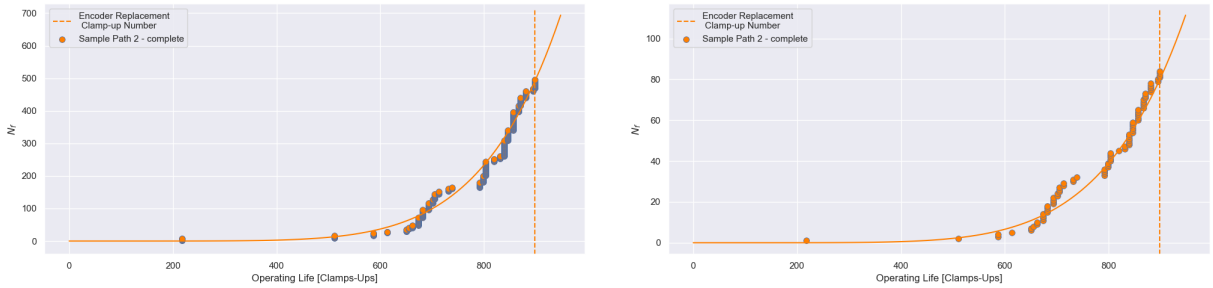


(a) Raw encoder error data (b) Processed encoder error data (unique faults)

Figure 5.5: Encoder error trend plots: encoder CA sample path 2 - complete lifetime

### Positive Implication With A Change In Interpretation

A positive implication in the processed data model can also occur through a change in interpretation. A change from increasing to constant failure rate or a change from constant to increasing failure rate occurs, and the processed model implicates positively with the lifetime type. Two examples from encoder CR are given for a right-censored and complete lifetime with sample path 7 in Figure 5.6 and sample-path 10 in Figure 5.7.

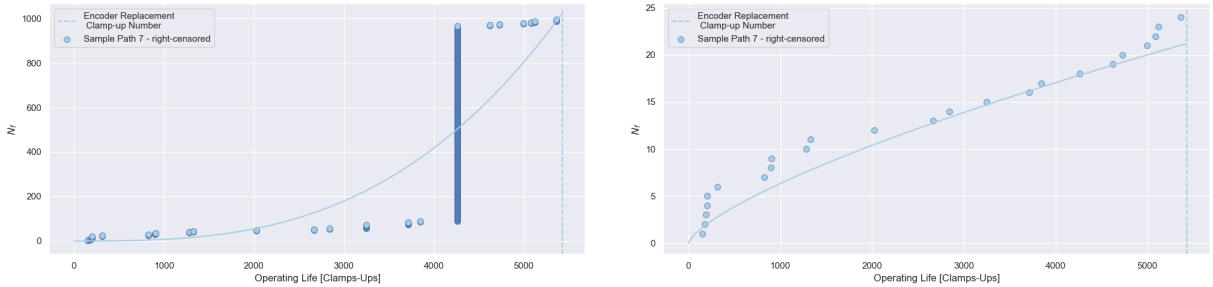


(a) Raw encoder error data (b) Processed encoder error data (unique faults)

Figure 5.6: Encoder error trend plots: encoder CR sample path 7 - right-censored lifetime

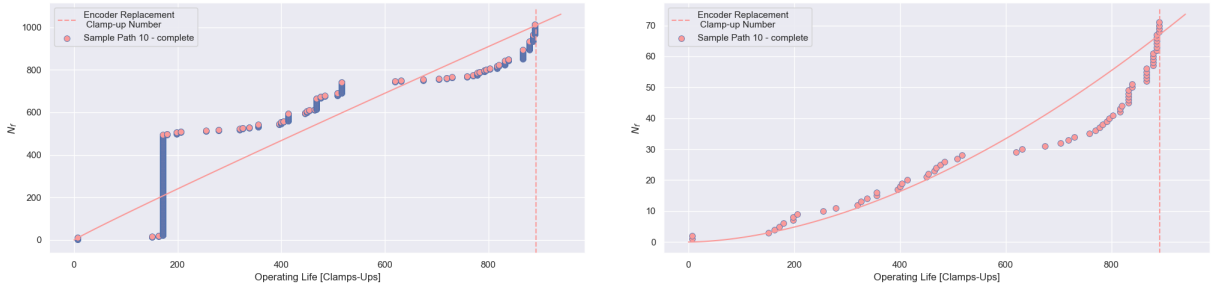


(a) Raw encoder error data (b) Processed encoder error data (unique faults)

Figure 5.7: Encoder error trend plots: encoder CR sample path 10 - complete lifetime

### Negative Implication With No Change In Interpretation

The negative implication involves a constant failure rate linked to a complete lifetime and an increasing failure rate linked with a right-censored lifetime. The unchanging interpretation means that the raw model indicates the same failure rate as the processed data model. Two examples are given for a right-censored and complete lifetime with sample-path 3 from encoder CR in Figure 5.8 and sample-path 5 from encoder CA in Figure 5.9.

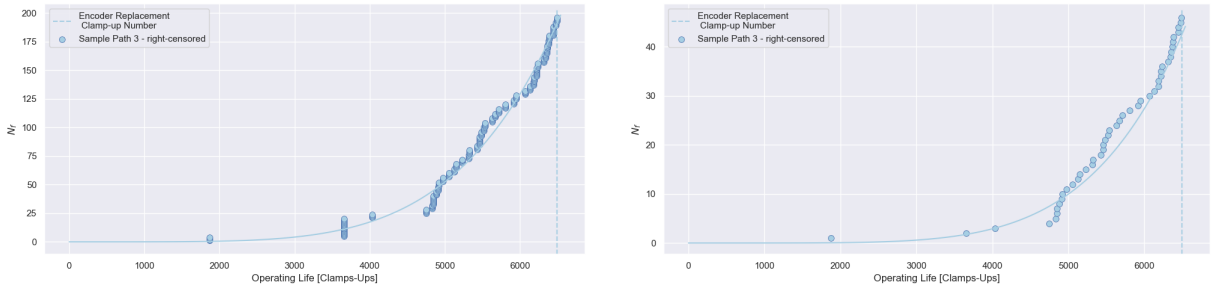


(a) Raw encoder error data (b) Processed encoder error data (unique faults)

Figure 5.8: Encoder error trend plots: encoder CR sample path 3 - right-censored lifetime

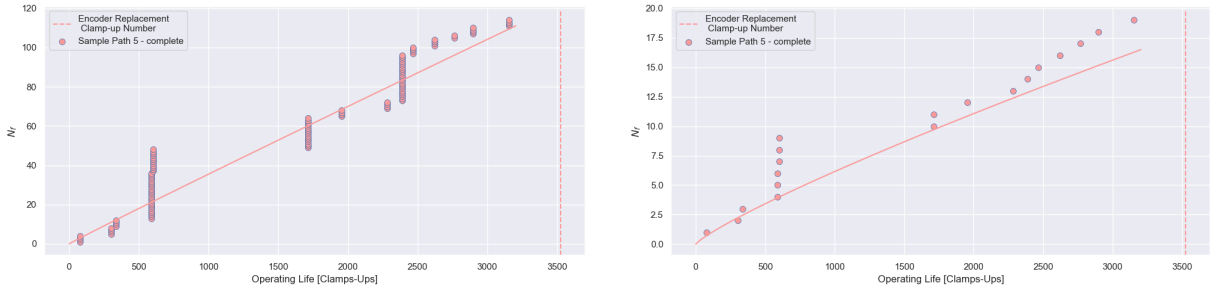


(a) Raw encoder error data (b) Processed encoder error data (unique faults)

Figure 5.9: Encoder error trend plots: encoder CA sample path 5 - complete lifetime

### Negative Implication With A Change In Interpretation

A negative implication in the processed data model can also occur through a change in interpretation. A change from increasing to constant failure rate or a change from constant to increasing failure rate occurs, and the processed model implicates negatively with the lifetime type. Within the 39 sample paths, a changing interpretation only created a negative implication with a complete lifetime type; with an example of this shown by Encoder RA's sample-path 5 in Figure 5.10.

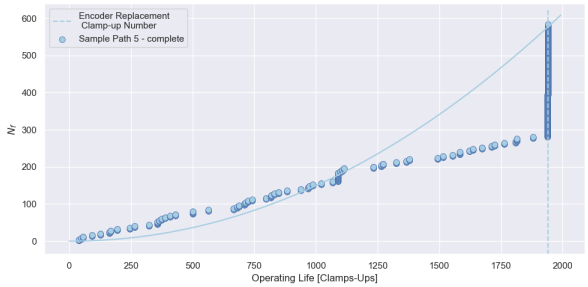


(a) Raw encoder error data

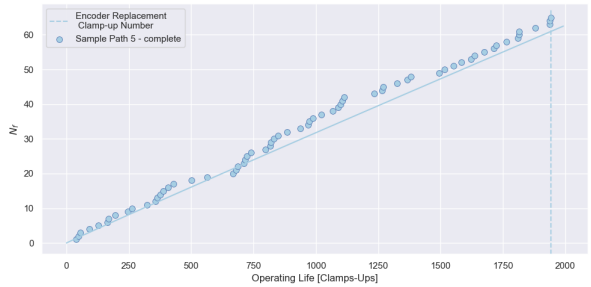


(b) Processed encoder error data (unique faults)

Figure 5.10: Encoder error trend plots: encoder RA sample path 5 - complete lifetime

### 5.4.1 Encoder CA

#### Sample Path 1

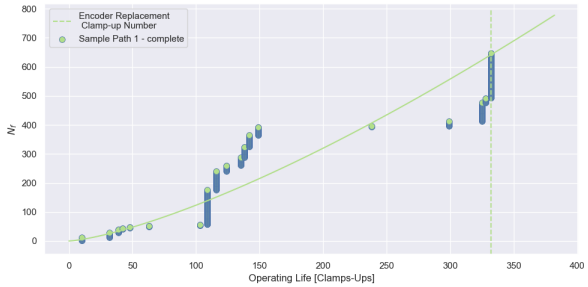


(a) Raw encoder error data

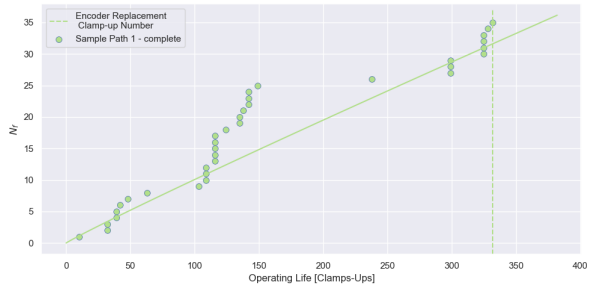


(b) Processed encoder error data (unique faults)

Figure 5.11: Encoder error trend plots: encoder CA sample path 1 - complete lifetime

### Sample Path 2

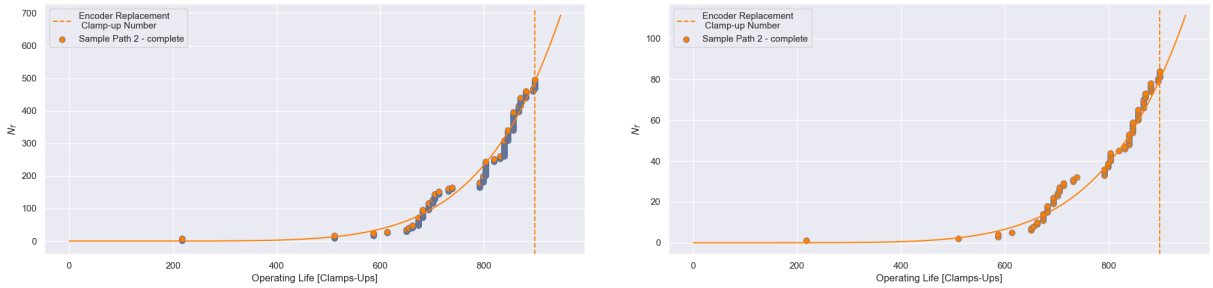


(a) Raw encoder error data (b) Processed encoder error data (unique faults)

Figure 5.12: Encoder error trend plots: encoder CA sample path 2 - complete lifetime

### Sample Path 3

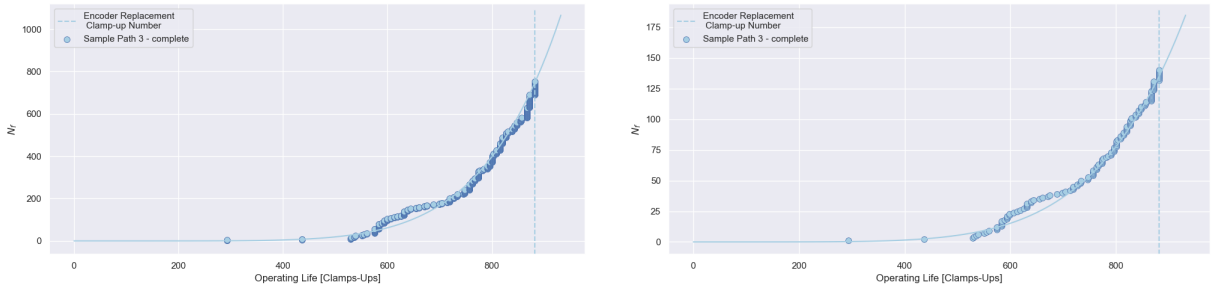


(a) Raw encoder error data (b) Processed encoder error data (unique faults)

Figure 5.13: Encoder error trend plots: encoder CA sample path 3 - complete lifetime

### Sample Path 4

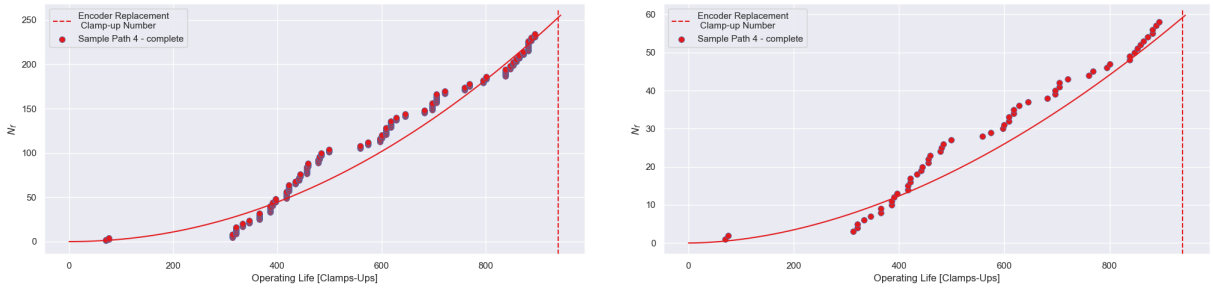


(a) Raw encoder error data (b) Processed encoder error data (unique faults)

Figure 5.14: Encoder error trend plots: encoder CA sample path 4 - complete lifetime

### Sample Path 5

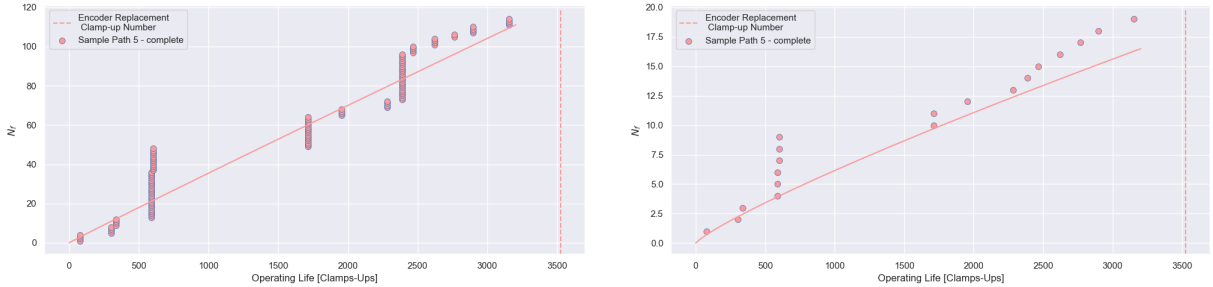


(a) Raw encoder error data (b) Processed encoder error data (unique faults)

Figure 5.15: Encoder error trend plots: encoder CA sample path 5 - complete lifetime

### Sample Path 6

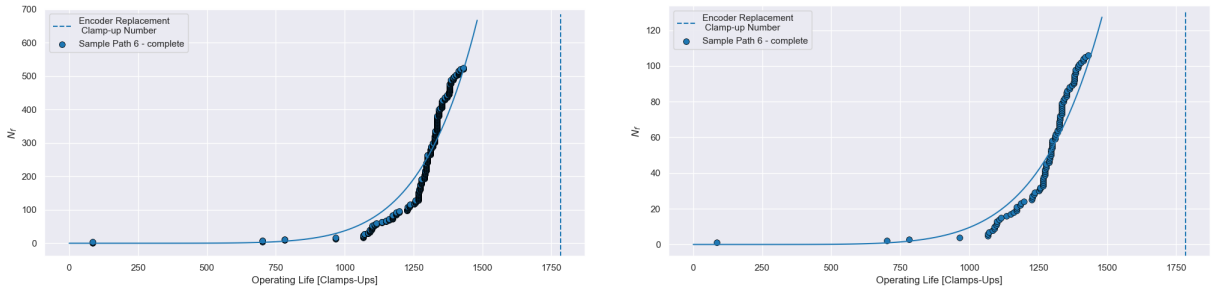


(a) Raw encoder error data (b) Processed encoder error data (unique faults)

Figure 5.16: Encoder error trend plots: encoder CA sample path 6 - complete lifetime

### Encoder CA Results Discussion

Table 5.2: Encoder CA sample path models information table

| Sample Path No. | Data Type | Encoder Name | Type of Lifetime | Lifetime (Clamp-ups) | No. of Data Points | beta | theta | beta > | beta < |
|---|---|---|---|---|---|---|---|---|---|
| 1 | Raw | CA | complete | 238 | 648 | 1.3739 | 3.005 | 0.9272 | 1.0818 |
| | Unique | CA | complete | 238 | 35 | 0.9536 | 8.226 | 0.7336 | 1.444 |
| 2 | Raw | CA | complete | 511 | 496 | 6.42 | 342.19 | 0.9174 | 1.0943 |
| | Unique | CA | complete | 511 | 84 | 6.1799 | 439.28 | 0.8155 | 1.2555 |
| 3 | Raw | CA | complete | 529 | 753 | 6.4614 | 316.83 | 0.9322 | 1.0755 |
| | Unique | CA | complete | 529 | 140 | 5.677 | 369.8075 | 0.8526 | 1.1895 |
| 4 | Raw | CA | complete | 313 | 234 | 2.033 | 61.7907 | 0.8831 | 1.1419 |
| | Unique | CA | complete | 313 | 58 | 1.8371 | 98.9859 | 0.7838 | 1.3203 |
| 5 | Raw | CA | complete | 3538 | 114 | 0.9798 | 26.1764 | 0.8385 | 1.2134 |
| | Unique | CA | complete | 3538 | 19 | 0.847 | 103.9496 | 0.6613 | 1.6873 |
| 6 | Raw | CA | complete | 1067 | 524 | 7.3552 | 611.8275 | 0.9195 | 1.0916 |
| | Unique | CA | complete | 1067 | 106 | 6.6098 | 707.7075 | 0.8332 | 1.2226 |

All six sample paths from encoder CA are complete lifetime types. Sample paths 1 and 5 can be defined as stationary. Sample paths 2, 3, 4, and 6 can be defined as non-stationary

or the rejection of the null hypothesis. Approximately 66.7% of encoder CA's sample paths positively implicate to their lifetime type. Sample-path 1 is the only path to have a change in interpretation. This change had adverse effects on the interpretation, given that the processed model negatively implicates with its lifetime type. Sample-path 5 is the only path where the raw and processed models negatively implicate with the lifetime type, meaning the processing made no difference. The stationary processed models have shape parameters ranging from 0.85 to 0.95 with a mean value of 0.9. For the non-stationary paths, the processing was passively effective in implicating them to their lifetime types. The non-stationary processed models have shape parameters ranging from 1.8 to 6.6 with a mean value of 5.08. The processing of the sample paths from encoder CA were 0% actively effective, 66.7% passively effective and 16.7% ineffective or adverse to the interpretation. The remaining paths did not make a difference to the interpretation. Without processing, the raw models would have been effective in determining failure or non-failure 83.3% over the set time period, meaning the raw models were more effective for interpreting the lifetime type regarding the encoder CA by approximately 16.6%.

The "encoder lifetimes" shown in the fifth column of Tables 5.2-5.4 are determined in the following way. In case of a right-censored dataset, the lifetime is essentially the same as the encoder replacement time (i.e., the censoring time). In case of a complete dataset, the lifetime is defined as the change point at which the NHPP curve begins to rise sharply. However, there are instances where the lifetime for complete dataset is also close to encoder replacement time.

### 5.4.2 Encoder CR

#### Sample Path 1

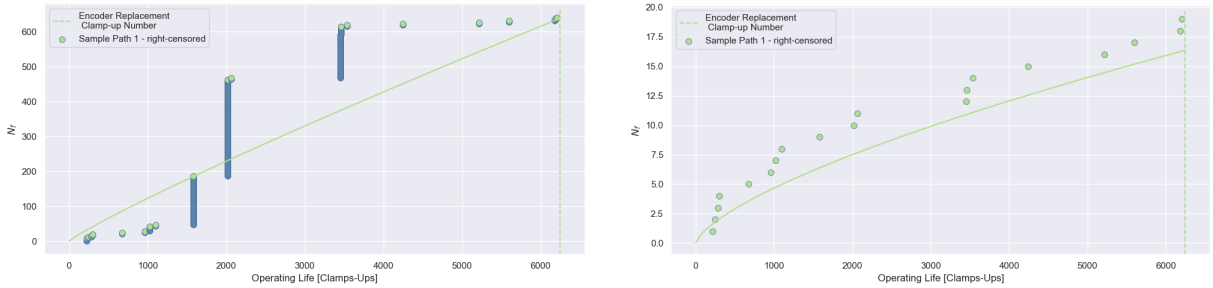


(a) Raw encoder error data (b) Processed encoder error data (unique faults)

Figure 5.17: Encoder error trend plots: encoder CR sample path 1 - right-censored lifetime

#### Sample Path 2

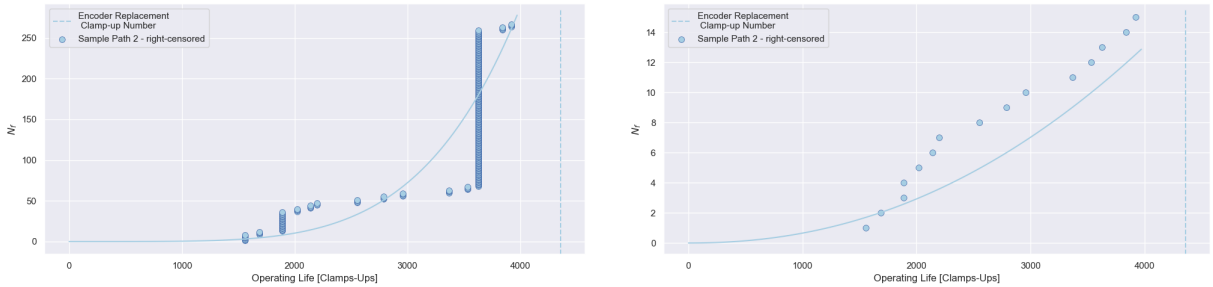


(a) Raw encoder error data (b) Processed encoder error data (unique faults)

Figure 5.18: Encoder error trend plots: encoder CR sample path 2 - right-censored lifetime

### Sample Path 3

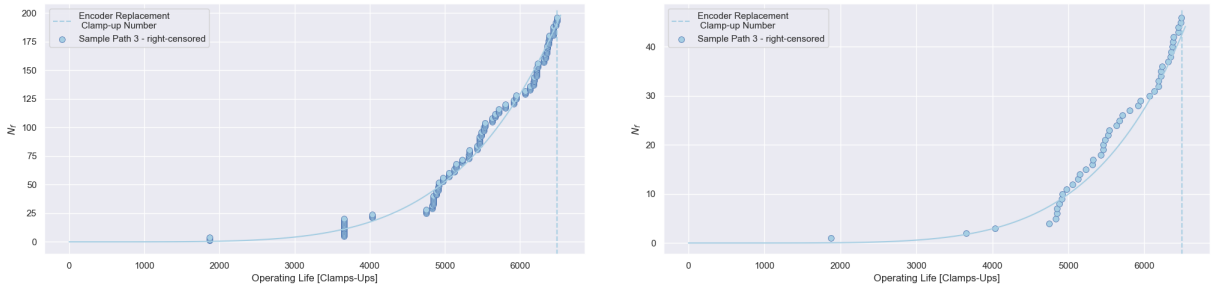


(a) Raw encoder error data (b) Processed encoder error data (unique faults)

Figure 5.19: Encoder error trend plots: encoder CR sample path 3 - right-censored lifetime

### Sample Path 4

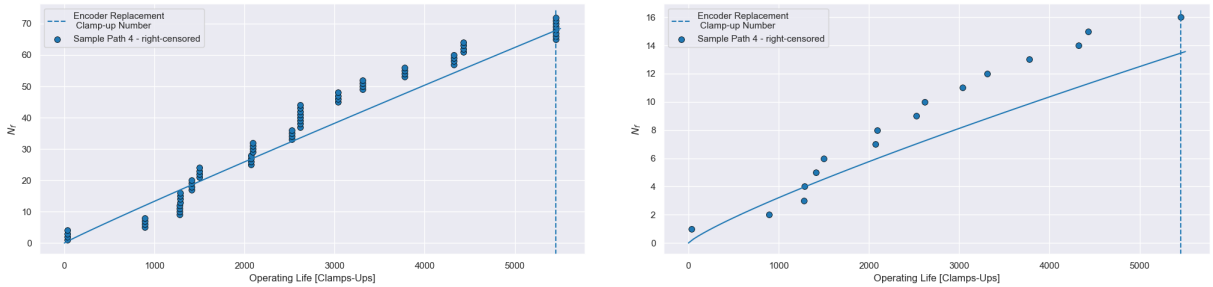


(a) Raw encoder error data (b) Processed encoder error data (unique faults)

Figure 5.20: Encoder error trend plots: encoder CR sample path 4 - right-censored lifetime

### Sample Path 5

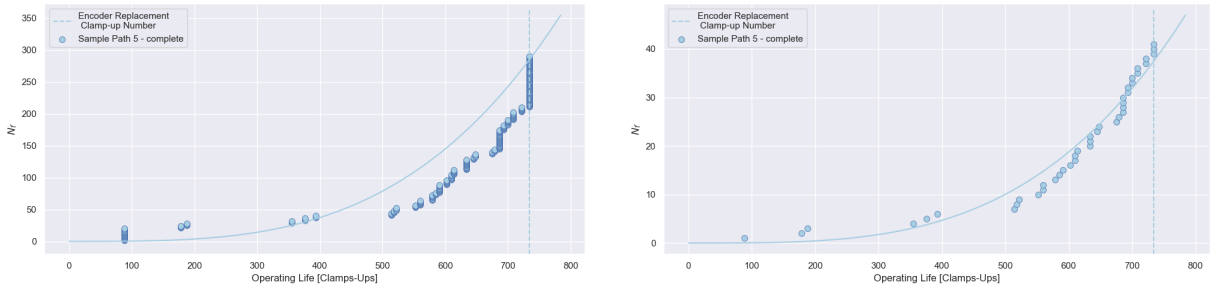


(a) Raw encoder error data (b) Processed encoder error data (unique faults)

Figure 5.21: Encoder error trend plots: encoder CR sample path 5 - complete lifetime

### Sample Path 6

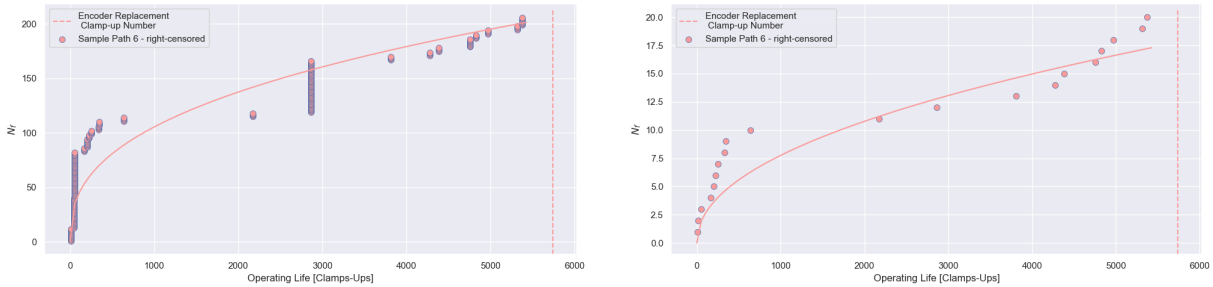


(a) Raw encoder error data (b) Processed encoder error data (unique faults)

Figure 5.22: Encoder error trend plots: encoder CR sample path 6 - right-censored lifetime

### Sample Path 7

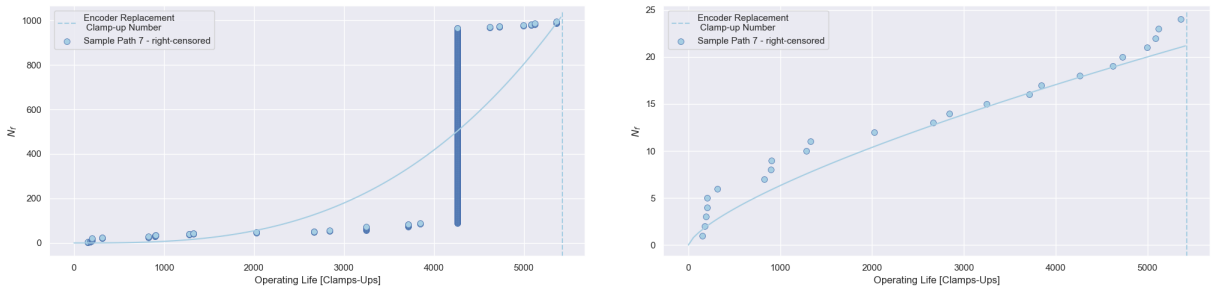


(a) Raw encoder error data (b) Processed encoder error data (unique faults)

Figure 5.23: Encoder error trend plots: encoder CR sample path 7 - right-censored lifetime

### Sample Path 8

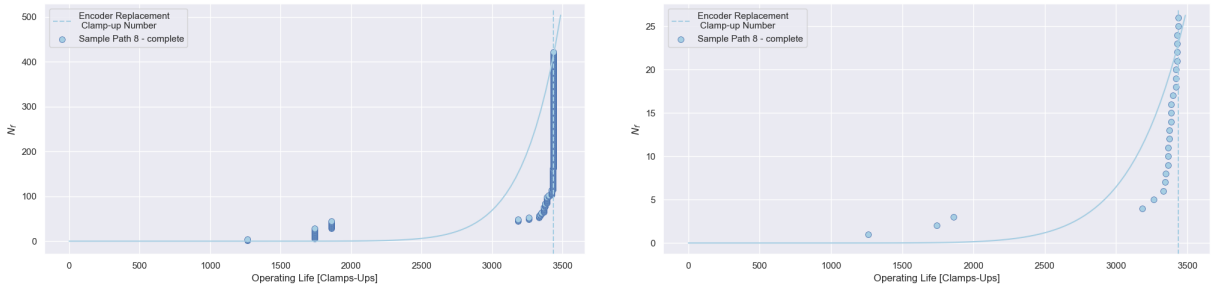


(a) Raw encoder error data (b) Processed encoder error data (unique faults)

Figure 5.24: Encoder error trend plots: encoder CR sample path 8 - complete lifetime

### Sample Path 9

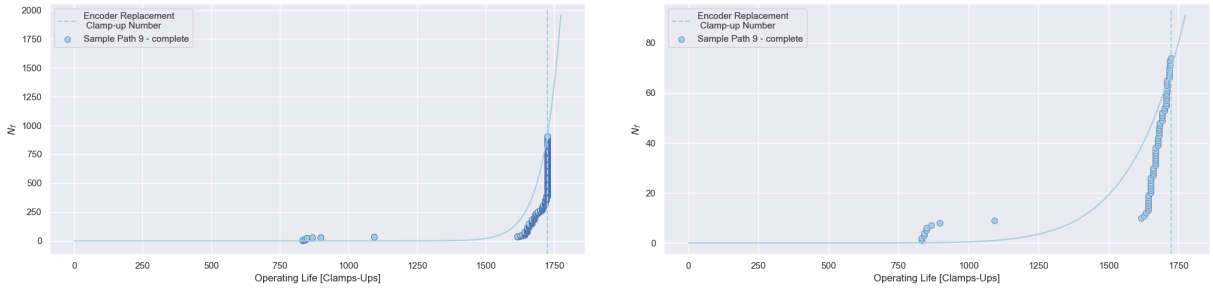


(a) Raw encoder error data (b) Processed encoder error data (unique faults)

Figure 5.25: Encoder error trend plots: encoder CR sample path 9 - complete lifetime

### Sample Path 10

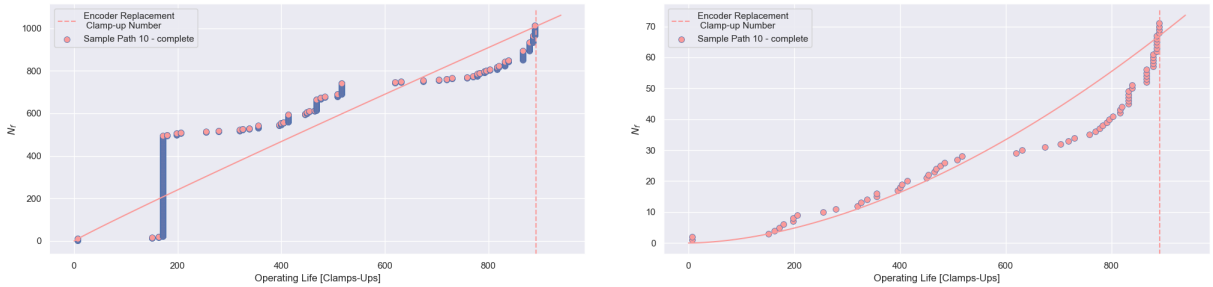


(a) Raw encoder error data (b) Processed encoder error data (unique faults)

Figure 5.26: Encoder error trend plots: encoder CR sample path 10 - complete lifetime

### Sample Path 11

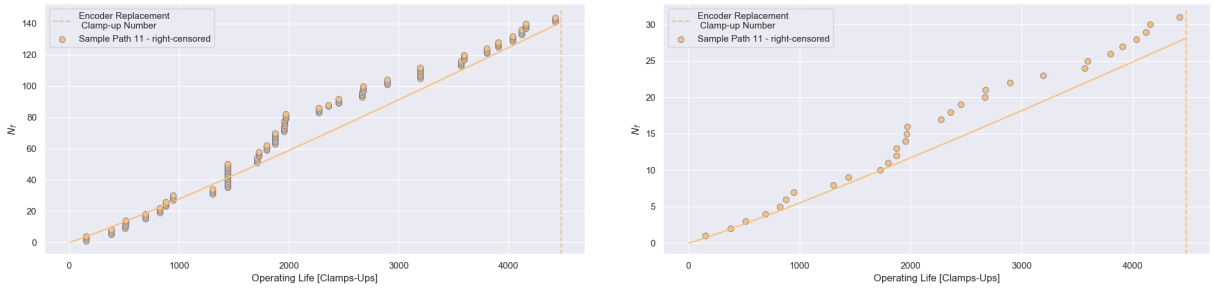


(a) Raw encoder error data (b) Processed encoder error data (unique faults)

Figure 5.27: Encoder error trend plots: encoder CR sample path 11 - right-censored lifetime

### Encoder CR Results Discussion

Table 5.3: Encoder CR sample path models information table

| Sample Path No. | Data Type | Encoder Name | Type of Lifetime | Lifetime (Clamp-ups) | No. of Data Points | beta | theta | beta > | beta < |
|---|---|---|---|---|---|---|---|---|---|
| 1 | Raw | CR | right-cens. | 6248 | 641 | 0.9 | 4.7731 | 0.9268 | 1.0822 |
| | Unique | CR | right-cens. | 6248 | 19 | 0.6843 | 90.8456 | 0.6613 | 1.6873 |
| 2 | Raw | CR | right-cens. | 4359 | 267 | 4.803 | 1231.1374 | 0.8899 | 1.132 |
| | Unique | CR | right-cens. | 4359 | 15 | 2.159 | 1155.487 | 0.6298 | 1.8291 |
| 3 | Raw | CR | right-cens. | 6494 | 196 | 4.9562 | 2249.5706 | 08732 | 1.1566 |
| | Unique | CR | right-cens. | 6494 | 46 | 5.5467 | 3267.33 | 0.7618 | 1.371 |
| 4 | Raw | CR | right-cens. | 5457 | 72 | 0.9599 | 67.4515 | 0.8028 | 1.2804 |
| | Unique | CR | right-cens. | 5457 | 16 | 0.8448 | 221.1878 | 0.6386 | 1.7867 |
| 5 | Raw | CR | complete | 514 | 290 | 3.3432 | 135.4239 | 0.894 | 1.1261 |
| | Unique | CR | complete | 514 | 41 | 3.4306 | 250.4403 | 0.7503 | 1.3997 |
| 6 | Raw | CR | right-cens. | 5738 | 206 | 0.3826 | 0.0052 | 0.8761 | 1.1524 |
| | Unique | CR | right-cens. | 5738 | 20 | 0.4742 | 10.809 | 0.6679 | 1.6609 |
| 7 | Raw | CR | right-cens. | 5429 | 994 | 2.9382 | 513.1967 | 0.9406 | 1.0652 |
| | Unique | CR | right-cens. | 5429 | 24 | 0.716 | 67.2311 | 0.6905 | 1.5775 |
| 8 | Raw | CR | complete | 3262 | 422 | 13.2574 | 2180.1982 | 0.911 | 1.1028 |
| | Unique | CR | complete | 3262 | 26 | 9.3344 | 2433.835 | 0.7001 | 1.5452 |
| 9 | Raw | CR | complete | 1615 | 906 | 27.1851 | 1342.3936 | 0.9379 | 1.0685 |
| | Unique | CR | complete | 1615 | 74 | 9.2878 | 1086.216 | 0.8051 | 1.2758 |
| 10 | Raw | CR | complete | 620 | 1014 | 0.9607 | 0.6661 | 0.9412 | 1.0646 |
| | Unique | CR | complete | 620 | 71 | 1.7622 | 79.8639 | 0.8016 | 1.2828 |
| 11 | Raw | CR | right-cens. | 4479 | 144 | 1.0839 | 46.5936 | 0.8544 | 1.1865 |
| | Unique | CR | right-cens. | 4479 | 31 | 1.088 | 194.167 | 0.7203 | 1.4821 |

Encoder CR sample paths consist of 7 right-censored lifetimes and 4 complete lifetimes. Sample paths 1, 4, 6, 7, and 11 can be defined as stationary, while sample paths 2, 3, 5, 8, 9, and 10 can be defined as non-stationary. The stationary processed models have shape parameters ranging from 0.5 to 1.1 with a mean value of 0.76. The non-stationary processed models have shape parameters ranging from 1.8 to 9.3 with a mean value of 5.2. 81.8% of the sample paths processed models positively implicate to their respective lifetime types. There are two changes in interpretation from the raw to the processed models in sample paths 7 and 10. Both changes were actively effective, with the processed

models implicating positively with the respective lifetime types. Sample paths 2 and 3 saw their raw and processed models negatively implicate with their lifetime types. Sample paths 1, 4, 5, 6, 8, 9, and 11 saw their positive implication remain positive from the raw to processed model. The processed models from encoder CR were actively effective 18.2%, passively effective 63.6%, and made no difference the remaining 18.2%. Without processing, the raw models would have been effective in determining failure or non-failure 63.6% over the set period, while with processing, the models would have been effective 81.8%. Meaning the processed models would have been more effective in determining the lifetime type of encoder CR by approximately 18.2%. Furthermore, sample path 2 and 3 show an inconsistency in the replacement decision taken by the operators or the lifetime has been erroneously classified in Chapter 4.

### 5.4.3 Encoder RA

#### Sample Path 1

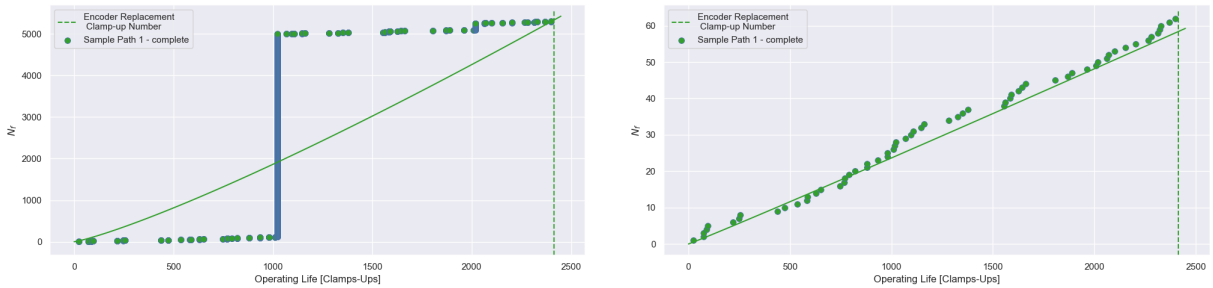


(a) Raw encoder error data

(b) Processed encoder error data (unique faults)

Figure 5.28: Encoder error trend plots: encoder RA sample path 1 - complete lifetime

### Sample Path 2

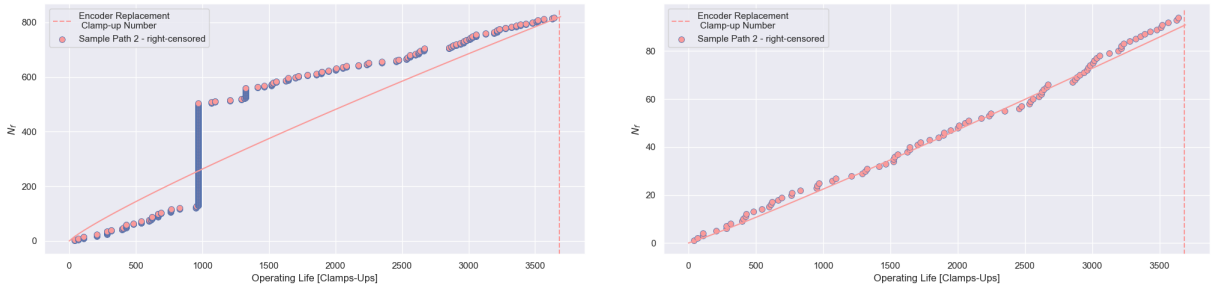


(a) Raw encoder error data (b) Processed encoder error data (unique faults)

Figure 5.29: Encoder error trend plots: encoder RA sample path 2 - right-censored lifetime

### Sample Path 3

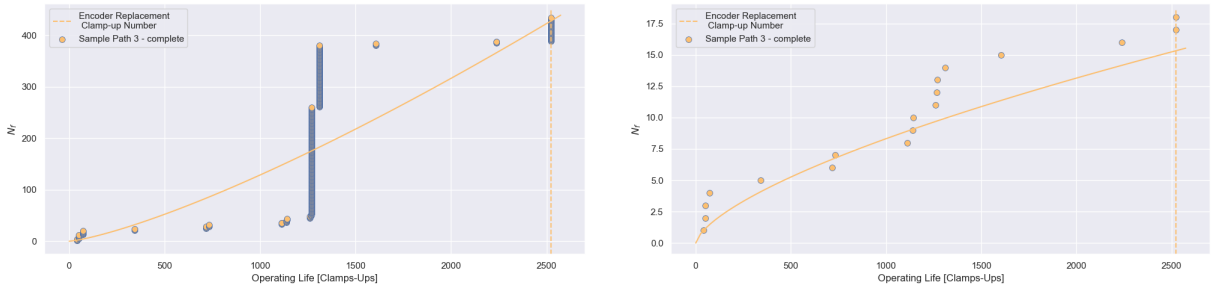


(a) Raw encoder error data (b) Processed encoder error data (unique faults)

Figure 5.30: Encoder error trend plots: encoder RA sample path 3 - complete lifetime

### Sample Path 4

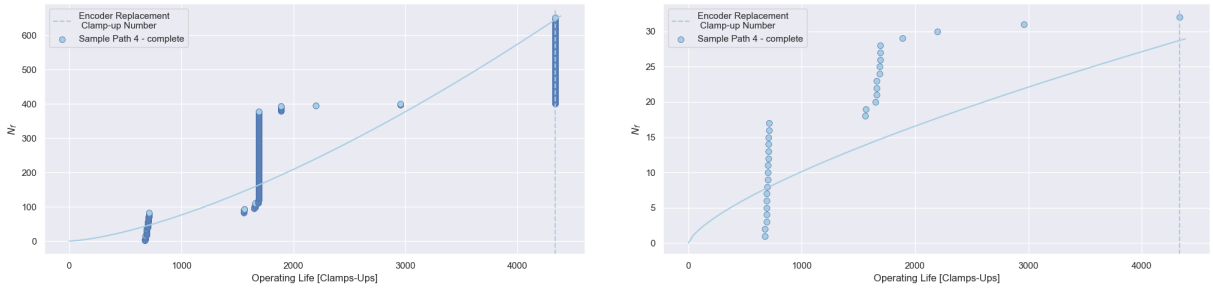


(a) Raw encoder error data (b) Processed encoder error data (unique faults)

Figure 5.31: Encoder error trend plots: encoder RA sample path 4 - complete lifetime

### Sample Path 5

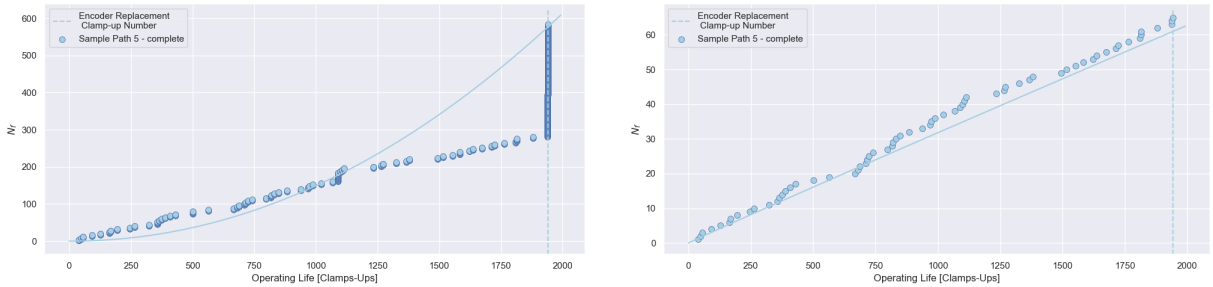


(a) Raw encoder error data (b) Processed encoder error data (unique faults)

Figure 5.32: Encoder error trend plots: encoder RA sample path 5 - complete lifetime

### Sample Path 6

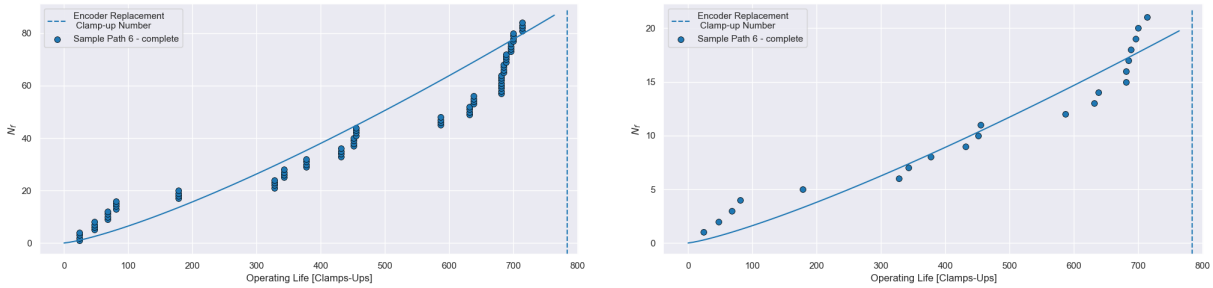


(a) Raw encoder error data (b) Processed encoder error data (unique faults)

Figure 5.33: Encoder error trend plots: encoder RA sample path 6 - complete lifetime

### Sample Path 7

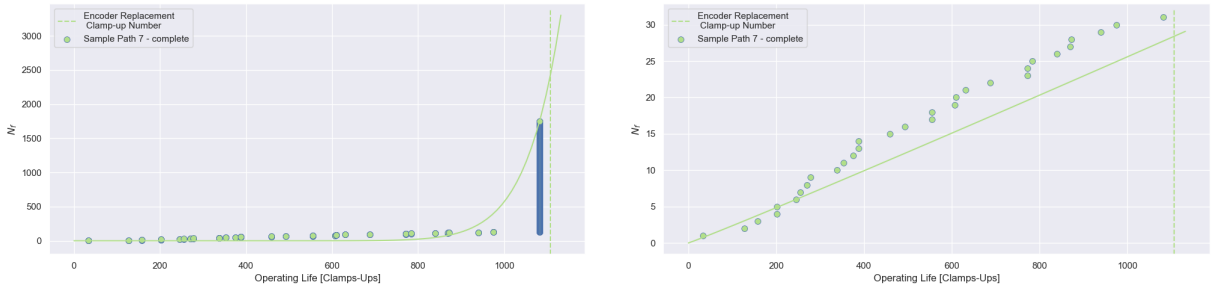


(a) Raw encoder error data (b) Processed encoder error data (unique faults)

Figure 5.34: Encoder error trend plots: encoder RA sample path 7 - complete lifetime

### Sample Path 8

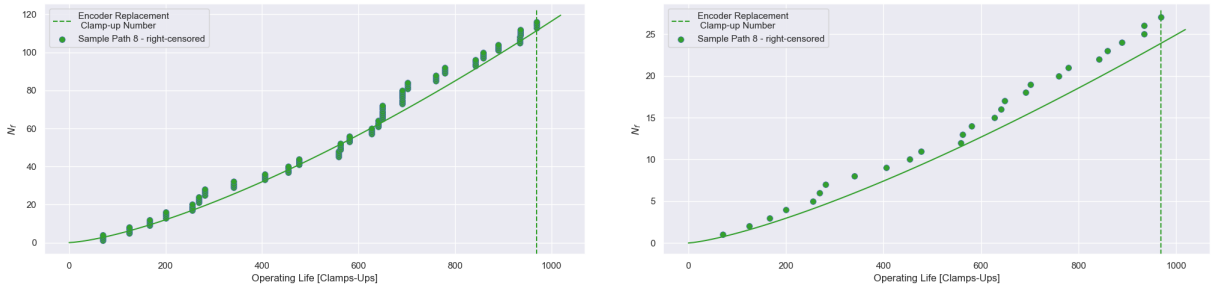


(a) Raw encoder error data (b) Processed encoder error data (unique faults)

Figure 5.35: Encoder error trend plots: encoder RA sample path 8 - right-censored lifetime

### Sample Path 9

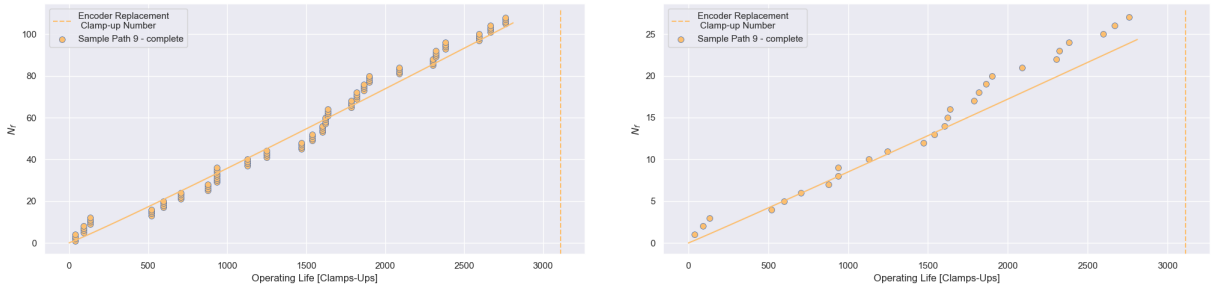


(a) Raw encoder error data (b) Processed encoder error data (unique faults)

Figure 5.36: Encoder error trend plots: encoder RA sample path 9 - complete lifetime

### Sample Path 10

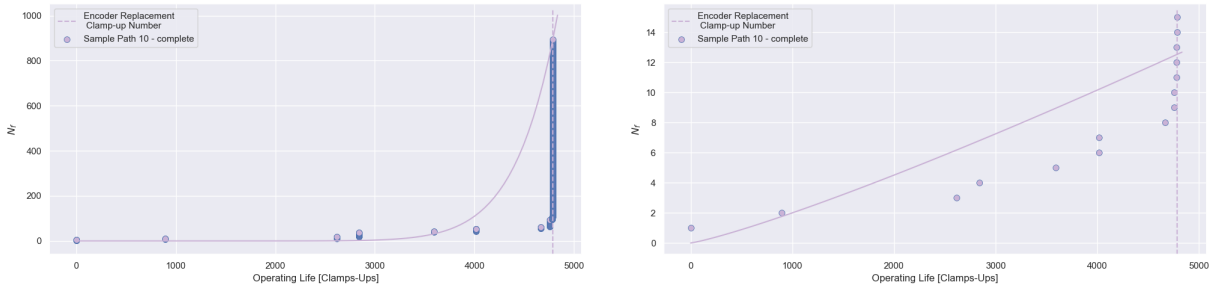


(a) Raw encoder error data (b) Processed encoder error data (unique faults)

Figure 5.37: Encoder error trend plots: encoder RA sample path 10 - complete lifetime

### Sample Path 11

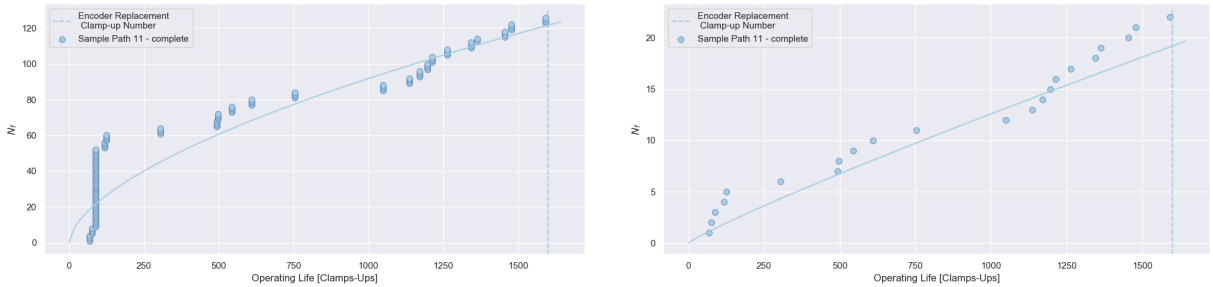


(a) Raw encoder error data (b) Processed encoder error data (unique faults)

Figure 5.38: Encoder error trend plots: encoder RA sample path 11 - complete lifetime

### Sample Path 12

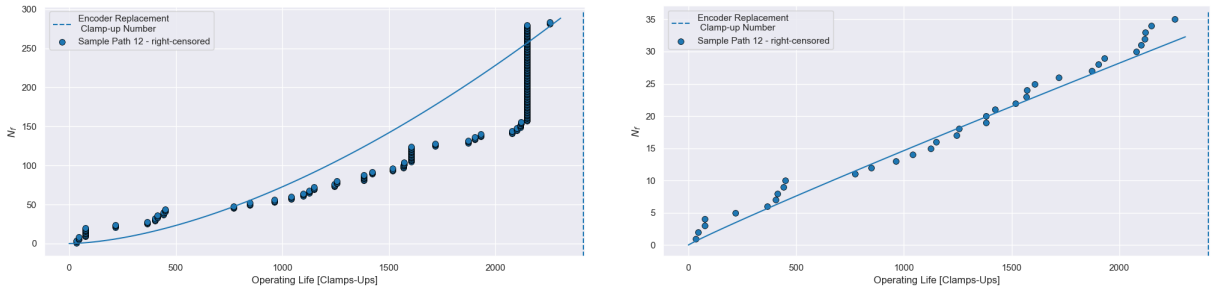


(a) Raw encoder error data (b) Processed encoder error data (unique faults)

Figure 5.39: Encoder error trend plots: encoder RA sample path 12 - right-censored lifetime

### Sample Path 13

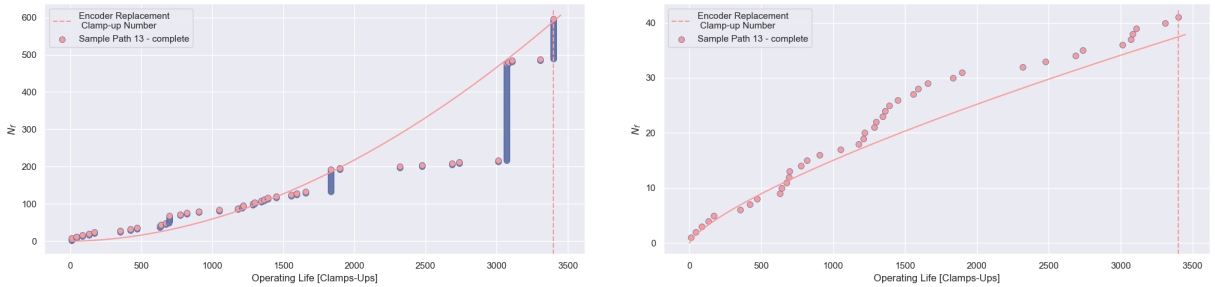


(a) Raw encoder error data (b) Processed encoder error data (unique faults)

Figure 5.40: Encoder error trend plots: encoder RA sample path 13 - complete lifetime

### Sample Path 14

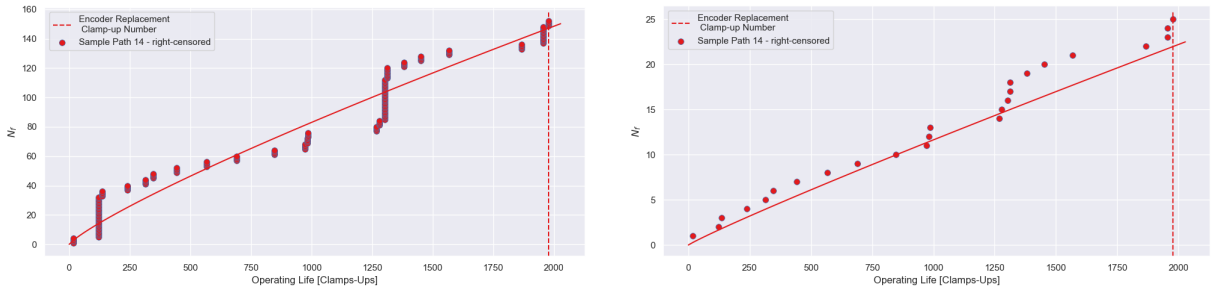


(a) Raw encoder error data (b) Processed encoder error data (unique faults)

Figure 5.41: Encoder error trend plots: encoder RA sample path 14 right-censored lifetime

### Sample Path 15

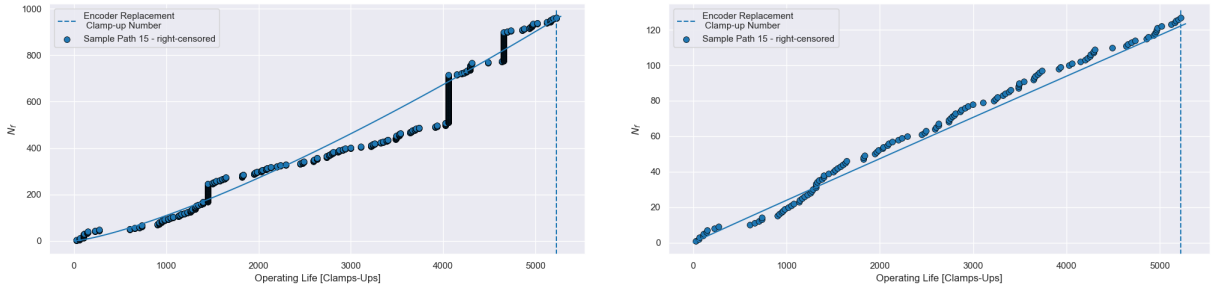


(a) Raw encoder error data (b) Processed encoder error data (unique faults)

Figure 5.42: Encoder error trend plots: encoder RA sample path 15 - right-censored lifetime

### Sample Path 16

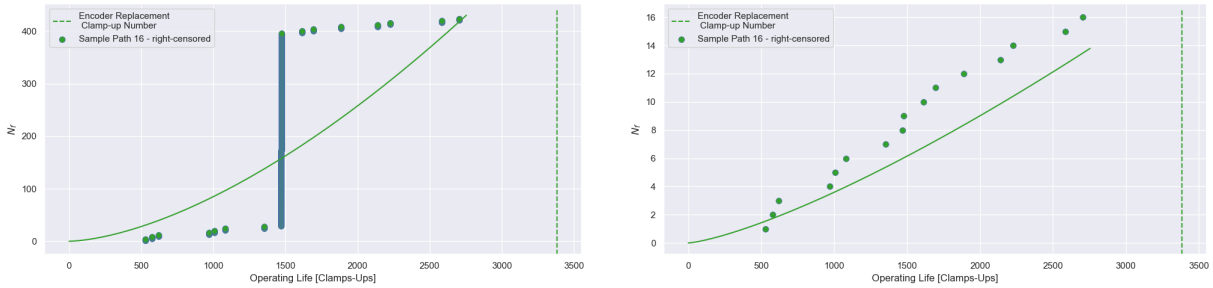


(a) Raw encoder error data (b) Processed encoder error data (unique faults)

Figure 5.43: Encoder error trend plots: encoder RA sample path 16 - right-censored lifetime

### Sample Path 17

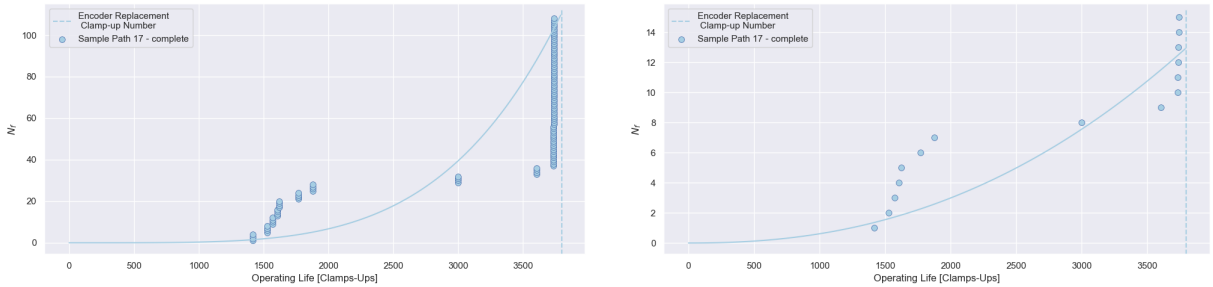


(a) Raw encoder error data (b) Processed encoder error data (unique faults)

Figure 5.44: Encoder error trend plots: encoder RA sample path 17 - complete lifetime

### Sample Path 18

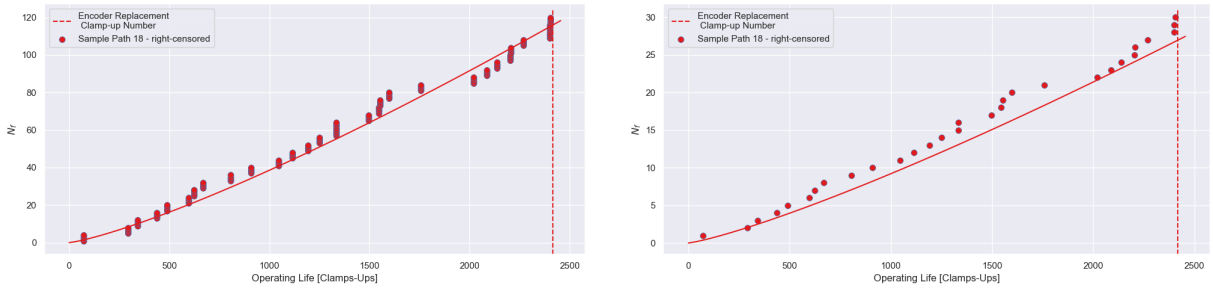


(a) Raw encoder error data (b) Processed encoder error data (unique faults)

Figure 5.45: Encoder error trend plots: encoder RA sample path 18 - right-censored lifetime

### Sample Path 19

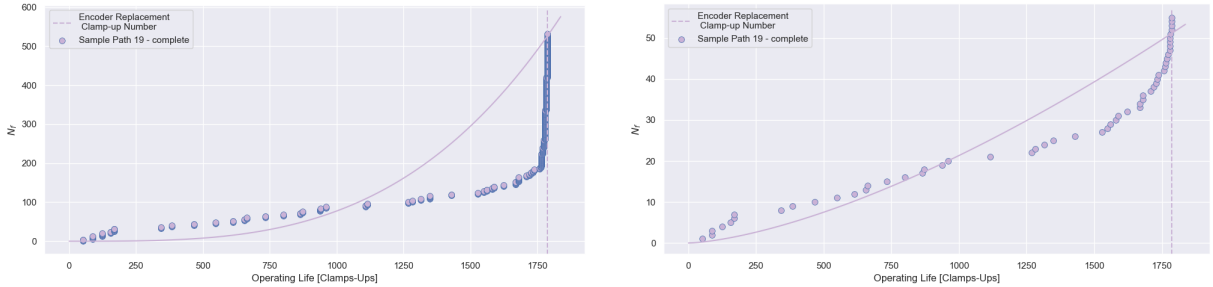


(a) Raw encoder error data (b) Processed encoder error data (unique faults)

Figure 5.46: Encoder error trend plots: encoder RA sample path 19 - complete lifetime

### Sample Path 20

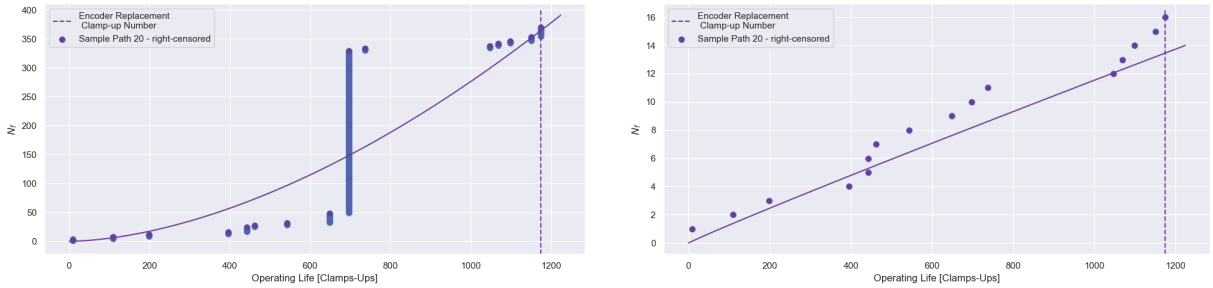


(a) Raw encoder error data (b) Processed encoder error data (unique faults)

Figure 5.47: Encoder error trend plots: encoder RA sample path 20 - right-censored lifetime

### Sample Path 21

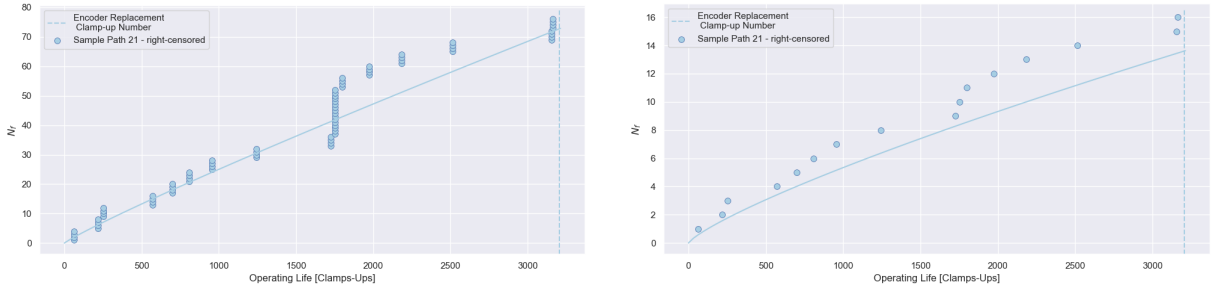


(a) Raw encoder error data (b) Processed encoder error data (unique faults)

Figure 5.48: Encoder error trend plots: encoder RA sample path 21 - right-censored lifetime

### Sample Path 22

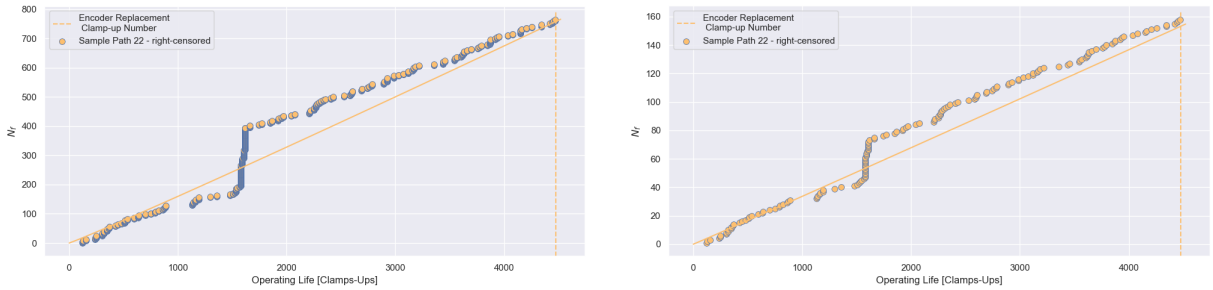


(a) Raw encoder error data (b) Processed encoder error data (unique faults)

Figure 5.49: Encoder error trend plots: encoder RA sample path 22 - right-censored lifetime

## Encoder RA Results Discussion

Table 5.4: Encoder RA sample path models information table

| Sample Path No. | Data Type | Encoder Name | Type of Lifetime | Lifetime (Clamp-ups) | No. of Data Points | beta | theta | beta > | beta < |
|---|---|---|---|---|---|---|---|---|---|
| 1 | Raw | RA | complete | 1805 | 5304 | 1.1939 | 1.8228 | 0.9736 | 1.0275 |
| | Unique | RA | complete | 1805 | 62 | 1.0261 | 43.6473 | 0.7898 | 1.3073 |
| 2 | Raw | RA | right-cens. | 3685 | 818 | 0.8708 | 1.6623 | 0.9348 | 1.0723 |
| | Unique | RA | right-cens. | 3685 | 94 | 1.0714 | 52.9644 | 0.8243 | 1.239 |
| 3 | Raw | RA | complete | 2524 | 434 | 1.2978 | 23.6898 | 0.9121 | 1.1013 |
| | Unique | RA | complete | 2524 | 18 | 0.6608 | 34.67 | 0.6543 | 1.7166 |
| 4 | Raw | RA | complete | 4334 | 652 | 1.4586 | 51.3341 | 0.9274 | 1.0815 |
| | Unique | RA | complete | 4334 | 32 | 0.7112 | 34.6762 | 0.7238 | 1.4718 |
| 5 | Raw | RA | complete | 1494 | 584 | 2.0408 | 86.1041 | 0.9235 | 1.0864 |
| | Unique | RA | complete | 1494 | 65 | 0.9813 | 28.0299 | 0.794 | 1.2985 |
| 6 | Raw | RA | complete | 587 | 84 | 1.2777 | 23.205 | 0.8154 | 1.2555 |
| | Unique | RA | complete | 587 | 21 | 1.2315 | 62.6985 | 0.6741 | 1.6371 |
| 7 | Raw | RA | complete | 1082 | 1747 | 14.1841 | 639.3977 | 0.9547 | 1.0486 |
| | Unique | RA | complete | 1082 | 31 | 1.0332 | 40.2258 | 0.7203 | 1.4821 |
| 8 | Raw | RA | right-cens. | 969 | 116 | 1.4106 | 34.305 | 0.8397 | 1.2112 |
| | Unique | RA | right-cens. | 969 | 27 | 1.3235 | 82.6455 | 0.7045 | 1.5308 |
| 9 | Raw | RA | complete | 2596 | 108 | 1.0478 | 32.9708 | 0.8346 | 1.2202 |
| | Unique | RA | complete | 2596 | 27 | 1.0184 | 112.5816 | 0.7045 | 1.5308 |
| 10 | Raw | RA | complete | 4669 | 894 | 11.6846 | 2676.0224 | 0.9375 | 1.069 |
| | Unique | RA | complete | 4669 | 15 | 1.1716 | 502.972 | 0.6298 | 1.8291 |
| 11 | Raw | RA | complete | 1592 | 126 | 0.5984 | 0.5245 | 0.8455 | 1.2014 |
| | Unique | RA | complete | 1592 | 22 | 0.8994 | 53.9391 | 0.6799 | 1.6155 |
| 12 | Raw | RA | right-cens. | 2413 | 284 | 1.6519 | 74.715 | 0.893 | 1.1276 |
| | Unique | RA | right-cens. | 2413 | 35 | 0.9467 | 54.4002 | 0.7336 | 1.444 |
| 13 | Raw | RA | complete | 3308 | 596 | 1.8776 | 113.7213 | 0.9243 | 1.0855 |
| | Unique | RA | complete | 3308 | 41 | 0.747 | 24.3616 | 0.7503 | 1.3997 |
| 14 | Raw | RA | right-cens. | 1978 | 152 | 0.8389 | 5.1599 | 0.8579 | 1.1808 |
| | Unique | RA | right-cens. | 1978 | 25 | 0.9314 | 65.2281 | 0.6954 | 1.5607 |
| 15 | Raw | RA | right-cens. | 5227 | 962 | 1.3097 | 27.7278 | 0.9397 | 1.0664 |
| | Unique | RA | right-cens. | 5227 | 127 | 0.988 | 39.1163 | 0.846 | 1.2004 |
| 16 | Raw | RA | right-cens. | 3382 | 424 | 1.6024 | 62.5496 | 0.9111 | 1.1026 |
| | Unique | RA | right-cens. | 3382 | 16 | 1.3268 | 351.2178 | 0.6386 | 1.7867 |
| 17 | Raw | RA | complete | 3732 | 108 | 4.3673 | 1298.9454 | 0.8346 | 1.2202 |
| | Unique | RA | complete | 3732 | 15 | 2.2875 | 1179.856 | 0.6298 | 1.8291 |
| 18 | Raw | RA | right-cens. | 2417 | 120 | 1.2484 | 53.6436 | 0.8421 | 1.2071 |
| | Unique | RA | right-cens. | 2417 | 30 | 1.2169 | 151.1479 | 0.7166 | 1.4932 |
| 19 | Raw | RA | complete | 1528 | 532 | 3.2994 | 267.6053 | 0.9201 | 1.0908 |
| | Unique | RA | complete | 1528 | 55 | 1.5067 | 126.5596 | 0.7789 | 1.3311 |
| 20 | Raw | RA | right-cens. | 1174 | 370 | 1.7187 | 37.9728 | 0.9053 | 1.1104 |
| | Unique | RA | right-cens. | 1174 | 16 | 0.9592 | 69.7548 | 0.6386 | 1.7867 |
| 21 | Raw | RA | right-cens. | 3207 | 76 | 0.9162 | 29.7938 | 0.8073 | 1.2714 |
| | Unique | RA | right-cens. | 3207 | 16 | 0.8025 | 108.2427 | 0.6386 | 1.7867 |
| 22 | Raw | RA | right-cens. | 4479 | 764 | 1.039 | 7.5722 | 0.9327 | 1.0749 |
| | Unique | RA | right-cens. | 4479 | 158 | 1.0116 | 30.1852 | 0.8603 | 1.1769 |

Encoder RA sample paths consist of 10 right-censored lifetimes and 12 complete lifetimes. Sample paths 1 to 16, 18, and 20 to 22 can be defined as stationary. Sample paths 17 and 19 can be defined as non-stationary. The stationary processed models have shape parameters ranging from 0.7 to 1.3 with a mean value of 1. The non-stationary processed models have shape parameters ranging from 1.5 to 2.3 with a mean value of 1.9. 54.5% of the sample paths processed models positively implicate to their respective lifetime types. Encoder RA's sample paths also have 13 changes in interpretation from the raw to the processed models. Of the thirteen, 6 of the changes were actively effective, and 7 were adversely effective. Of the remaining nine sample paths where no change in interpretation occurs, 6 were passively effective, and 3 made no difference. The processed models from encoder RA were actively effective 27.3%, passively effective 27.3%, adversely effective 31.8%, and made no difference the remaining 13.6%. Without processing, the raw models would have been effective in determining failure or non-failure 59.1% over the period, while with processing, the models would have been effective 54.5%. Meaning the raw models would have been more effective in determining lifetime type, in regards to encoder RA, by approximately 4.6%. Furthermore, encoder RA also shows inconsistencies in replacement decisions taken by the operators or an erroneous lifetime classification, as shown by sample path 1 and 2.

## 5.5 Overall Results Discussion

Of the 39 sample paths, 17 are right-censored and 22 are complete. With the right-censored sample paths, 88.2% are correctly identified by the processed model, and 52.9% are correctly identified by the raw model. The processed model correctly identifies the complete sample paths 45.4% and 77.3% are correctly identified by the raw model. Out of the 27 processed stationary models, 15 or 55.6% are right-censored lifetime types. Out of the 12 processed non-stationary models or the models that reject the null hypothesis, 10 or 83.3% are complete lifetime types. Out of the 12 raw stationary models, 8 or 66.7% are right-censored lifetime type, and out of the 27 raw non-stationary models, 18 or 66.7% are complete lifetime type. Overall the encoders sample paths, the processed and raw models, were equally effective at interpreting the lifetime type at 64.1%. The raw and processed models were adversely effective at interpreting the lifetime type with 8 sample paths, and processed models were also adversely effective with another 8 independent sample paths, which is 20.5% over the set period. Together, the raw and processed models made no

difference in determining the correct lifetime type with 6 sample paths, which is 15.4% of the time over the set period, respectively. 7 of the 8 adversely effective raw models are of right-censored lifetime type. All 8 of the adversely effective processed models are of the complete lifetime type, highlighting the respective model sets weakness.

Some accuracy issues for using an NHPP model to determine the lifetime type can be attributed to WOs. All the right-censored lifetime types replacements for the non-stationary models occur on Overhaul intervals. Since the encoders are within the FM head system, the Overhauls are encapsulated by the FM head SCI number within the maintenance system. They do not usually indicate the replacement/repairs under the encoder SCI number. The Overhaul work reports could identify that the encoders did indeed fail or that the encoders operated with the knowledge that their replacement would occur at the upcoming FM head Overhaul. There also could be issues in regards to the assumptions made for determining a failure did indeed occur when looking at the WOs. Looking at each specific work report could be necessary to confirm the assumptions.

Given that raw models better identify complete lifetime types and processed models better identify right-censored lifetime types, another potential place of inaccuracy is in the number of data points necessary for the model to create a good understanding of the trend. For this study, the minimum number of data points was 15. Encoder RA's sample-path 17 proves this is enough data points to correctly identify a complete lifetime (which theoretically should be the more challenging lifetime type to determine correctly with a low number of data points). Where the processed models were ineffective, the average number of data points was 31.8. Where the processed models were effective, the average number of data points was 53. Therefore, the models could become more accurate with increased data points or modification of the current processing procedures to find a better way to reduce the noise while limiting the removal of potentially essential data points. Another consideration would be to develop a better model or some form of spline curve to match the encoder error data better and more accurately implicate to its lifetime type.

## 5.6 Summary

In this chapter, sample paths of sequence jump errors over lifetimes of different encoders were analyzed. Each sample-path, with at least 15 errors, was fitted by an NHPP model.

The idea is to determine the sample path's lifetime type (complete or right-censored) using the trend of the models'. The chapter further identifies a processing technique of consolidating the errors by clamp-up number to reduce the noise within the encoder error data and increase the accuracy of determining lifetime type. Models are fitted to both raw and processed data and compared to one another. This comparison found that the raw models outperformed the processed models in determining complete lifetimes, and the processed models outperformed the raw models in determining the right-censored lifetimes. Overall, when used separately, both model sets were equally effective in determining the lifetime type at 64.1%. In the end, this chapter identifies the merit of modelling sequence jump error data to determine a failing or non-failing encoder which will be further discussed and investigated in Chapter 7, as it presents a concept for a health monitoring strategy.

# Chapter 6

# Probabilistic Assessment of Bit Mismatch Patterns

The sequence jump error is caused by two main reasons; the encoder moving faster than expected or a faulty data bit (see Section 3.3). Each sequence jump error presents the cause of an error via the previous and current bit patterns creating a respective Bit Mismatch (BM). This chapter presents a methodology for using this data to aid in determining an encoder failure or non-failure. It will then take a look at two complete lifetimes with clear failing trends and replacement WOs and two right-censored lifetimes with corresponding steady trendline and WOs to prove the logical rationale. This chapter demonstrates the value of tracking BM patterns and the rational use of identified bit information in each error log, which is presently not used by the FMH.

## 6.1 Bit Mismatch Pattern: Definition

This chapter takes the sequence jump error logs, creates the BM patterns and correlates them to complete and right-censored lifetimes. An example of error logs is given by Table 6.1. Each entry logs a previous and current bit pattern for both bus 1 and 2, respectively and is shown in Table 6.1. The bit pattern is a 13-bit binary number that identifies the position of the encoder. The English code column separates each bus's initial error logs and return logs (RTN). The sequence jump error logs when the current value for an encoder has changed too much from the previous value, and the sequence jump return error logs when the sequence jump has been detected and logged, and sequencing returns to normal values [4]. Therefore, the BM comes from the bit differences in the bit patterns between the previous and current position values on each respective bus.

Looking at the index number 1285485 in Table 6.1, the previous and current columns for both bus 1 and 2 indicate the encoder position values as 0000000111010 and 0000000101111.

Table 6.1: Sequence Jump Error Logging Example - Encoder RA Head 1

| **Index** | **English Code** | **Prev. Bus 1** | **Cur. Bus 1** | **Prev. Bus 2** | **Cur. Bus 2** | **Bus 1 BM** | **Bus 2 BM** |
|---|---|---|---|---|---|---|---|
| 1285485 | SEQ JUMP 1 | 0000000111010 (72 - octal) | 0000000101111 (57 - octal) | 0000000111010 (72 - octal) | 0000000101111 (57 - octal) | 0,2,4 | 0,2,4 |
| 1285486 | SEQ JUMP 2 | 0000000111010 (72 - octal) | 0000000101111 (57 - octal) | 0000000111010 (72 - octal) | 0000000101111 (57 - octal) | 0,2,4 | 0,2,4 |
| 1285487 | SEQ JUMP RTN 1 | 0000000101111 (57 - octal) | 0000000100110 (46 - octal) | 0000000101111 (57 - octal) | 0000000100110 (46 - octal) | 0,3 | 0,3 |
| 1285488 | SEQ JUMP RTN 2 | 0000000101111 (57 - octal) | 0000000100110 (46 - octal) | 0000000101111 (57 - octal) | 0000000100110 (46 - octal) | 0,3 | 0,3 |

Table 6.2: Index number 1285485 bit mismatch example

| **Bit No.** | **12** | **11** | **10** | **9** | **8** | **7** | **6** | **5** | **4** | **3** | **2** | **1** | **0** |
|---|---|---|---|---|---|---|---|---|---|---|---|---|---|
| Prev. | 0 | 0 | 0 | 0 | 0 | 0 | 0 | 1 | 1 | 1 | 0 | 1 | 0 |
| Cur. | 0 | 0 | 0 | 0 | 0 | 0 | 0 | 1 | 0 | 1 | 1 | 1 | 1 |

In this case, the previous column was the last known position where the encoder exhibited normalcy, and the current column is an unexpected position occurrence. Each bit pattern has 13-bits identified as bit numbers ranging from 0 to 12, moving from the right side of the number to the left. In the 1285485 index number example, when comparing the bit patterns over the previous and current columns, the 0, 2, and 4 bit numbers do not match and are identified as the BM pattern; this is shown in preceding columns and is executed on both buses separately (see Table 6.2 where the BM pattern is shown in yellow). An illustration of the mismatching can be found in Figure 6.1, where the black squares equals to 1 and the white squares equals to zero. Looking at a return log example of index 1285487, the previous and current columns for both bus 1 and 2 indicate the encoder position values as 0000000101111 and 0000000100110. In this case, the previous column is an unexpected position, and the current column is the position when the encoder returns to normal or expected operation. The 13-bits are identified in the same manner stated above in the initial error logging example, and in this case, the 0 and 3 bit numbers do not match and are the BM pattern for this error log. This process is done for each entry within the time frame of interest and each respective set of previous and current bus columns.

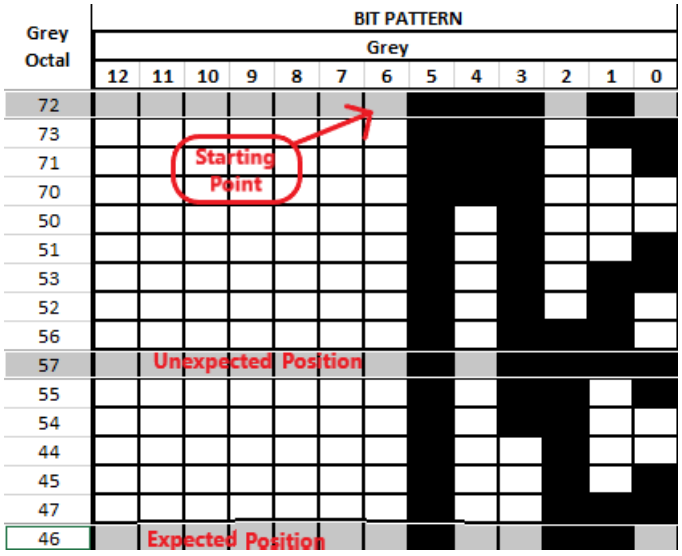


Figure 6.1: Bit Mismatch Example Visualization

## 6.2 Methodology

The sequence jump error logs involves four different types of entries; the initial error logging for either bus 1 or 2 and the return to normal operation for bus 1 or 2. The logging of the sequence jump error identifies the change from correct position to incorrect, and a return log identifies the change from an incorrect position to correct. For the initial logging of the error, the previous column is the accurate position with the current column identifying the inaccurate position, and in a return log entry the previous column holds the incorrect position and the current column holds the correct position. The BM is the difference between previous and current columns for each respective bus, therefore, there are two BMs for each log. When identifying the BM from the sequence jump error log, the identified bit changes is either expected or unexpected with the movement of the encoder. Meaning an error log and positional movement has bits that changed expectantly and unexpectedly. With the initial log, it is impossible to tell which bit changes fall into which category. However, the returning records were the only entries to hold bit changes identified as only being from bad bits or the unexpected bit changes. This is confirmed by the encoder technical document stating that "If this is the result of a bad bit only, the delta count will be zero" [4] and the delta count only registers as zero solely for return

logs. These are the bit changes that are of interest in this study and are the reason for only considering the return logs for the BM assessment. However, return logs do not hold only delta count zero entries, meaning an understanding of the exact nature of the delta count value could uncover further processing techniques to achieve further understanding of BMs in identifying failing encoders. For this study, looking at the example in Table 6.1, the return logs BMs of 0,3 would be the ones considered given the higher potential to hold the unexpected bit changes as explained above and the initial error logs will be removed from consideration.

Table 6.3: Encoder error processing for bit mismatch patterns example

| Entry No. | Clamp-up No. | BM Bus 1 | BM Entered into Histogram |
|---|---|---|---|
| 1 | 150 | 0,5,6 | |
| 2 | 150 | 0,1,6 | |
| 3 | 150 | 5,6,7 | 0,1,5,6,7 |
| 4 | 210 | 0,3 | 0,3 |
| 5 | 225 | 9 | |
| 6 | 225 | 11 | 9,11 |

Most commonly, the sequence jump error logs on both bus 1 and 2 simultaneously, and identical BMs show in the logs as shown by Table 6.1. For this reason, both bus 1 and 2 BM histograms should be close to identical at all times. Comparing the BM patterns over all the intervals for bus 1 and 2 confirms the usual similarity (see Figure 6.2). To reduce redundancy, BM patterns of bus 1 is the focus of the study. The focus of the study will again be on lifetime intervals that log 15 or more unique faults, the same as the NHPP analysis in Chapter 5 further described in Section 5.2. However, each unique fault will consider the bits that mismatch over all the consolidated errors, an example of this processing is shown in Table 6.3. The error logs are consolidated by what clamp-up number they occur on in each respective interval, and all the bits causing the error are relevant. However, this does not always occur in the first or a single log of the error and using all the errors creates the possibility for skew to the analysis if certain bits receive numerous entries over the same clamp-up number. Considering and merging all the bits that mismatch over all the faults in each consolidation will help maintain accuracy and reduce the skew of the analysis. Also, the removal of encoder MR from this chapter is for

the same reasons identified in Chapter 5, which is due to lack of data.

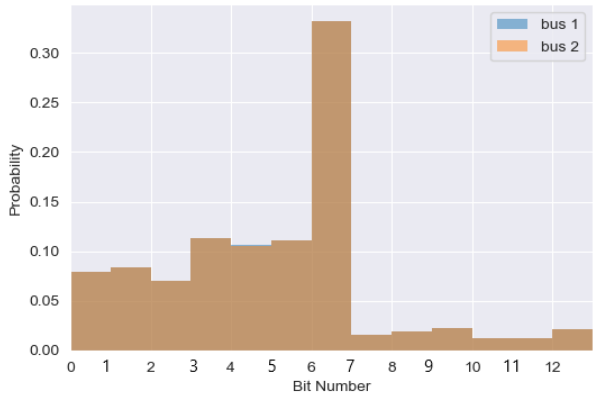


Figure 6.2: Bit Mismatch Histogram Comparison Between all Sequence Jump 1 and 2 Error Entries for Encoder RA

Only taking the return logs gives the failure causing bits, which are the bits of interest. Taking either bus 1 or 2 reduces redundancy of the bit retrieval. Consolidating the errors and the bits that mismatch with their identified clamp-up count number provides the most accurate and reduces the skew when analyzing the bit mismatch patterns. These three points propose the most logical way to monitor and utilize this data to glean the most information.

## 6.3 Case Study

The case study will use the methodology formed above to look into two complete and right-censored lifetimes to demonstrates the results. It will present a bit mismatch histograms over each lifetime and include the respective NHPP graph with an annotation of the bit pattern logging for each unique fault. The potential overuse of encoder CR is due to its WO clarity over the other two encoders given the work reports, which was defined in Section 3.2. For Figure 6.4, the removal of 60% of the annotations occurs for a clearer graph.

Each BM histogram identifies the count of the bit number fault with the x-axis distinguishing the appropriate bit number. The title of each histogram indicates the interval

number and lifetime data type (complete or right-censored). The python code found in Section of the appendix shows the creation process of the following histograms in this section.

### 6.3.1 Complete Lifetimes

The two complete lifetimes are encoder CA sample path 6 and encoder CR sample path 8. For the encoder CA lifetime, the number of unique faults is 106, with the overall faults totalling 131. The encoder CR lifetime divides its total of 105 errors into 26 clamp-up numbers. Both of the complete lifetimes show a clear bit pattern as it ages. Most of the unique faults of the encoder CA lifetime include the bit numbers 1, 2,4, and 5. With the encoder CR lifetime, most of the error logs involve the first seven bits. The same bit pattern further identifies these lifetimes as complete with NHPP graphs that are getting worse with clamp-ups.

#### Encoder CA - Sample Path 6

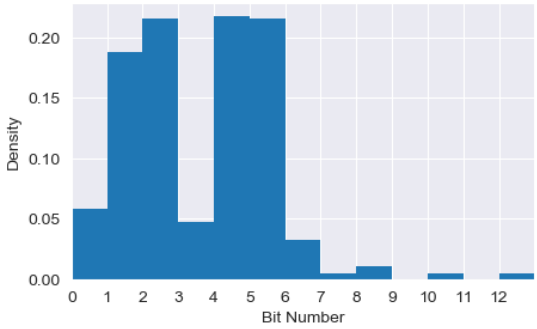


Figure 6.3: Bit Mismatch Plot of Unique SEQ Jump Error Encoder CA Sample Path 6

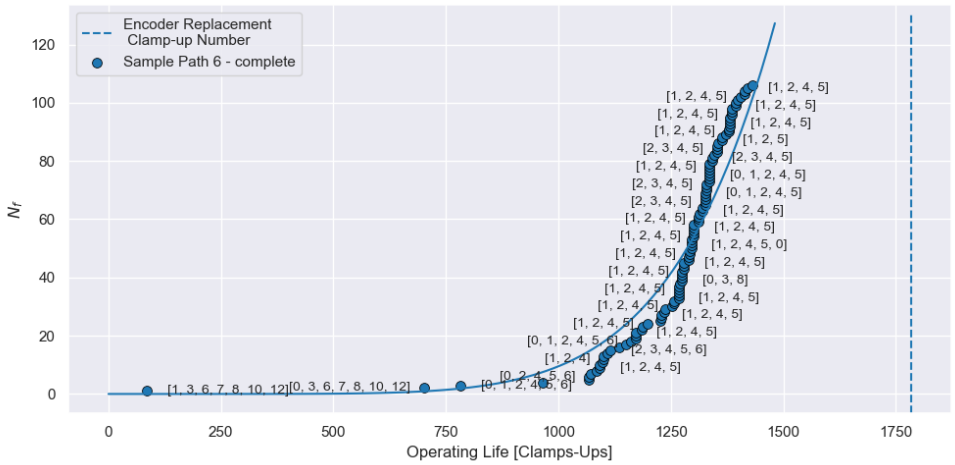


Figure 6.4: Error trend plot: encoder CA sample path 6 annotated with bit mismatches

### Encoder CR - Sample Path 8

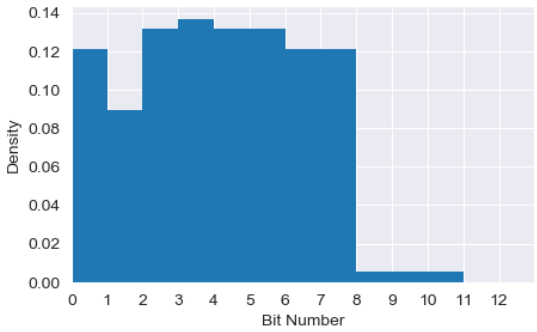


Figure 6.5: Bit Mismatch Plot of Unique SEQ Jump Error Encoder CR Sample Path 8

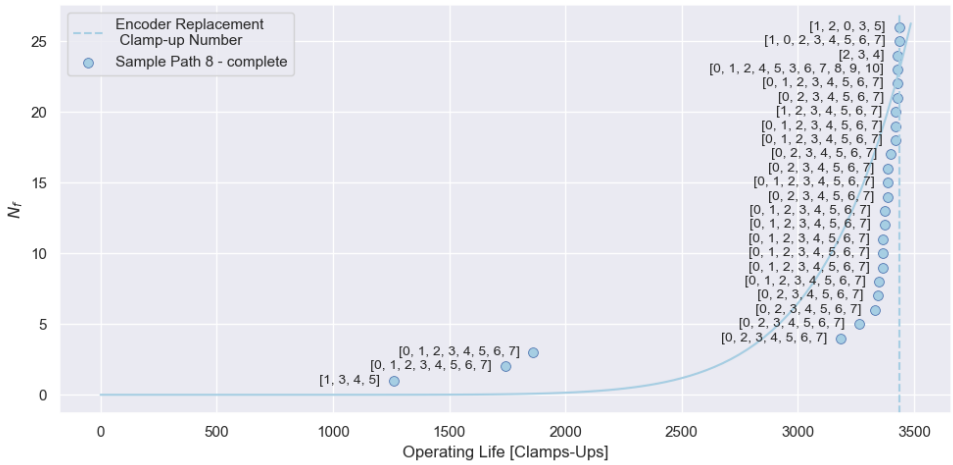


Figure 6.6: Error trend plot: encoder CR sample path 8 annotated with bit mismatches

### 6.3.2 Right-Censored Lifetimes

The two right-censored lifetimes are encoder CR sample path 4 and 7. Sample path 4 logs a total of 18 errors, with 16 occurring on different clamp-up counts. Sample path 7 has a total of 466 individual errors that consolidate into 24 unique faults. Both of the right-censored lifetimes show unclear bit patterns as the encoders age past 5000 clamp-ups. The sample path 4 pattern, in particular, has only one bit that occurs in half of the unique faults. These unclear bit patterns that occur over long clamp-up counts in a relatively steady fashion further show these lifetimes as encoders that were not defective.

### Encoder CR - Sample Path 4

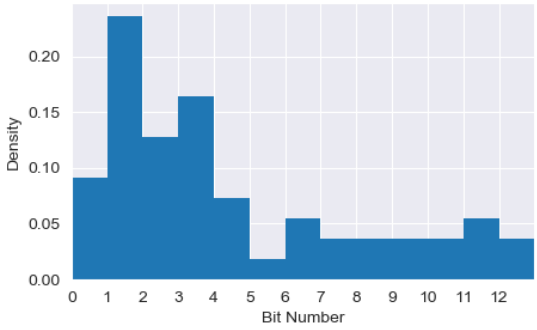


Figure 6.7: Bit Mismatch Plot of Unique SEQ Jump Error Encoder CR Sample Path 4

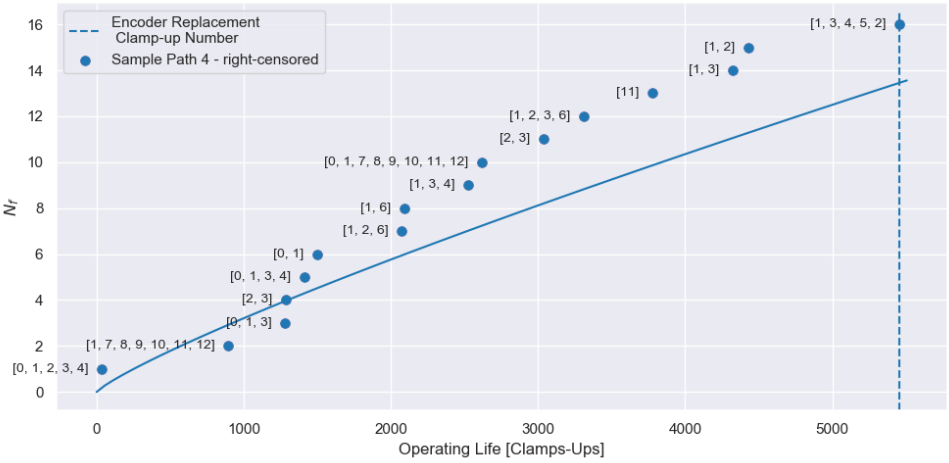


Figure 6.8: Error trend plot: encoder CR sample path 4 annotated with bit mismatches

**Encoder CR - Sample Path 7**

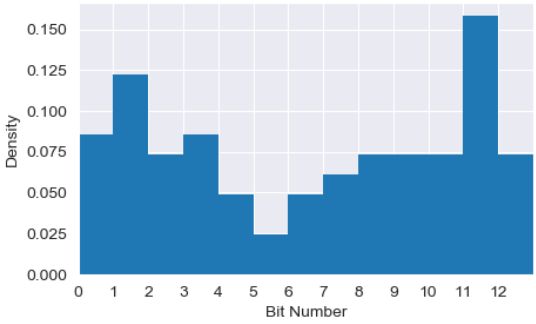


Figure 6.9: Bit Mismatch Plot of Unique SEQ Jump Error Encoder CR Sample Path 7

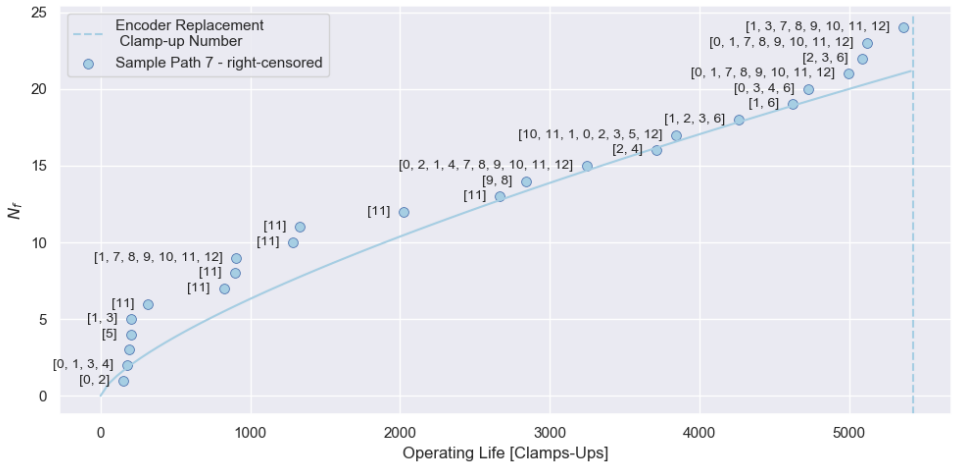


Figure 6.10: Error trend plot: encoder CR sample path 7 annotated with bit mismatches

## 6.4 Summary

In this chapter, a methodology for utilizing the bit data information within the sequence jump error logs is defined, which is currently not in use. It aims to make the information useful to determine defective encoders and prove this is the most rational way to handle the

data to maximize this ability. Presenting a case study on two complete and right-censored lifetimes allows for the discovery of the methodology's effectiveness and demonstrates how defective and non-defective encoder lifetime's BM patterns can occur and resemble. It also proves that BM monitoring can be an effective health monitoring tool for the encoder components. The BM monitoring strategy consists of identifying repeating bit patterns, combining that with the knowledge of an increasing NHPP error trend plot would then indicate the encoder is approaching its end of life. This is further discussed in the Chapter 7.

# Chapter 7

# Applications

This chapter will describe how the analyses from Chapter 4 - 6 can aid preventative maintenance procedures and overall enhance expert knowledge throughout the workforce. Furthermore, a monitoring strategy on the health of the encoders will be created and will consist of a diagnostic part with the NHPP complete analysis and correlation with the lifetime distributions and a prognostic part with the tracking of bit mismatch patterns.

## 7.1 Preventive Maintenance

Preventative maintenance is about fixing or replacing components as close to the onset of ageing as possible. The lifetime distributions and stochastic process modelling can calculate reliable estimates for the expected life of the encoders, the remaining life of the encoders, and expected occurrences of errors. This information can then aid in updating the maintenance procedures currently employed on this component.

### 7.1.1 Lifetime Distribution

The lifetime distribution of each of the four encoders was estimated in Chapter 4. Using the lifetime distributions, the mission reliability over an operating interval can be predicted. Equation (7.1) defines the mission reliability for a component.

$$R(t, t+x) = \frac{R(t+x)}{R(t)} \tag{7.1}$$

Where $R(t)$ is the reliability at the current age of the component, $R(t+x)$ is the reliability of the current age of the component at the end of the mission. In this case, the Weibull reliability function, defined by Equation (4.7), will determine the mission reliability of

the component. Figure 7.1 shows the mission reliability for encoder CA for a mission of 0 to 6,000 clamp-ups with increments of 500 clamp-ups. The increments represent the times when to perform a theoretical and reasonable in-service testing (IST). Therefore, the mission reliability can be calculated for any desired IST increment and for any of the three encoders.

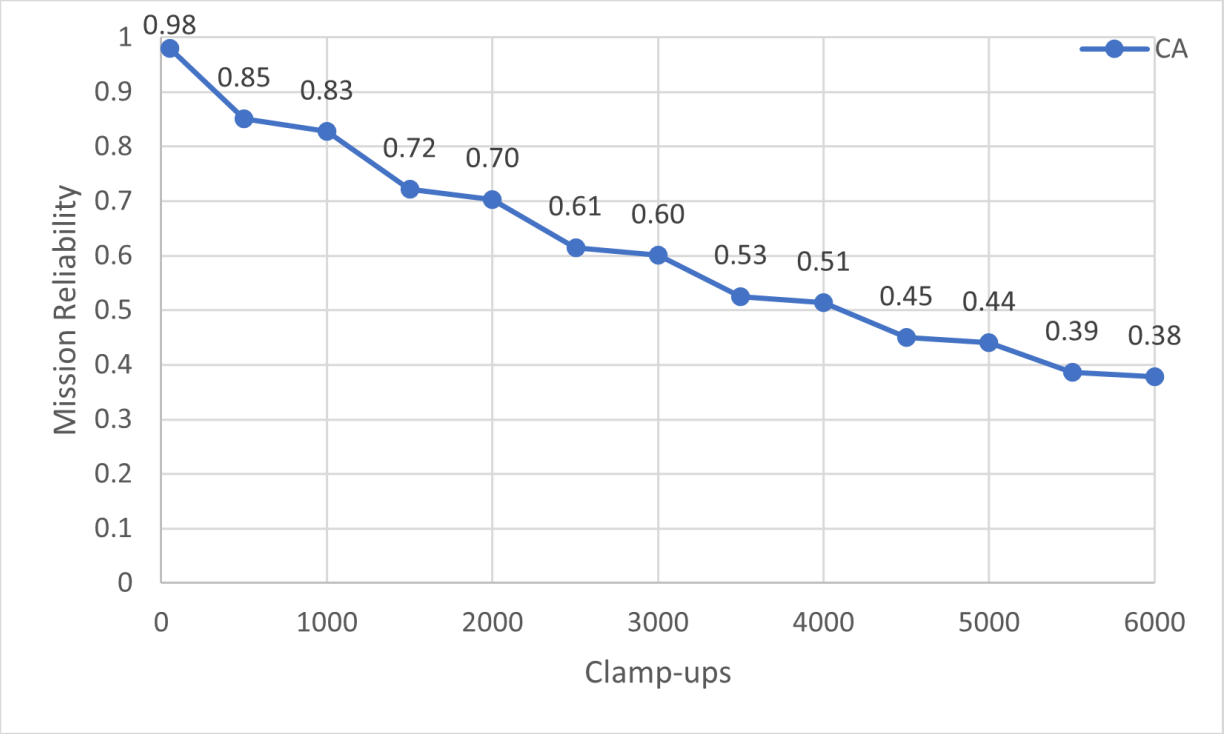


Figure 7.1: Example mission reliability graph for encoder CA with a 500 clamp-up interval

The points identify the probability of surviving to the specified age given the encoder is in good condition upon the previous IST.

## 7.2 Encoder Health Monitoring Strategy

This section will present a plan for applying the information from the NHPP and BM chapters. It will create a real-time monitoring strategy for the health of the encoders consisting

of a diagnostic part using the NHPP analysis in correlation with the lifetime distributions and a prognostic part using the bit mismatch pattern tracking concept described in Chapter 6.

### 7.2.1 Monitoring Error Trendline

The diagnostic part involves looking at the current rate of errors of the encoder and the change in that rate. An efficient and accurate way to monitor this would be by creating a NHPP model and determining the $\beta$ value, which provides the current deterioration. Using the logic in Chapter 5 will allow for accurate tracking of the rate, utilizing unique faults and the logging of a singular bus number. The proposed method is to make sure the $\beta$ value remains close to 1 and follows a tolerable trend, and, once it does not, to initiate a repair/replace order.

### 7.2.2 Monitoring Bit Mismatch Patterns

The monitoring of the bit mismatches should occur using the methodology from Chapter 6 for accurately retrieving the bit patterns. Therefore, unclear bit patterns with no significantly recurring bit(s) identify a healthy encoder and significant recurring bit(s) mismatching identify a faulty encoder. For example, an increase in fault rate could mean that the health of the encoder has deteriorated and a replacement is necessary. However, matched with inconclusive bit patterns, this can be postponed until further information. On the other hand, the same bit(s) mismatching provides an extra guarantee that a replacement WO is necessary.

### 7.2.3 Example - 1

An example of this monitoring strategy application is presented. A complete lifetime of CA encoder i.e. sample-path 2, is chosen. It is a complete lifetime with 124 total and 84 unique faults. The NHPP model also has a $\beta$ of 6.18. An increasing error trend and a dominant bit mismatch pattern, can be seen in Figures 7.2 and 7.3, respectively. This overall NHPP graph does not annotate all the data points for the ease of viewing of the BM pattern and the orange line is the fitted NHPP model.

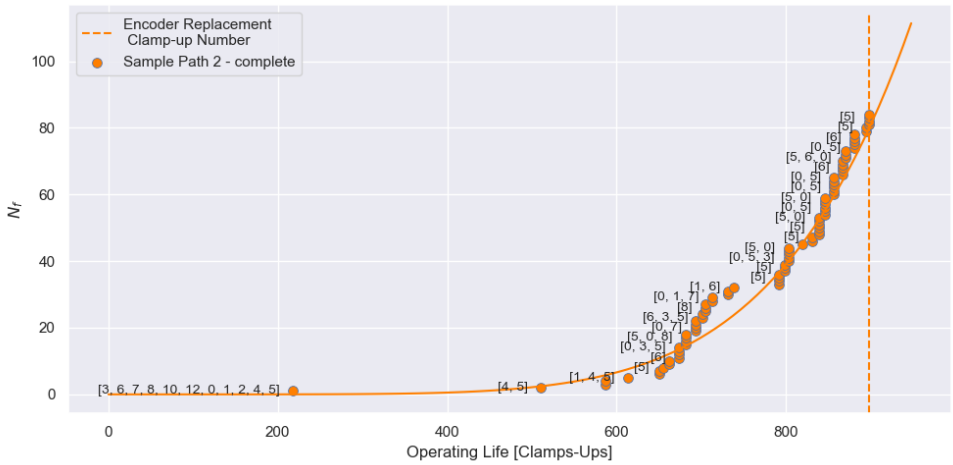


Figure 7.2: Encoder error trend plot: encoder CA sample path 2 annotated with bit mismatches

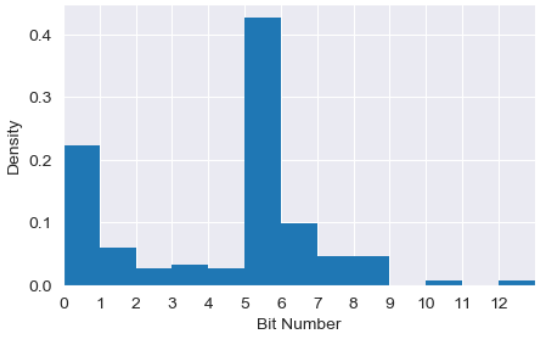


Figure 7.3: Bit mismatch plot of unique SEQ jump error encoder CA sample path 2

Figure 7.4 shows a relatively sharp increase in errors starting at about the 600 clamp-ups. Eventually the encoder was replaced at about 900 clamp-ups. Furthermore, Figure 7.3 shows 2 dominantly recurring bits in bit 0 and 5.

Figures 7.4 and 7.5, shows the theoretical NHPP model and BM histogram output of the monitoring tool near the 650 clamp-up count with 10 unique faults. With the bit mismatch pattern histogram, bit number 5 shows up in all of the unique fault logs, while the other bits do not even show up in half. With the annotations on the NHPP model, it is

clear that bit number 5 has an abnormal high occurrence and points to a defective encoder. Both parts of the health monitoring tool point to a deteriorating encoder clearly near 700 clamp-ups. The encoder performance continues to deteriorate until the replacement near $\approx 900$ clamp-ups.

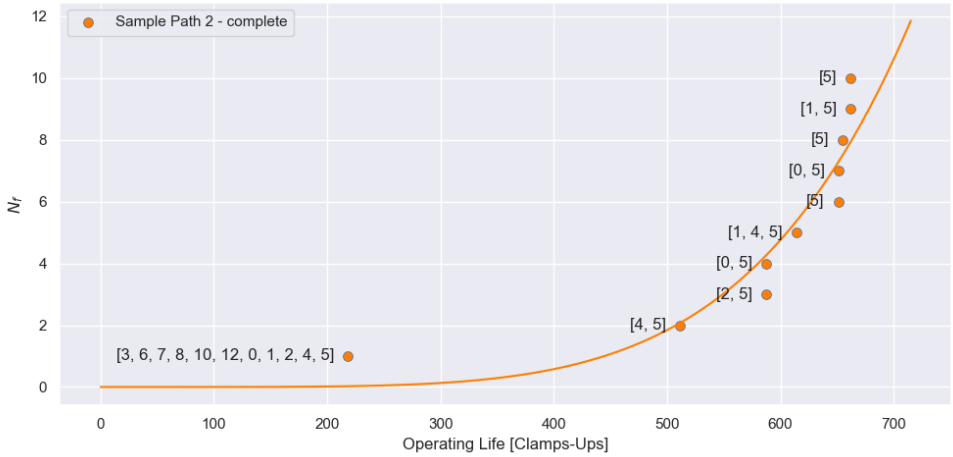


Figure 7.4: Encoder error trend plot: encoder CA sample path 2 annotated with bit mismatches up to theoretical defective encoder detection

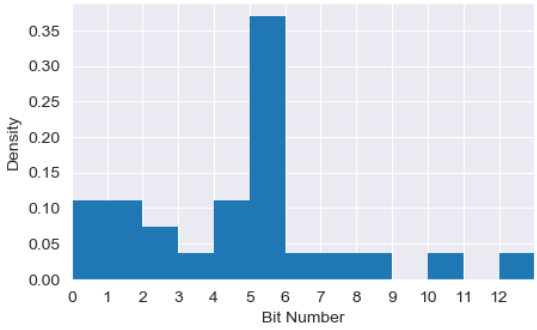


Figure 7.5: Bit mismatch plot of unique SEQ jump error encoder CA sample path 2 at theoretical defective encoder detection

### 7.2.4 Example - 2

The second example is based on encoder CR, sample-path 4. It is presented to show the ability of the monitoring strategy to determine a non-failing encoder. It is a right-censored lifetime with 72 total and 16 unique faults and also has a $\beta$ value of 0.84. The error trend line does not have any sharp change (Figure 7.6) and the BM histogram has sole dominant mismatch in bit 1 (Figure 7.7), showing the need for them to be used in conjunction. Also, within the following error trend graphs the blue line is the fitted NHPP model.

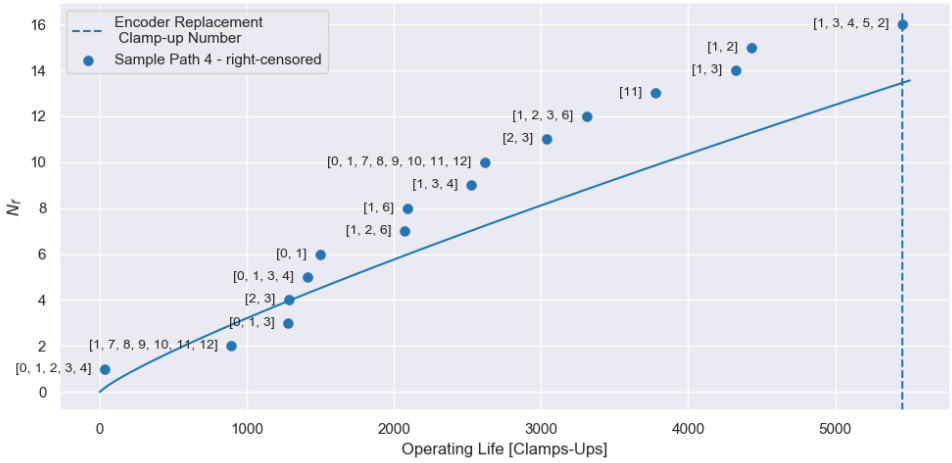


Figure 7.6: Encoder error trend plot: encoder CR sample path 4 annotated with bit mismatches

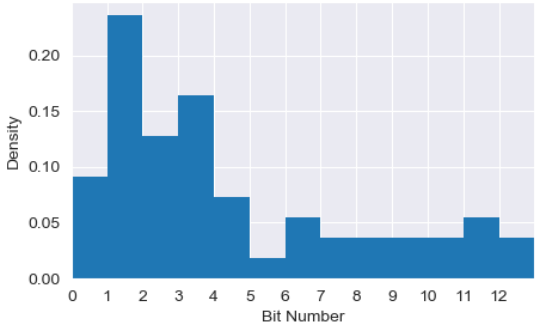


Figure 7.7: Bit Mismatch Plot of Unique SEQ Jump Error Encoder CR Sample Path 4

Figure 7.6 shows a linear relationship between the number errors and the number of clamp-ups. The encoder is able to survive past the desired mission of 5,000 clamp-ups.

Figures 7.4 and 7.5, shows the theoretical NHPP model and BM histogram output of the monitoring tool near the 3,000 clamp-up count with 10 unique faults. The $\beta$ value is 1.2624. The error trend identifies a non-failing trend with the bit mismatch pattern histogram showing a dominant bit 1. However, you can see that when used in conjunction the dominant bit has less meaning and still identifies a healthy encoder that was able to survive the desired mission. At approximately 3000 clamp-ups, the health monitoring tool points to a stable encoder. The encoder lifetime continues to approximately 5500 clamp-ups with a steady error trendline, surviving till its replacement at the next FM head overhaul.

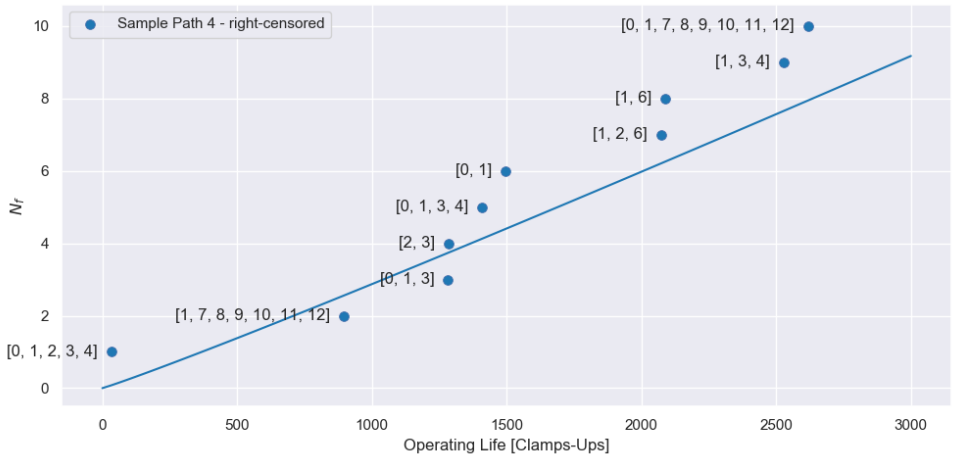


Figure 7.8: Encoder error trend plot: encoder CR sample path 4 annotated with bit mismatches up to theoretical defective encoder detection

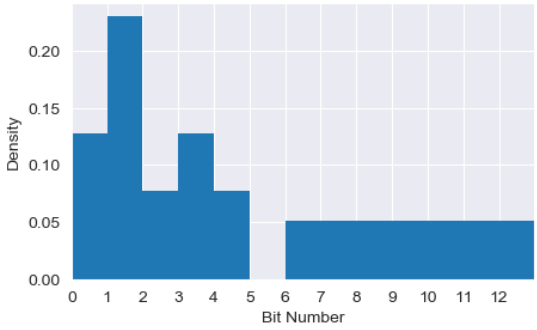


Figure 7.9: Bit mismatch plot of unique SEQ jump error encoder CA sample path 2 at theoretical defective encoder detection

## 7.3 Remarks

Both the lifetime distributions and the NHPP modelling allows for a better understanding of the reliability of the components and give information in terms of maintenance needs and remaining lifetime. The two-part health monitoring tool can be useful to determine the current health of an encoder and detect deteriorating encoders in real-time without removing them from service.

# Chapter 8

# Conclusion

This thesis presents analyses of historical data of the four encoders used in the Fueling Machine Head that is used to fuel and defuel a CANDU reactor. The nuclear reactors need to be continuously fuelled to maintain optimum power generation at all times. Encoder reliability is important to ensure reliable performance of the fuelling process.

The lifetime distribution analysis uses all three historical data types with the WOs, encoder errors, and clamp-ups in the estimation of distribution parameters for each of the four encoders using the MLE method. The distributions were then used to estimate the MTTFs. Encoders CA, CR, and RA are fitted well by the Weibull distribution and gave MTTF estimates of 3083, 11773, and 3698 clamp-ups, respectively. This indicated that the encoder CA and RA are less likely to reach the desired overhaul interval of 5000 clamp-ups. Due to lack of data encoder MR was not analyzed in the study. With the estimated Weibull parameters for the remaining three encoders, a reliability curve, hazard rate plot, and mission reliability curve are presented. The reliability curve identifies the reliability of the encoder CA, CR, and RA at 5000 clamp-ups to be 19.83%, 71.01%, and 26.21%, respectively.

The stochastic process model chapter utilizes the encoder error versus clamp-up data to estimate the NHPP model parameters. It takes the unique faults, consolidates the logs to each respective clamp-up count number, and only considers lifetimes with 15 or more of them. This outputs 39 sample paths from the historical data for encoder CA, CR, and RA. The NHPP models are then fitted to both the raw and processed versions of the data and compared. The NHPP model helps to identify deteriorating condition of the encoder when its shape parameter is greater than one, $\beta > 1$. When $\beta$ is close to 1, it implies that errors are occurring at random and no systematic trend is present in the data. The maintenance WOs tend to support the implication of NHPP model. For example, when NHPP model shows a sharply deteriorating trend, the encoders tend to undergo an emergency replacement.

The probabilistic assessment of the bit mismatch patterns, can help identify defective bit(s). The NHPP and bit mismatch analysis allow for the development of a health monitoring strategy, with the effectiveness of this methodology being shown by two examples.

Lifetime distribution MTTF estimates can be used for date of replacement or repair of the encoder components. Furthermore, the lifetime distributions can be used to create mission reliability curves based on an in-service testing desired interval. The bit mismatch patterns are useful in identifying dominant recurring failed bits, to confirm failed encoders. Finally, the NHPP modelling and bit mismatch histogram methodology can be put together into a two-part health monitoring tool. With one part consisting of analyzing the NHPP models determining the rate of the faults, and the other part consisting of the bit mismatch histograms to identify recurring patterns. Using the two parts in conjunction creates an efficient rationale for monitoring the health of the encoders.

# References


[1] O. P. Generation, "Inroduction to CANDU processes," Clarington, Ontario, Canada, 1993, accessed: (2021/11/04). Available: http://canteach.candu.org/_layouts/15/WopiFrame.aspx?sourcedoc=/Content%20Library/20042609.pdf&action=default. x, 2

[2] ——, "Nuclear Power Demonstration g.s. system training manual 053 reactor boiler and auxiliaries fuel handling system," Clarington, Ontario, Canada, 1968, accessed: (2021/02/15). Available: https://canteach.candu.org/_layouts/15/WopiFrame.aspx?sourcedoc=%2FContent%20Library%2FNPD053%2D352%2Epdf&action=view. x, xiii, 4, 5, 6, 7, 8, 102, 103, 104, 105

[3] R. W. Doran, "The gray code," *Journal of Universal Computer Science*, vol. 13, no. 11, pp. 1573–1597, 2007. x, 9

[4] GEH-C, "Ge hitachi nuclear energy canada encoder error format," Ontario Power Generation, Clarington, Ontario, Canada, Tech. Rep. TD 38-69842-071-530 R005, - -. 14, 15, 16, 77, 79

[5] M. Pandey and M. I. Jyrkama, "Fall 2017 engineering risk and reliability," 2017. 22, 23, 24

[6] W. Nelson, *Applied Life Data Analysis*. New York, USA: John Wiley & Sons Inc., 1982. 22, 24

[7] ——, "Theory and applications of hazard plotting for censored failure data," *Technometrics*, vol. 14, no. 4, pp. 945–966, 1972. 26, 27

[8] Z. Yang, S. Li, C. Chen, H. Mei, and Y. Liu, "Reliability prediction of rotary encoder based on multivariate accelerated degradation modeling," *Measurement*, vol. 152, 2020. 35

[9] S. E. Rigdon and A. P. Basu, *Statistical Methods for the Reliability of Repairable Systems*, 1st ed. Wiley-Interscience, April 14, 2000. 38, 39, 41

[10] W. J. Garland, "Candu in context," in *The Essential CANDU*, W. J. Garland, Ed. Hamilton, Ontario, Canada: UNENE, 2014, ch. Prologue, pp. 1–11.

[11] R. Chaplin, "Introduction to nuclear reactors," in *The Essential CANDU*, W. J. Garland, Ed. Hamilton, Ontario, Canada: UNENE, 2014, ch. 1, pp. 13–37.

[12] ——, "Genealogy of candu reactors," in *The Essential CANDU*, W. J. Garland, Ed. Hamilton, Ontario, Canada: UNENE, 2014, ch. 2, pp. 47–94.

[13] ——, "Nuclear plant systems," in *The Essential CANDU*, W. J. Garland, Ed. Hamilton, Ontario, Canada: UNENE, 2014, ch. 8, pp. 611–668.

[14] ——, "Nuclear plant operation," in *The Essential CANDU*, W. J. Garland, Ed. Hamilton, Ontario, Canada: UNENE, 2014, ch. 9, pp. 669–738.

[15] D. Damario, "Fuel handling an storage," in *The Essential CANDU*, W. J. Garland, Ed. Hamilton, Ontario, Canada: UNENE, 2014, ch. 20, pp. 1507–1546.

[16] A. Sun, E. J. kee, W. Yu, E. Popova, R. Grantom, and D. Richards, Eds., *Application Of CROW-AMSAA Analysis To Nuclear Power Plant Equipment Performance ICONE-13*, Beijing, China, May 16-20, 2005.

[17] H. M. Taylor and S. Karlin, *An Introduction to Stochastic Modeling*, 3rd ed. San Diego, CA: Academic Press, 1998.

[18] H. C. Tijms, *A First Course in Stochastic Models*. New York, USA: John Wiley & Sons, 2003.

[19] N. Manzana, "Stochastic renewal process models for structural reliability analysis," Ph.D. dissertation, University of Waterloo, Waterloo, ON, CA, 2018.

[20] R. E. Barlow and F. Proschan, *Mathematical Theory of Reliability*. New York, NY: John Wiley & Sons, 1965.

[21] M. E. Flygare, J. A. Austin, and R. M. Buckwalter, "Maximum likelihood estimation for the 2-parameter weibull distribution based on interval-data," *Transactions on Reliability*, vol. R-34, pp. 57–59, April, 1985.

[22] H. Guo, A. Mettas, G. Sarakakis, and P. Niu, "Piecewise nhpp models with maximum likelihood estimation for repairable systems," in *2010 Proceedings - Annual Reliability and Maintainability Symposium (RAMS)*, 2010, pp. 1–7.

# APPENDICES

# Appendix A

# FM Head Main Drive Systems

## A.1 Charge Tube Axial

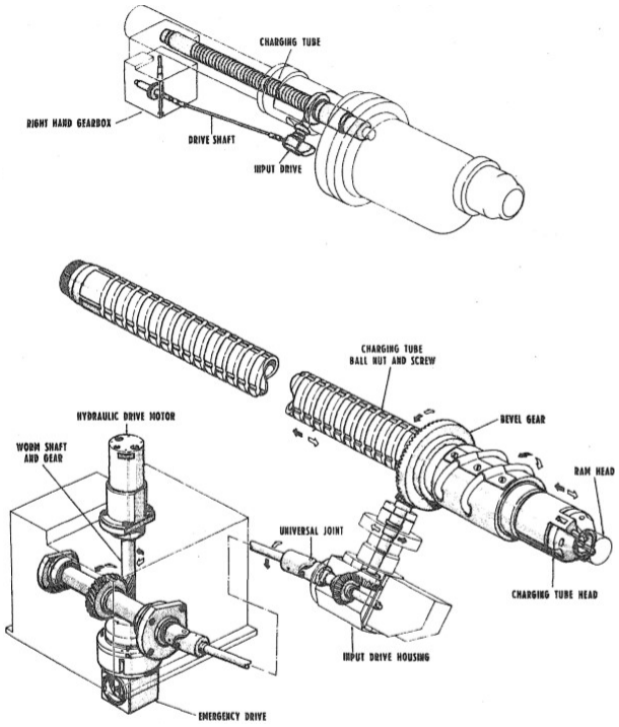


Figure A.1: Charge Tube Axial Drive System [2]

## A.2 Charge Tube Rotary

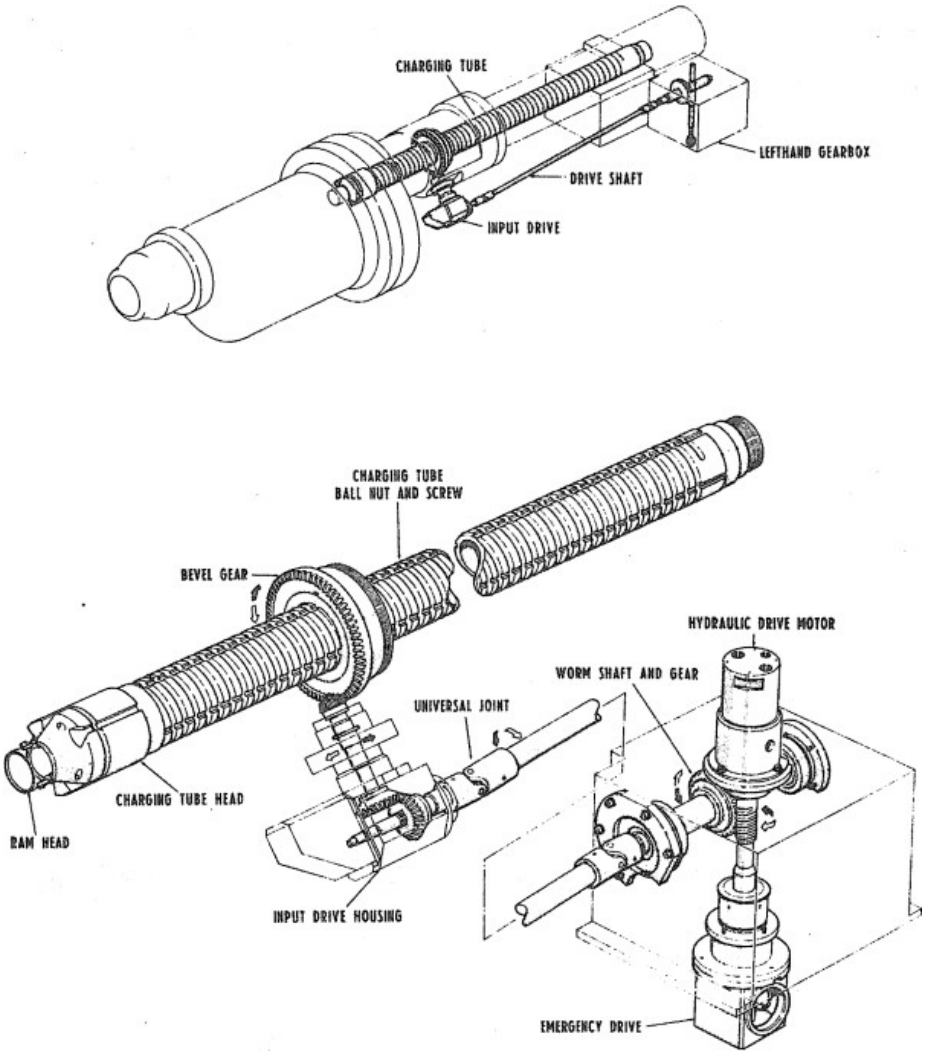


Figure A.2: Charge Tube Rotary Drive System [2]

## A.3 Ram Axial

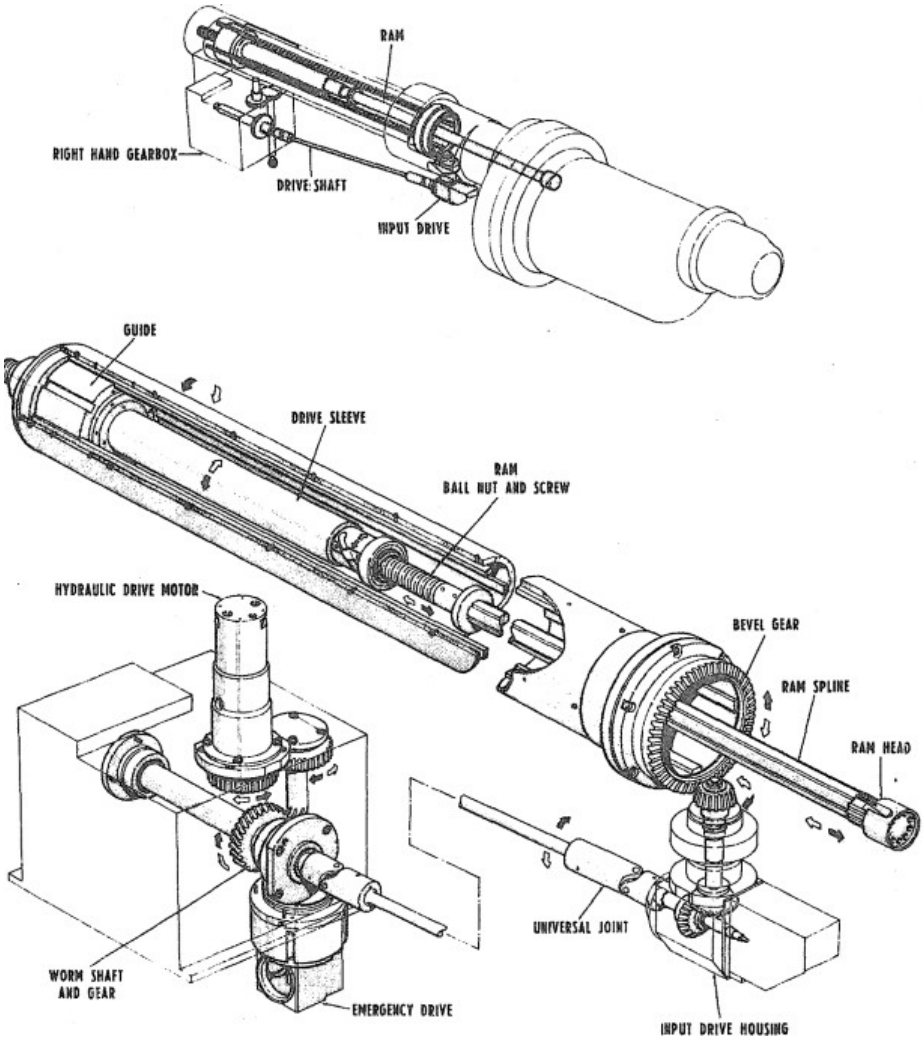


Figure A.3: Ram Axial Drive System [2]

## A.4 Magazine Rotary

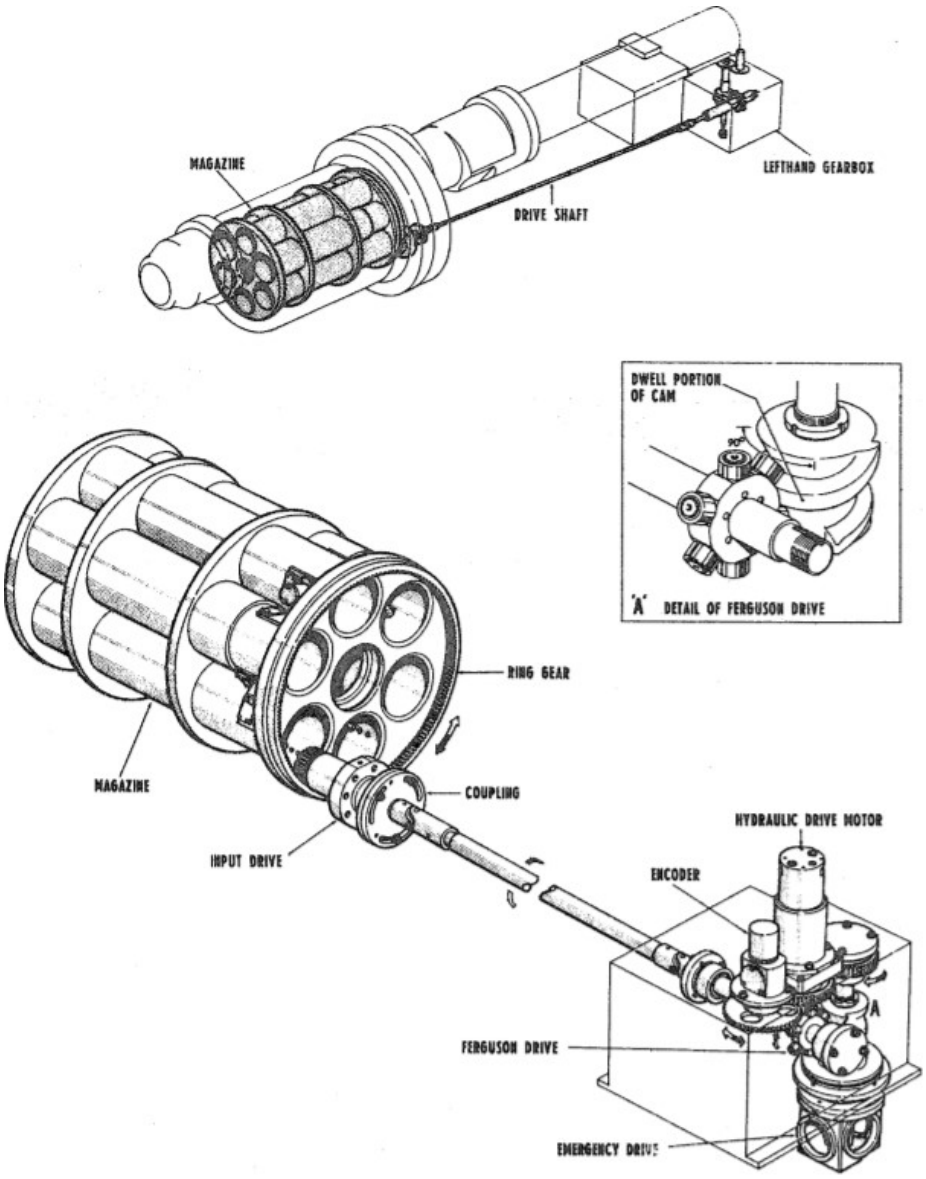


Figure A.4: Magazine and Drive System [2]

# Glossary

**bus** A bus is a subsystem that is used to connect computer components and transfer data between them. For example, an internal bus connects computer internals to the motherboard. A "bus topology" or design can also be used in other ways to describe digital connections. 14–17, 79, 80, 90

**CANDU** CANada Deuterium Uranium - the generic name for Canadian heavy water power reactors iii, 1, 96, 98

**Nuclear Power Demonstration** The Nuclear Power Demonstration or NPD Reactor was partially modelled on the NRU reactor and was intended to be the first Canadian nuclear power reactor and a prototype for the CANDU design. 98